# UC Merced

## UC Merced Electronic Theses and Dissertations

### Title

Deletion of Vhl in Dmp1-expressing cells causes microenvironmental impairment of hematopoiesis

### Permalink

https://escholarship.org/uc/item/0m12p9wf

### Author

Chicana, Betsabel

### Publication Date

2022

### Copyright Information

This work is made available under the terms of a Creative Commons Attribution License, availalbe at https://creativecommons.org/licenses/by/4.0/

Peer reviewed|Thesis/dissertation

eScholarship.org Powered by the California Digital Library
University of California

UNIVERSITY OF CALIFORNIA, MERCED

Deletion of *Vhl* in Dmp1-expressing cells causes microenvironmental impairment of hematopoiesis

A dissertation submitted in partial satisfaction of the requirements for the degree Doctor of Philosophy in Quantitative and Systems Biology

by

Betsabel Chicana Romero, M.S.

Committee in charge:

Professor Joel A. Spencer, Chair

Professor Gabriela G. Loots

Professor Stefan Materna

Professor Jennifer O. Manilay

2022

Copyright ©

Betsabel Chicana, 2022

*All rights reserved*

The Dissertation of Betsabel Chicana is approved, and it is acceptable in quality and form for publication on microfilm and electronically:

---

Dr. Jennifer O. Manilay

---

Dr. Gabriela G. Loots

---

Dr. Stefan Materna

---

Dr. Joel A. Spencer, Chair

University of California, Merced

2022

# DEDICATION

The entirety of this work as a culmination of my extensive education journey is dedicated to my family for their continuous support to my goals and dreams.

Martha Trinidad

Marco Segovia

Lorena Reyes

Mario Reyes

Carl Sandstrom

Thank you for all the support, courage, and strength you all provide me.

Gracias por todo el apoyo, ánimo, y valor que siempre me dan ♥.

TABLE OF CONTENTS

LIST OF ABBREVIATIONS

| | |
|---|---|
| Ab | Antibody |
| B1a | sub-class of B cell lymphocytes |
| B1b | sub-class of B cell lymphocytes |
| BGLAP | Bone Gamma-Carboxyglutamate protein |
| BM | Bone marrow |
| BMSC | Bone marrow stromal cells |
| CLP | Common lymphoid progenitor |
| CXCL12 | C-X-C Motif Chemokine Ligand 12 |
| DMP1 | Dentin Matrix Acidic Phosphoprotein 1 |
| EC | Endothelial cell |
| EMH | Extramedullary hematopoiesis |
| EPO | Erythropoietin |
| EPOR | Erythropoietin receptor |
| Glut1 | Glucose transporter 1 |
| HIF | Hypoxia-inducible factor |
| HSC | Hematopoietic stem cell |
| IL | Interleukin |
| i.p. | Intraperitoneal |
| Lin | Lineage |
| LSK | Lineage$^{-}$, Sca1$^{+}$, cKIT$^{+}$ |
| LT-HSC | Long-term hematopoietic stem cell |
| 2-NBDG | 2-(N-(7-Nitrobenz-2-oxa-1,3-diazol-4-yl)Amino)-2-Deoxyglucose |
| MFI | Mean fluorescent intensity |
| MPP2 | Multipotent progenitor 2 |
| MPP3 | Multipotent progenitor 3 |
| MPP4 | Multipotent progenitor 4 |

| | |
|---|---|
| MSC | Mesenchymal stem cell |
| $\mu$CT | Micro-computed tomography |
| NK | Natural Killer cells |
| OB | Osteoblast |
| OC | Osteoclast |
| OCY | Osteocyte |
| OPG | Osteoprotegerin |
| PB | Peripheral blood |
| PBS | Phosphate buffered saline |
| PerC | Peritoneal Cavity |
| PHD | HIF prolyl hydroxylase |
| PIM | Pimonidazole |
| SA | Streptavidin |
| SPL | Spleen |
| ST-HSC | Short-term hematopoietic stem cell |
| SOST | Sclerostin |
| VHL | von-Hippel Lindau |
| VEGF | Vascular endothelial growth factor |

LIST OF SYMBOLS

| | |
|---|---|
| α | alpha |
| β | beta |
| ° | degree |
| ε | epsilon |
| γ | gamma |
| μ | micro |
| + | positive expression |
| - | negative expression |

LIST OF TABLES

LIST OF FIGURES

ACKNOWLEDGEMENTS

The work presented in this dissertation has been made possible by the contributions of many people; I wish to thank my family, friends, and colleagues for all their contributions to my dissertation and educational career. I am thankful to all my mentors and positive influences I've had in my journey thus far. Dr. Terrence Satterfield and Dr. Dorothy Jones-David for their guidance at San Francisco Community College, you inspired me to pursue a career in science and your continued guidance over the years has set the foundation of my career. Dr. Vance Vredenburg and Dr. Andrea Swei for their support since my early research days as an undergraduate student to a master's student at San Francisco State University. Dr. Ruth Globus, Dr. Steve Weinstein, and Dr. Ronald Drucker for believing that I can pursue and succeed in graduate school before I could even see it myself. Dr. Frank T Bayliss and Dr. Megumi Fuse for their support through the Bridges to Doctorate Program guiding my path towards graduate school. Dr. Josh Alwood, Dr. Ann-Sofie Schreurs, Dr. Yasaman Shirazi, and Dr. Candice Tahimic whose journeys through their own postdoc inspired me to pursue mine, and for their constant support through my scientific journey.

Special thanks to my advisor Dr. Jennifer O. Manilay for her continued investment and mentoring leading to this dissertation. She has been a wonderful mentor and a strong role model to my academic and research learning structure. During my time in her lab, she has guided me through experimental techniques, critical thinking, teaching skills, scientific writing and more, allowing me grow as a scientist. I would also like to thank my colleagues Dr. Cristine Donham and Dr. Alberto Millan for their support and guidance in lab. Additionally, the undergraduate students "wondergrads" who have contributed to this work: Hanna Taglinao, Hawa Padmore, William Pratcher, Bryan Hom, Samantha Hernandez, and Jazmin Reyes Servin.

My sincere thanks to my committee members, Dr. Anna Beaudin whose initial guidance set the groundwork for this dissertation, Dr. Gabriela Loots and Dr. Joel Spencer, for their continued guidance and support during this work, and Dr. Stefan Materna for joining my committee providing crucial guidance and advice. A special thanks to graduate students Negar Seyedhassantehrani, Nastaran Abbasizadeh, and Christian Burns, for their friendship and support with this work.

Additionally, I would like to acknowledge the staff of the Department of Animal Research Services (DARS) and Dr. David Gravano from the Stem Cell Instrumentation Foundry (SCIF) at UC Merced for the excellent animal care and technical support. As well as the Health Sciences Research Institute (HSRI) at UC Merced for their administrative support. I cannot express my gratitude enough to all the people who have helped one way or another, all which accentuates how my scientific journey has been collaborative and supportive.

FUNDING, COPYRIGHTS, AND CONTRIBUTIONS

**CHAPTER 1-4**

This work was funded by the University of California, and UC graduate student fellowships. NIH grants R15 AI154245-01 to Dr. Jennifer O. Manilay and Dr. Joel A. Spencer and NIH F31 AI154815 fellowship to Betsabel Chicana.

**CHAPTER 2: Deletion of *Vhl* in Dmp1-expressing cells causes microenvironmental impairment of B cell lymphopoiesis**

This section of the dissertation is a reprint of the material as it appears in *Frontiers Immunology* with no format changes. All data collected and figures created by B.C. except for the following: Fig1a, Fig.6 and Supplemental Fig.7 by Nastaran Abbasizadeh.; Fig.7 and Videos 1-10 by Christian Burns; Fig.5D as well as assistance collecting crucial experimental data by Hanna Taglinao.

Betsabel Chicana, Nastaran Abbasizadeh, Christian Burns, Hanna Taglinao, Joel A. Spencer, Jennifer O. Manilay. Deletion of *Vhl* in Dmp1-expressing cells causes microenvironmental impairment of B cell lymphopoiesis. Frontiers in Immunology. February 2022. DOI: https://doi.org/10.3389/fimmu.2022.780945

Copyright © 2022 Chicana, Abbasizadeh, Burns, Taglinao, Spencer and Manilay. This is an open-access article distributed under the terms of the Creative Commons Attribution License (CC BY). The use, distribution or reproduction in other forums is permitted, provided the original author(s) and the copyright owner(s) are credited and that the original publication in this journal is cited, in accordance with accepted academic practice. No use, distribution or reproduction is permitted which does not comply with these terms.

There is a preprint copy of this manuscript prior to peer review in BioRxiv doi: https://doi.org/10.1101/2021.09.10.459794

**CHAPTER 3 *Vhl* deficiency in Dmp1-expressing cells affects myeloid development and erythropoiesis: possible effects on myeloerythroid metabolism**

Betsabel Chicana*, Janna Emery*, Hanna Taglinao, Cristine Donham, Jennifer O. Manilay. *Vhl* deficiency in Dmp1-expressing cells affects myeloid development and erythropoiesis: possible effects on myeloerythroid metabolism. *In preparation.* *Betsabel Chicana and Janna Emery equally share first authorship of this work.

The parts that are described in this chapter are focused on the bone marrow defects of myeloid development and erythropoiesis, while the systemic effects, metabolism and blood disorders found will be part of Janna Emery's master thesis. Specific contributions by each author to any figure presented in this chapter will be acknowledged in the figure legends.

CURRICULUM VITAE

## EDUCATION

2022 **Doctor of Philosophy**, Quantitative and Systems Biology

University of California, Merced

2016 **Master of Science**, Cell and Molecular Biology

San Francisco State University

2013 **Bachelor of Science**, Molecular, Cell & Developmental Biology

University of California Santa Cruz

2011 **Associate in Science**, 1) Social and Behavioral Sciences,

2) Science and Mathematics, 3) Chemistry

City College of San Francisco

## RESEARCH & PROFESSIONAL EXPERIENCE

2016-2022 University of California Merced

Mentor: Dr. Jennifer O. Manilay

Ph.D. thesis aims to understand the interactions between the skeletal system and B lymphocyte development. I propose to define the role of von-Hippel Lindau tumor suppressor in immune cell development to understand the molecular mechanisms underlying the effects of altered osteocyte signaling on hematopoiesis.

2014-2016 San Francisco State University

Mentor: Dr. Andrea Swei

Master thesis focused on investigating transcriptomic profiles in different virulent strains of the bacteria *Borrelia burgdorferi*, the causative agent of Lyme disease. The goal of this study was to identify key virulence genes that are differentially expressed in strains of B. burgdorferi to understand role in the dissemination and pathogenicity of *B. burgdorferi*.

2012-2014 NASA Ames Research Center

Mentor: Dr. Ruth Globus

Project: Ionizing radiation induced gene expression analysis of key osteoclastogenic cytokines.

Performed molecular and microscopic analyses of samples from experiments designed to understand mechanisms involved in bone loss, radiation, and microgravity effects. Measured expression of selected cytokines known to stimulate osteoclastogenesis and contribute to inflammatory bone disease.

2011 BioMarin Pharmaceutical Inc.

Mentor: Dr. Terrence Satterfield

Implemented molecular biology and cell culture techniques to determine if supplementing enzymes to disease-model cells ameliorates specific cellular phenotypes, developing assays that will be used to quantify cellular responses to specific stimuli, and assisting with general lab organization.

2010 San Francisco State University

Mentor: Dr. Vance Vredenburg and Dr. Tina Cheng

Project: Monteverde Amphibian Decline Due to Outbreak of an Emerging Disease.

Performed real-time PCR assay to detect *Batrachochytrium dendrobatidis* on formalin preserved museum specimens from Monteverde, Costa Rica to understand the role of the disease on the decline and extinction of amphibians in the area from 1970-1990.

**PUBLICATIONS**

*In preparation* ***Chicana B**, *Emery J, Taglinao H, Donham C, Manilay JO. *Vhl* deficiency in Dmp1-expressing cells affects myeloid development and erythropoiesis: possible effects on myeloerythroid metabolism. *Shared first authorship

2022 **Chicana B**, Abbasizadeh N, Burns C, Taglinao H, Spencer JA, Manilay JO. Deletion of *Vhl* in Dmp1-expressing cells causes microenvironmental impairment of B cell lymphopoiesis. Frontiers in Immunology. Jan 2022. BioRxiv preprint doi: https://doi.org/10.1101/2021.09.10.459794.

2021 Donham C, **Chicana B**, Robling A, Mohamed A, Ellizaldi S, Chi M, Freeman B, Millan A, Murguesh D, Loots GG, Manilay JO. Sclerostin depletion induces inflammation in the bone marrow of mice. Int J Mol Sci. 2021 Aug 24;22(17):9111. doi: 10.3390/ijms22179111. PMID: 34502021.

2019 **Chicana B***, Donham C*, Millan AJ*, Manilay JO. Wnt Antagonists in Hematopoietic and Immune Cell Fate: Implications for Osteoporosis Therapies. Curr Osteoporos Rep. 2019;17(2):49-58. Epub 2019/03/06. doi:

10.1007/s11914-019-00503-3. PubMed PMID: 30835038; PMCID: PMC6715281. *Shared first authorship

2019 **Chicana B**, Couper LI, Kwan JY, Tahiraj E, Swei A. Comparative Microbiome Profiles of Sympatric Tick Species from the Far-Western United States. Insects Vectors and Vector-borne Diseases. 2019;10(10). Epub 2019/10/23. doi: 10.3390/insects10100353. PubMed PMID: 31635285; PMCID: PMC6836157.

2017 Kwan JY, Griggs R, **Chicana B**, Miller C, Swei A. Vertical vs. horizontal transmission of the microbiome in a key disease vector, Ixodes pacificus. Mol Ecol. 2017 ;26(23):6578-89. Epub 2017/11/28. doi: 10.1111/mec.14391. PubMed PMID: 29178531

2014 Alwood JS*, Shahnazari M*, **Chicana B**, Schreurs AS, Kumar A, Bartolini A, Shirazi-Fard Y, Globus RK. Ionizing Radiation Stimulates Expression of Pro-Osteoclastogenic Genes in Marrow and Skeletal Tissue. J Interferon Cytokine Res. 2015;35(6):480-7. Epub 2015/03/04. doi: 10.1089/jir.2014.0152. PubMed PMID: 25734366; PMCID: PMC4490751. *Shared authorship

**PRESENTATIONS**

2022 **Chicana B.,** Abbasizadeh N., Christian Burns., Taglinao H., Spencer JA., Manilay JO. Deletion of *Vhl* in Dmp1-expressing cells causes microenvironmental impairment of B cell lymphopoiesis. Oral presentation delivered at Indiana University. February 17th, 2022 (hybrid).

2022 **Chicana B.,** Abbasizadeh N., Christian Burns., Taglinao H., Spencer JA., Manilay JO. Deletion of *Vhl* in Dmp1-expressing cells causes microenvironmental impairment of B cell lymphopoiesis. Oral presentation delivered at University of Connecticut (UConn Health). February 14th, 2022 (hybrid).

2022 **Chicana B.,** Abbasizadeh N., Christian Burns., Taglinao H., Spencer JA., Manilay JO. Deletion of *Vhl* in Dmp1-expressing cells causes microenvironmental impairment of B cell lymphopoiesis. Oral presentation delivered at Fred Hutch Cancer Research Center. February 11th, 2022 (virtual).

2022 **Chicana B.,** Abbasizadeh N., Christian Burns., Taglinao H., Spencer JA., Manilay JO. Deletion of *Vhl* in Dmp1-expressing cells causes microenvironmental impairment of B cell lymphopoiesis. Oral presentation delivered at Lawrence Livermore National Laboratory. December 15th, 2021 (hybrid).

2021 **Chicana, B**., Abbasizadeh N., Burns C., Taglinao H., Spencer JA., Manilay JO. Exploring the B cell microenvironment in bones from von-Hippel Lindau (*Vhl*) Dmp1-specific knockout mice. Poster presentation selected for the Annual Society of Bone and Mineral Research (ASBMR) conference. San Diego; October 2021.

2021 **Chicana, B**., Abbasizadeh N., Burns C., Spencer JA., Manilay JO. Exploring the B cell microenvironment in von-Hippel Lindau (*Vhl*) Dmp1-specific knockout mice. Oral and poster presentation selected for the annual American Association of Immunologists (AAI) conference. Virtual; May 2021. Award: AAI-Thermo Fisher Trainee Achievement Award

2020 **Chicana, B**., Taglinao H., Donham C., Abbasizadeh N., Burns C., Spencer JA., Manilay JO. Deletion of von-Hippel Lindau in Dmp1-expressing cells impairs B cell development. Poster presentation selected for the American Society for Bone and Mineral Research. Virtual; October 2020

2020 Taglinao H (presenter), **Chicana B.**, Donham C., Manilay JO. Immune cell alterations in the deletion of oxygen sensing gene (*Vhl*) in bone cells. Annual Society for Advancement of Chicanos/Hispanics and Native Americans in Science (SACNAS) Virtual; October 2020.

2020 **Chicana, B**., Burns C., Spencer JA., Manilay, J.O. Deletion of von-Hippel Lindau in Dmp1-expressing cells impairs B cell development. Poster presentation selected for the Annual American Association of Immunologists (AAI) conference. Honolulu, HI, May 2020 (cancelled due to COVID-19).

2019 **Chicana, B**. and Manilay, J.O. The role of the von-Hippel Lindau gene in osteocytes on B lymphocyte maturation and Activation. Poster presentation delivered at the annual American Association of Immunologists (AAI) conference. San Diego, CA, May 2019.

2018 **Chicana, B**., Genetos, D., Yellowley, C., Murguesh, D., Loots, G.G., Manilay, J.O. Loss of the von-Hippel Lindau gene in osteocytes alters B lymphocyte development and immune response. Poster presentation delivered at the Annual American Association of Immunologists (AAI) conference. Austin, TX, May 2018.

2017 Hernandez, S. (presenter), **Chicana, B**., Loots, G.G., Manilay, J.O. Investigating the role that VHL-deficiency plays in B cell development and immune response. Poster presentation delivered at the Annual Society for Advancement of Chicanos/Hispanics and Native Americans in Science (SACNAS) conference. Salt Lake City, UT., October, 2017.

2016 **Chicana, B.,** Swei, A. (2016) Comparison of Borrelia burgdorferi strains and their virulence using whole transcriptome analysis. Poster presentation delivered at the Annual Society for Advancement of Chicanos/Hispanics and Native Americans in Science (SACNAS) conference. Long Beach, CA., October, 2016. Presentation Award: Microbiology Division presentation award.

2015 Cerna, L.(presenter), **Chicana, B**., Kwan, J., O'Connell, K., Swei, A. Characterizing the distribution of Borrelia burgdorferi outer-surface protein C (ospC) genotypes in Ixodes pacificus and a vertebrate reservoir. Poster presentation delivered at the Society for Advancement of Chicanos/Hispanics and Native Americans in Science (SACNAS), Washington, D.C. November, 2015.

2015 **Chicana, B**., Swei, A. (2015). Understanding the disease potential of tick-borne bacteria, Borrelia burgdorferi, using next-generation sequencing. Oral presentation delivered at the City College of San Francisco Seminar, San Francisco, CA. September, 2015.

2015 **Chicana, B.** and Swei A. (2015) Comparison of Borrelia burgdorferi strains and their virulence transmission using whole transcriptome analysis. Oral presentation delivered at the SFSU level 29th Annual CSU Student Research Competition, San Francisco, CA. February 2015.

2015 **Chicana, B**., Kwan, J., Swei, A. Comparison of Borrelia burgdorferi strains and their pathogenicity using whole transcriptome analysis. Poster presentation delivered at the San Francisco State University Annual Biology Department Retreat, Tiburon, CA. January 2015.

2015 Kwan, J (Presenter), **Chicana, B**., Swei, A. Abiotic and Biotic Determinants of Ixodes pacificus Tick Microbiome Diversity. Poster presentation delivered at the San Francisco State University Annual Biology DepartmentRetreat, Tiburon, CA. January 2015.

2012 **Chicana, B**., Kumar, A., Schreurs, A.S., Globus, R.K. Radiation Induced Changes in Osteoclast Growth and Activity. Oral presentation delivered at the City College of San Francisco Seminar, San Francisco, CA. September, 2012.

2010 **Chicana, B**., Cheng, T., Vredenburg, VT. Monteverde Amphibian Decline Due to Outbreak of an Emerging Disease. Poster presentation delivered at the Annual Biomedical Research Conference for Minority Students (ABRCMS), Charlotte, NC. November, 2010.

2010 **Chicana, B.,** Cheng, T., Vredenburg, VT. Amphibian Decline Driven by an Emerging Infectious Disease. Oral talk delivered at SFSU Summer Research Symposium, San Francisco, CA. August, 2010.

2009 **Chicana, B**. and Campbell, B. Effects of Psuedoephedrine on Zebrafish Embryos and the Blocking Abilities of Melatonin. Poster presentation delivered at the SFSU Summer Research Symposium, San Francisco, CA. August, 2009.

## HONORS & AWARDS

2022 American Association of Immunologists (AAI) Trainee Abstract Award
2022 American Association of Immunologists Minority Scientist Travel Award
2021 ASBMR Young Investigator Travel Grant
2021 AAI-Thermo Fisher Trainee Achievement Award
2021 National Science Policy Network - Professional Development Award
2021 ASBMR Student Cohort Program Trainee
2020 American Association of Immunologists Minority Scientist Travel Award (conference canceled due to COVID-19)
2019-2020 Miguel Velez Scholarship
2019 American Association of Immunologists Minority Scientist Travel Award
2018 FASEB Excellence in Science Travel Award
2017 Manilay Lab Research Award
2016 Graduate Dean's Relocation Award UC Merced
2016 SACNAS Microbiology Division presentation Award
2015 NSF Graduate Research Fellowship Honorable Mention
2010-2011 Mathematics Engineering Science Achievement (MESA) Trainee
2010-2011 Building Diversity in Science Trainee
2009-2011 NIH Bridges to the Baccalaureate Trainee
2008 Medlink (Healthlink) UCSF Future Scientist of America Award

## FUNDING AWARDS

2021-2022 Graduate Bobcat Fellowship
2021-2022 Graduate Division Fellowship
2021 UC Merced QSB Summer Research Fellowship
2021 F31 Ruth L. Kirschstein Predoctoral National Research Service Award
2020 Graduate Dean's Dissertation Fellowship
2018 UC Merced QSB Summer Research Fellowship
2017 UC Merced Fall QSB Fee and Tuition Fellowship
2015 Graduate Student Council in Biology (GSCB) Research Grant
2014-2016 NIH MA-MS/PhD Bridge Graduate Fellowship
2014 Instructionally Related Activities (IRA) Research Grant Award

## SYNERGISTIC ACTIVITIES

### Teaching experience at University of California Merced

| | |
|---|---|
| Instructor of Record | Bio140 Genetics (Summer 2021) |
| Teaching Assistant | Bio140 Genetics (4 semesters) |
| Teaching Assistant | Bio001 Contemporary Biology (4 semesters) |
| Teaching Assistant | Bio110 Cell Biology (1 semester) |
| Teaching Assistant | Bio060 Nutrition (2 semesters) |
| Teaching Assistant | Bio161 Physiology (1 semester) |

### Mentoring Experience

| | |
|---|---|
| January 2020 – May 2022 | Jazmin Reyes Servin, University of California, Merced, CA |
| March 2019 – May 2022 | Hanna Taglinao, University of California, Merced, CA |
| May 2019 – December 2019 | Bryan Hom, University of California, Merced, CA |
| January 2019 – May 2019 | Amanda Shein, University of California, Merced, CA |
| June 2018 – December 2018 | Hawa Padmore, University of California, Merced, CA |
| June 2018 – August 2018 | William Pratcher, University of California, Merced, CA |
| June 2017 – May 2018 | Samantha Hernandez, University of California, Merced, CA |
| June 2015 – August 2016 | Enxhi Tahiraj, San Francisco State University, CA |
| June 2015 – August 2016 | Liliana Cerna, San Francisco State University, CA |
| June 2015 – May 2016 | Shivang Kaushik Mehta, San Francisco State University, CA |
| June 2015 – May 2016 | Jonathan Bertram, San Francisco State University, CA |
| September 2014 – June 2015 | Arnold Shir, San Francisco State University, CA |

### Membership to Professional Societies

| | |
|---|---|
| 2021-Present | National Science Policy Network (NSPN) |
| 2020-Present | American Society for Bone and Mineral Research (ASBMR) |
| 2019-Present | American Association for the Advancement of Science (AAAS) |
| 2017-Present | American Association of Immunologists (AAI) |
| 2010-Present | Society for Advancement of Chicanos/Hispanics and Native Americans in Science (SACNAS) |

**Service Promoting Science**

2016-2022 Merced City School District STEAM center volunteer. Ask-a-Scientist speaker for 5th and 6th graders to help provide support to their science fair project. Science fair judge for the city and county of Merced.

2017-2022 RadioBio member since 2017 and Fundraiser coordinator/Grant writer since 2018. RadioBio is a UC Merced graduate student-run science communication organization. We produce and distribute open access biology educational podcasts from molecules to ecosystems. (radiobio.net)

2014-2018 Bio-Link Depot Volunteer to help sort and organize donated scientific supplies and equipment from biotech companies to provide educators and researchers tools to promote scientific training to students.

Deletion of *Vhl* in Dmp1-expressing cells causes microenvironmental impairment of hematopoiesis

by

Betsabel Chicana

Doctor of Philosophy in Quantitative and Systems Biology

University of California, Merced 2022

Professor Jennifer O. Manilay

How changes in bone homeostasis affect immune development is not fully understood. The von-Hippel Lindau protein (VHL) regulates hypoxia-inducible factor (HIF) degradation, which is involved in cellular adaptation to low oxygen environments. Conditional deletion of *Vhl* in osteoblasts and hematopoietic progenitors have demonstrated a role for VHL in these cell types. Studies have demonstrated that the B cell development is mediated by crosstalk between the skeletal and hematopoietic systems. To understand how changes in bone homeostasis may affect immune cell development, we utilized *Dmp1*-Cre;$Vhl^{fl/fl}$ conditional knockout mice (***VhlcKO***), in which *Vhl* is deleted primarily in osteocytes, mature osteoblasts, and a small subset of MSCs. The *VhlcKO* mice display dysregulated bone growth, high bone density, smaller bone marrow (BM) cavity volume, and an overall decrease in BM cellularity compared to wild-type (WT) controls. In line with this, the frequencies, and numbers of B cells in the BM were significantly decreased. These data suggest that changes in bone homeostasis may adversely affect B cell development in a cell-extrinsic manner. We **hypothesized** that normal B cell development was not supported in *VhlcKO* mice due to alterations of the microenvironment niche, such as reduction of key niche cells and decreased production of B cell-supporting cytokines. Furthermore, we have obtained evidence that *Vhl* deletion also affects myeloid and erythroid development. We found elevated Epo levels in cKO peripheral blood serum and BM fluid by 6 weeks of age, and evidence for dysregulated erythropoiesis. Moreover, the cKO displayed an increased frequency of common myeloid progenitors, CD11b+ Gr1- monocytes, and CD11b+ Gr1+ granulocytes by 10 weeks of age. We also **hypothesized** that alterations in skeletal glucose metabolism directly affect myeloerythroid development in the BM through increased Epo-receptor (EpoR) signaling. EpoR is expressed on osteoprogenitors, hematopoietic stem cells, and B cells, but whether it is expressed on myeloid progenitors is unclear. Studies are in progress to test the hypothesis that overproduction of Epo by *Vhl*-deficient Dmp1+ cells result in elevated EpoR signaling in myeloid progenitors and lineages; this in turn, results in an increase in myeloid cell glycolysis and Glut1 expression. These studies are relevant for the understanding how BM microenvironmental changes can dysregulate B cell development and trigger adaptations in immunometabolism of myeloid cells. My thesis works expands on the potential mechanisms by which VHL in Dmp1-expressing cells regulate the development of distinct hematopoietic cell lineages in the BM, further elucidating and expanding our definition of "immune niches" to include osteocytes, bone, and vasculature.

# CHAPTER 1

## Background and Introduction

## 1.1 Hematopoiesis – Lymphoid vs. Myeloid Cells

Blood cells are continuously replenished by differentiation and maturation of hematopoietic stem cells (HSCs) into either lymphoid or myeloid lineage cells, this process is known as hematopoiesis. Hematopoiesis is the formation of blood cells from embryonic development through adulthood in order to produce and replenish the blood system. Hematopoiesis occurs in two waves, 1) the primitive wave and 2) the definitive wave (1). The primitive wave, which occurs during early embryonic development is transitory and its main purpose is to produce red blood cells to facilitate oxygenation to embryo tissue during rapid growth (2, 3). Definitive hematopoiesis, which involves HSCs in the adult bone marrow can give rise to all blood lineages (4)**.** Other tissues such as spleens, liver, lymph nodes, and other organs can also support formation and development of blood cells, a process known as extramedullary hematopoiesis (EMH). EMH is generally defined as production of mature blood cells outside of the bone marrow, a compensatory expansion that occurs as a pathological change to defective hematopoiesis or insufficient bone marrow function (5). The understanding of primitive, definitive and extramedullary hematopoiesis has helped scientists better understand immunodeficiencies, blood disorders, and cancers allowing for disease treatment development. For example, the clinical benefits of stem cell transplant and immune-based therapies against cancers and disease treatment (6). Further understanding of hematopoiesis and replicating the developmental process in vivo remains to be achieved.

In this dissertation I will mainly focus on definitive hematopoiesis. Here I present a simplified version of the classical hematopoietic hierarchical model for the purpose of this dissertation (**Figure 1**). It has been established that hematopoiesis starts with hematopoietic stem cells (HSCs). Differentiation into lineage cells starts from long-term-hematopoietic stem cells (LT-HSCs) which differentiate into short-term hematopoietic stem cells (ST-HSCs), which have low self-renewal capacity compared to LT-HSCs (7). ST-HSCs then differentiate into multipotent progenitors (MPPs) which have no detectable self-renewal abilities yet keeping full lineage differentiation potential (7-9). Multipotent progenitors (MPPs) have been shown to be comprised of distinct myeloid-biased subsets (MPP2 and MPP3) and lymphoid primed MPP4s which gives rise to myeloid and lymphoid mature lineages (10). The lymphoid and myeloid cell lineages are the two major branches of hematopoietic cells. Lymphoid lineage cells include T cells, B cells, and natural killer (NK) cells, myeloid lineage cells include megakaryocytes and erythrocytes, granulocytes and macrophages (11, 12). These two lineages are separable at the progenitor level. MPPs give rise to oligopotent progenitors, either common lymphoid progenitors (CLPs) (13, 14) or common myeloid progenitors (CMPs) (15). CLPs can develop into B cells, T cells or NK cells, all which leave the bone marrow into the periphery to finish development in other organs such as the spleen or thymus. CMPs have myeloid, erythroid, and megakaryocytic potential and can form granulocyte-macrophage progenitors (GMPs) and megakaryocyte-erythrocyte progenitors (MEPs). MEPs can develop into erythrocytes or megakaryocytes which then breaks into platelets. GMPs differentiate into granulocytes such as neutrophils, basophils and eosinophils, or into monocytes which in turn become macrophages, osteoclasts, or myeloid dendritic cells (DCs) (15-19). The molecular regulation of the process of hematopoietic differentiation involves cytokines and transcription factors

governing lineage commitment decisions for proper blood development (20-24). This overview of hematopoiesis remains under exploration and is constantly updating to better understand the differentiation of each lineage cell (25-27).

There are two branches within the B cell population, conventional B-2 cells and unconventional B-1 cells. In mice, B-1 and B-2 cells differ in function and development. B-2 cells are first generated in fetal liver during development, and in the bone marrow in adults (28). B1 cells are a fetal-derived population localized mainly in the peritoneal cavity (PerC) and persists in adults (29-31). Although initially B-1 cells were believed to only originate from fetal progenitors (neonatal livers) (32), there have been newer reports that show that bone marrow progenitors can also produce B1 cells, but a much lower rate than conventional B2 cells (33-36). Whether B-1 cells are derived from a distinct adult-derived bone marrow or splenic precursor cell, still remains controversial (34, 35, 37). B-1 cells spontaneously secrete natural antibodies, and are considered to be the first line of defense against pathogens in a T-independent manner (33, 38). This allows these cells to provide immediate defense against microbial infections (39, 40). Conventional B-2 cells cooperate with T cells in the splenic germinal centers to provide high-affinity antibody responses against pathogens (41). We will focus on B-2 conventional cells which will be referred to as "B cells" for the remainder of this dissertation unless otherwise stated. Hardy et al. divided B cell precursors into subpopulations we now know as "the Hardy fractions", based on the cell's expression of various cell surface proteins (42). Hardy et al. proposed to identify the relatively abundant small pre-B cells (designated fraction D) as $B220^{+}CD43^{-}IgM^{-}$, whereas more primitive cells were resolved and designated fractions A, B, and C (42). Bone marrow B cells with functional heavy and light chains express B cell receptors (BCRs) on the cell surface were called immature B cells (fraction E) and identified as $IgM^{hi}$, $IgD^{-}$, $B220^{int}$, $HSA^{hi}$ (42, 43). Before fraction E leaves the BM for the periphery it undergoes several types of negative selection to avoid autoreactivity, including clonal deletion (44) and receptor editing (45, 46). Fraction E subsequently differentiates into mature B cells (Hardy fraction F) (47), which express surface $IgM^{int}$, $IgD^{hi}$, $B220^{hi}$, $HSA^{int}$ (42). We will be using the Hardy nomenclature to identify B cell development in our studies (**Figure 2**). Furthermore, B cell development in the BM occurs in stages that rely on growth factors that are produced by osteolineage derived cells from the BM microenvironment, in a crosstalk between the skeletal and hematopoietic systems (48-51).

### 1.2 Bone Marrow Microenvironment – "Niche"

The bone marrow microenvironment also called the "niche" is essential for the maintenance and support of hematopoiesis. Studies have revealed that this niche controls the regulation of quiescence, self-renewal and differentiation of HSCs (52). The BM niche can be divided into the vascular niche, perivascular niche and endosteal niche. The vascular niche (sinusoids, arterioles, transition zone) indicates a site rich in blood vessels where endothelial cells (ECs) and mural cells (pericytes and smooth muscle cells), create a microenvironment that affects hematopoiesis (53). The perivascular niche describes the microenvironment around a vessel and includes distinct cell types and stroma such as Nestin+ ECs, CXCL12-abundant reticular (CAR) cells, and Leptin receptor (LepR) expressing cells (54), which are involved in hematopoietic maintenance and leukocyte

trafficking (55-58). The endosteal niche located in the endosteum region comes in close contact with calcified bones, osteoblasts and osteoclasts which provides support for proper maintenance of HSC activity (59, 60). Initial studies found that HSCs colonize near the endosteal part of the bone marrow (61, 62). Spatial distribution studies using fluorescent HSCs transplanted into ablated recipients revealed a selective redistribution and enrichment within the endosteal region (60), but subsequent studies found HSCs located closer to the bone marrow sinusoids in the central niche (63, 64). These data altogether indicates that HSCs reside in spatially distinct niches (65, 66), with approximately 85% of HSCs reside within 10 μm of a sinusoidal blood vessel within the perivascular niche (67). The endosteal niche was thought to be involved in hematopoietic quiescence (68), but recent studies revealed the role of the perivascular niche. Acar et al. found that dividing and non-dividing HSCs reside mainly in perisinusoidal niches with $LepR^{+}CXCL12^{high}$ cells throughout the bone marrow (67). Hematopoietic progenitor commitment into mature lineage cells is also regulated in the endosteal, perivascular and vascular niches. Deletion of *Cxcl12* from perivascular stromal cells depleted HSCs and mobilized these cells into circulation (65). Deletion of *Cxcl12* from endothelial cells depleted HSCs, but not myeloerythroid or lymphoid progenitors (56). Deletion of *Cxcl12* from osteoblasts depleted early lymphoid progenitors and maintenance, but not HSCs or myeloerythroid progenitors (65). An osteoblast population (Lin- CD31- Sca1- CD51+) expressing PDGFRα and PDGFRβ, also high in LeptinR gene expression, was found to support pre-B lymphopoiesis in culture assays (69). These PDGFRα and PDGFRβ expressing populations localized near the growth plate and trabecular bone and were rarely found near cortical bone regions or in central bone marrow (69). Additionally, perivascular MSCs provide important signals such as CXCL12 and IL-7 which are critical for lymphoid and B cell development (28, 51, 70-72). These results suggests that HSCs tend to occupy the perivascular niche while early lymphoid progenitor occupy an endosteal niche, but the heterogeneity of distinct spatial niche for HSCs remains under exploration. What these observations reveal is that hematopoietic lineage cells development is coordinated by supporting cells and cytokine signals that guide them to specialized niches for differentiation.

The BM microenvironment is composed of hypoxic heterogeneities of local $pO_2$ (73), however the implications of these oxygen tension differences have on hematopoiesis is not well characterized. Studies in hypoxic conditions (<1-13% $pO_2$) or manipulation of the hypoxia-inducible factor-1α (HIF-1α) pathway by von-Hippel Lindau protein (VHL) or $O_2$-dependent prolyl hydroxylase domain (PHD) deletion gives us an insight of the important role of oxygen adaptation in osteogenesis. Activation of HIF-1α accelerates bone regeneration (74), promotes osteoblast differentiation into osteocytes (75), and can stimulate osteoclast formation (76). Studies have shown HIF-1α stabilization as a therapeutic option for treating bone fractures (77, 78) and osteoporosis (79-81), but the underlying molecular mechanism remains poorly understood. VHL plays an important role regulating HIF-1α expression, and disruption of *Vhl* in bone cells leads to improper bone homeostasis. Disrupting *Vhl* in osteoblasts induces expression of β-catenin, revealing an insight to the mechanism by which VHL/HIF pathway promotes bone formation through the Wnt pathway (74, 82-84). *Vhl* deletion in osteochondral progenitor cells and osteocalcin-positive osteoblasts leads to an increase in bone mass through an increase in

osteoblast number (83, 85). Mice lacking HIF-1α in the osteoblast lineage have narrow, poorly vascularized long bones at 3 weeks of age, despite normal expression of HIF-1α in the surrounding tissues (83). However, by 24 weeks of age, bones from mice lacking HIF-1α in osteoblasts have normal cortical thickness and increased bone area compared to controls (86). These results indicate that HIF-1α plays an age dependent and complex role in osteogenesis. However, these studies of *Vhl* deletion in osteolineage cells have not examined the cell-extrinsic effects that these bone changes have on the immune niche nor immune cells residing in the BM.

### 1.3 The role of *Vhl* in bone and immune development

The VHL protein functions as a regulator of hypoxia-inducible factor (HIF-1α) degradation (83, 87). When HIF-1α accumulates under hypoxic conditions (or VHL deletion), it travels to the nucleus to activate over 100 hypoxia-inducible target genes (83) (**Figure 3**). The role of HIF-1α and its regulation on the immune system has been extensively reviewed, but the mechanism of *Vhl* deletion (or HIF-1α stabilization) in specific immune cell lineages has not fully been addressed (88). Deletion of *Vhl* stabilizes HIF-1α, and its deletion in bone cells leads to an increase in bone mass by regulating bone formation activity of osteoblasts and bone resorption activity of osteoclasts (83, 85, 89-91). Localized hypoxia and HIF-1α stabilization are normal features of germinal centers in spleens. Development of robust antibody responses from conventional B lymphocytes (a.k.a. B2 cells) is diminished by the relatively low oxygen levels in the germinal centers of the spleen and lymph nodes (92). Deletion of *Vhl* in B cells stabilizes HIF-1α levels and affects B cell function by impairing cell proliferation, antibody class-switching, generation of high affinity antibodies, antibody responses, and impairs metabolic balance is essential for naive B cell survival (92, 93). VHL is expressed ubiquitously in many cell types, and global deletion of the *Vhl* gene results in embryonic lethality, so conditional knockout approaches are necessary to investigate the cell-specific roles of *Vhl* in specific microenvironments.

#### *Vhl deletion in skeletal cells*

A list and summary of key publications in which conditional knockout models of *Vhl* have been utilized to study cell intrinsic effects in skeletal and immune cells are described in Table 1 and Table 2. Mangiavini et al. deleted *Vhl* utilizing *Prx1-Cre;Vhl$^{fl/fl}$*, which targets mesenchymal progenitors. This generated shorter and developmentally delayed fetal bones by impairing proliferation of chondrocytes and by delaying their terminal differentiation. They also found increased trabecular bone with dilated BM vessels and few hematopoietic cells in perinatal mice (94). Wang et al. showed evidence that deletion of *Vhl* from osteoblasts using *OC-Cre;Vhl$^{fl/fl}$*, which targets the osteoblast bone gamma carboxyglutamate protein (BGLAP, also known as osteocalcin) promoter/enhancer, led to an increase in osteogenesis, bone mass and also increase in angiogenesis (83). Wan et al. also deleted *Vhl* from osteoblasts (*OC-Cre;Vhl$^{fl/fl}$*) and found that bones in this model had increased vascularity and higher bone mass in response to distraction osteogenesis, they suggested the HIF1α pathway as a critical mediator of angiogenesis required for skeletal regeneration HIF activators as therapies to improve bone

healing (74). Zhang et al. also utilized *OC-Cre;Vhl$^{fl/fl}$*, which led to the development extremely dense and highly vascularized long bones. They found that osteoblasts lacking *Vhl,* overexpress and secrete high levels of VEGF, promoting the proliferation and osteogenic differentiation of bone marrow stromal cells (BMSC) by promoting expression of Heme oxygenase-1 (HO-1) in BMSC. This study suggested that osteoblasts promote the proliferation and osteogenic differentiation of BMSC by VEGF/HO-1 pathway (91). Zuo et al. (*OC-Cre;Vhl$^{fl/fl}$*) found significantly increased cortical bone area resulting from enhanced proliferation and osteogenic differentiation of BMSCs by inducing the expression of β-catenin in the BMSC and disrupting the canalicular network (82). Kang et al. (*OC-Cre;Vhl$^{fl/fl}$*) found upregulated OPG, as well as osteoblast HIF-1α activation which led to an increased interleukin-33 (IL-33) expression, which was found to inhibit osteoclastogenesis (90). Weng et al. deleted *Vhl* from osteochondral progenitor cells using *Col2-CreER$^{T2}$;Vhl$^{fl/fl}$*, which targets Collagen type 2, and found that deletion of *Vhl* at the postnatal stage (2 months old) developed a progressive accumulation of cancellous bone with increased microvascular density and bone formation. This was accompanied with a significant increase in osteoblast proliferation, upregulation of differentiation marker Runx2 and osteocalcin, and elevated expression of vascular endothelial growth factor (VEGF) and phosphorylation of Smad1/5/8 (85). Rankin et al. showed evidence that *Vhl* deletion from osteoprogenitors using *Osx-Cre;Vhl$^{fl/fl}$*, which targets osterix, a transcription factor essential for osteoblasts differentiation, led to a HSC niche expansion associated with selective expansion of the erythroid lineage, revealing an unexpected role for osteoblasts in the production of EPO and modulation of erythropoiesis (95). Dirckx et al. showed evidence that *Vhl* deletion from osteoprogenitors using *Osx-Cre;Vhl$^{fl/fl}$*, led to low blood glucose levels, lower glucose tolerance, and enhanced clearing of glucose from the blood following i.p. glucose injection during a glucose tolerance test. They also found increased mRNA expression of key glycolytic enzymes Pgk1 and Pdk1, and Glut1. To visualize the uptake of glucose in situ, they administered 2-NBDG to control and mutant mice and assessed the uptake and accumulation of the compound in the tibia, particularly in osteoblast lineage cells on and around the bone surfaces and found increased presence of GLUT1 in the mutant bones lining (osteoblasts) (96). Loots et al. deleted *Vhl* from osteocytes and mature osteoblasts using *Dmp1-Cre;Vhl$^{fl/fl}$*, which targets the dentin matrix protein 1 (DMP1), which is an extracellular matrix protein involved in bone and dentin mineralization, highly expressed in osteocytes, mature osteoblast and a small subset of MSCs. They found abnormal bone phenotype increase in both trabecular and cortical bone thickness, these results demonstrated that manipulating *Vhl* in bone cells influences skeletal development and osteogenesis. This bone growth led to a dysfunctional bone marrow cavity and analysis of immune cells in the BM found that B cells were decreased, suggesting that *Vhl* deletion in Dmp1-expressing cells influences hematopoiesis (89). These results have been confirmed in a B6 background mice (*Dmp1-Cre;Vhl$^{fl/}$*) by Chen et al. that additionally found decreased osteoclastogenesis and that cell-to-cell contact between stromal cells and monocytes is required for osteoclast differentiation (97).

*Vhl deletion in hematopoietic cells*

The cell-intrinsic effects of *Vhl* has been described in various papers. For example, Takubo et al. showed evidence that deleting *Vhl* in hematopoietic cells using the *Mx1-*

*Cre;Vhl*$^{fl/fl}$ model affects quiescence and transplantation experiments showed that *Vhl* deleted HSCs no longer supported hematopoiesis (98). Cho et al. showed evidence of the role of *Vhl* in B cells using an inducible *ER*$^{T2}$*-Cre;Vhl*$^{fl/fl}$. They performed adoptive transfers into mice homozygous for the Rag mutation (which produce no mature T cells or B cells) and studied B cell activation response. They found that deletion of *Vhl* decreases germinal center B cells and memory B cells as well as reduced generation of high affinity antibodies. This study only looked at mature B cells and not developing B cells in the BM. They performed a set of in vitro experiments to show that hypoxia (1% and 5% $pO_2$) also led to similar results, decreasing proliferation and survival of B cells (92). Xu et al. deleted *Vhl* from B cells using B lineage-restricted *CD19-Cre;Vhl*$^{fl/fl}$ and found disturbed glycolytic and oxidative metabolic balance which led to severe reduction of mature B cells (93), this study highlights that metabolic balance is essential for B cell survival. Burrows et al. deleted *Vhl* from B cell progenitors by utilizing *Mb1-Cre;Vhl*$^{fl/fl}$, which targets cells expressing the Ig-α signaling subunit of the B cell antigen receptor, which is expressed exclusively in the early pro-B cell stage in the bone marrow and found severe peripheral B cell lymphopenia (low B cell frequency), as well as defects in B cell receptor (BCR) signaling, editing, and BIM (Bcl-2-like 11) dependent death (99).

As summarized in Table 2, and described above, these studies focused on the cell-intrinsic role of *Vhl*, and the cell extrinsic role in bone formation. The high bone mass described by deletion of VHL in bone cells or in other words HIF stabilization has provided a possible route against bone loss. HIF stabilizers such as PHD inhibitors (iron chelators such as desferrioxamine or 2-oxylutarate analogues such as dimethyloxalylglycine) that stabilized HIF in a similar manner as VHL inhibitors, have been shown to protect against bone loss in postmenopausal osteoporosis (100, 101). PHD enzyme inhibitor FG-4592 has been shown to improve bone formation in vitro studies and has promising results as treatment of osteolytic pathologies (102). New VHL inhibitors to stabilize HIF have been recently developed (VH032 and VH298) with high pharmacological importance of VHL blockade (103). But the implications of HIF stabilizing treatments on immune development remain unclear. None of these studies have focused on the cell extrinsic effects that altered bone has on hematopoiesis, which is key focus of my dissertation studies and Chicana et al. 2022 (104). **Our studies indicate that HIF stabilizing in bone cells, negatively alters B cell development, effects myelopoiesis and erythropoiesis, affecting patients' health.**

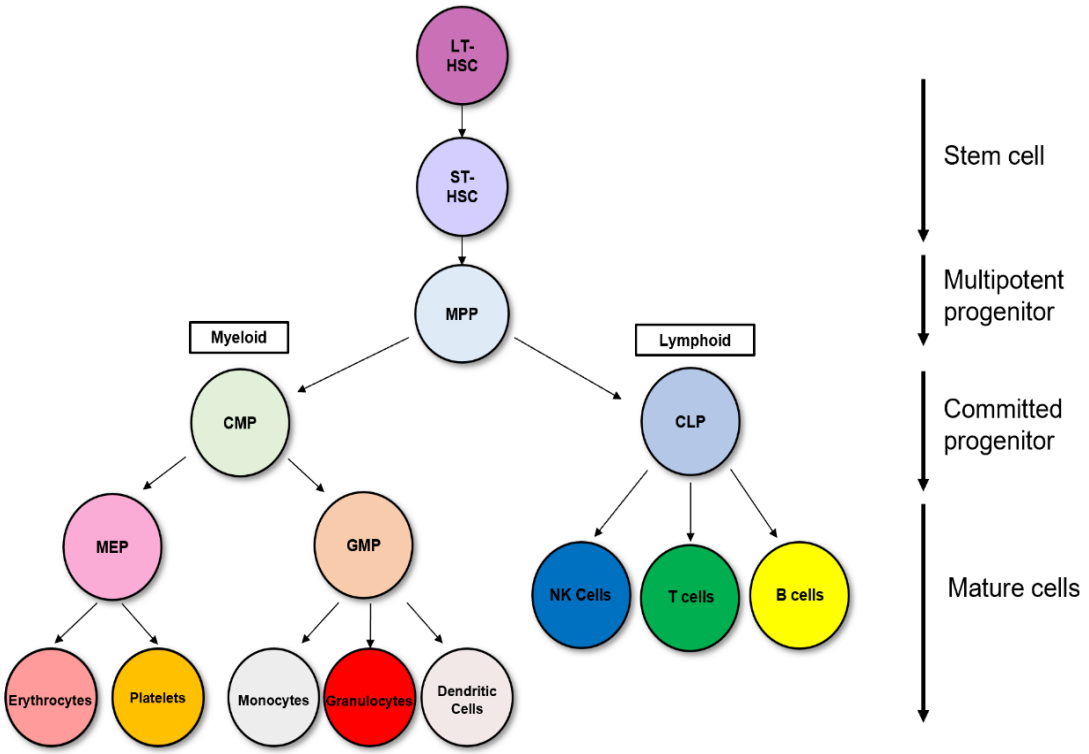


**Figure 1. Hematopoiesis Hierarchical Model.** Hematopoietic development starting from long-term hematopoietic stem cell (LT-HSC); Short term hematopoietic stem cell (ST-HSC); Multipotent progenitor (MPP); Common myeloid progenitor (CMP); Common lymphoid progenitor (CLP); Megakaryocyte erythroid progenitor (MEP); granulocyte monocyte progenitor (GMP); Erythrocytes; Platelets; Monocytes; Granulocytes; Dendritic cell (DC); NK cells; T cells; B cells.

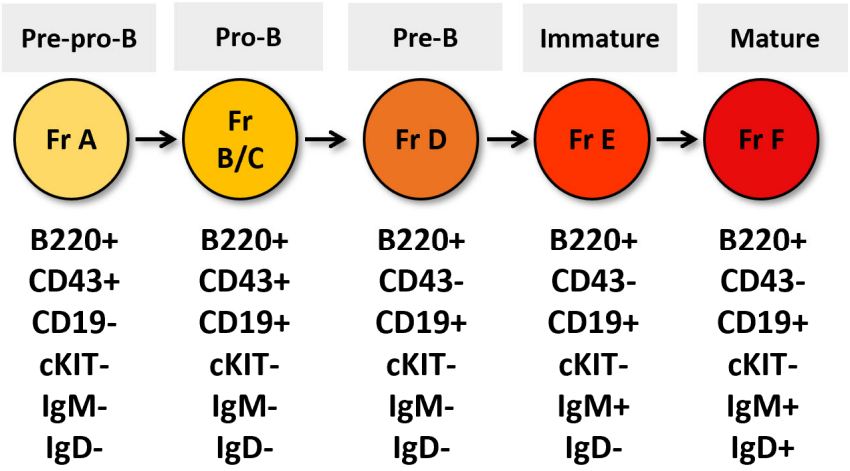


**Figure 2. Schematic of B cell development by Hardy Fractions.** Antigen markers used to identify and distinguish B cell development stages by flow cytometry.

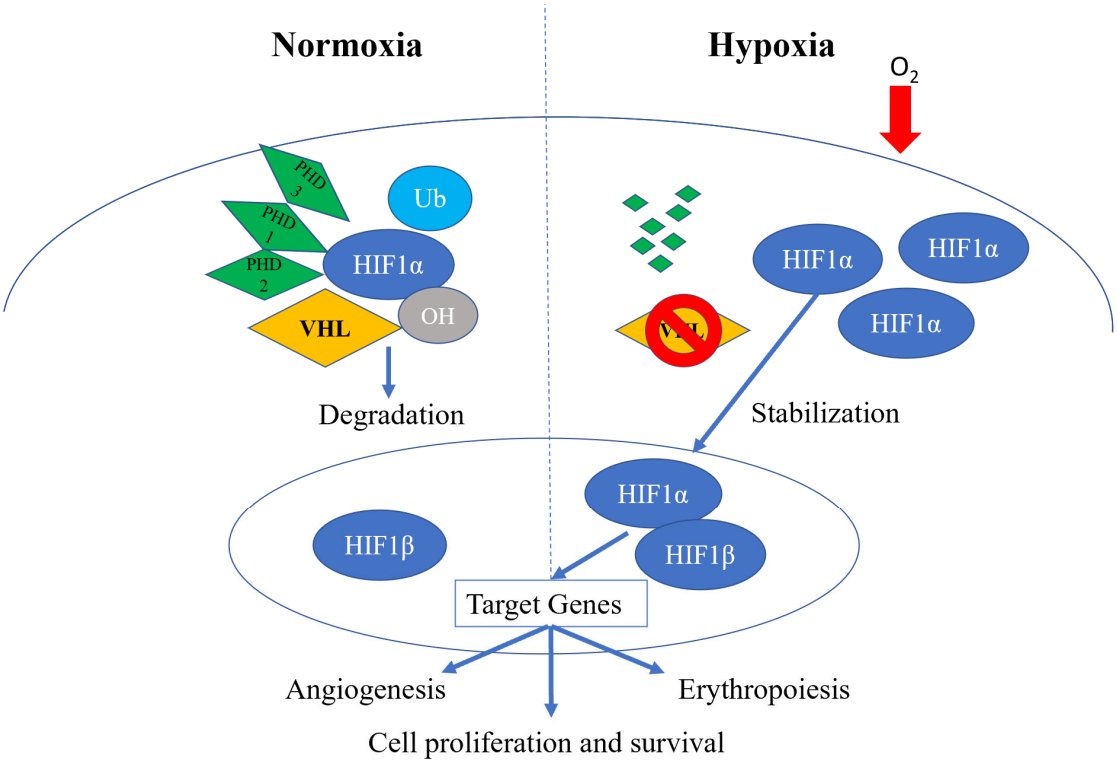


**Figure 3. VHL/HIF Pathway under normoxic and hypoxic conditions.** Left: under normoxic conditions, PHDs hydroxylate HIF1α, allowing VHL to add a ubiquitin tag for degradation; Right: under hypoxic conditions PHDs do not hydroxylate HIF1α and VHL does not bind, allowing HIF1α to accumulate in the cytoplasm and translocate to the nucleus to activate transcription of hypoxia induced genes. Similarly, in the absence of VHL, HIF1α accumulates and translocates to the nucleus in the same manner as it would under hypoxic conditions, therefore mimicking hypoxia in the cell.

**Table 1. *Vhl* Conditional Knock-Out studies targeting skeletal or hematopoietic lineages.** Conditional knock out studies of *Vhl* using the flox-Cre system.

| Target | Citation | Vhl target | Cre target | Target cell |
|---|---|---|---|---|
| Skeletal | Mangiavini et al. 2014 (94) | *Vhl* $^{fl/fl}$ | *Prx1-Cre* | Mesenchymal progenitors |
| | Wang et al. 2007 (83) | *Vhl* $^{fl/fl}$ | *OC-Cre* | Osteoblasts |
| | Wan et al. 2008 (74) | *Vhl* $^{fl/fl}$ | *OC-Cre* | Osteoblasts |
| | Zhang et al. 2014 (91) | *Vhl* $^{fl/fl}$ | *OC-Cre* | Osteoblasts |
| | Zuo et al. 2015 (82) | *Vhl* $^{fl/fl}$ | *OC-Cre* | Osteoblasts |
| | Kang et al. 2017 (90) | *Vhl* $^{fl/fl}$ | *OC-Cre* | Osteoblasts |
| | Weng et al. 2014 (85) | *Vhl* $^{fl/fl}$ | *Col2-CreER* $^{T2}$ | Osteochondral progenitors |
| | Rankin et al. 2012 (95) | *Vhl* $^{fl/fl}$ | *Osx-Cre* | Osteoprogenitors |
| | Dirckx et al. 2018 (96) | *Vhl* $^{fl/fl}$ | *Osx-Cre* | Osteoprogenitors |
| | Loots et al. 2018 (89) | *Vhl* $^{fl/fl}$ | *Dmp1-Cre* | Osteocytes, mature OBs, small subset of MSCs |
| | Chen et al. 2022 (97) | *Vhl* $^{fl/fl}$ | *Dmp1-Cre* | Osteocytes, mature OBs, small subset of MSCs |
| Hematopoietic | Takubo et al. 2007 (98) | *Vhl* $^{fl/fl}$ | *Mx1-Cre* | Hematopoietic Stem cells |
| | Cho et al. 2016 (92) | *Vhl* $^{fl/fl}$ | *ER* $^{T2}$*-Cre* | Mature B cells from spleens |
| | Xu et al. 2019 (93) | *Vhl* $^{fl/fl}$ | *CD19-Cre* | Mature B cells |
| | Burrows et al. 2020 (99) | *Vhl* $^{fl/fl}$ | *Mb1-Cre* | B cell progenitors |
| | Chicana et al. 2022 (104) | *Vhl* $^{fl/fl}$ | *Dmp1-Cre* | Osteocytes, mature OBs, small subset of MSCs |

**Table 2. Summary of findings from different *Vhl* conditional knock-out targets.** Osteoblasts (OBs), bone marrow stromal cells (BMSC) and osteocytes (OCYs).

| Target | Citation | BM B cell development | Peripheral B cell function | Glucose metabolism | Oxygen levels | Bone density | Bone marrow space | Niche cells | Vascularity |
|---|---|---|---|---|---|---|---|---|---|
| Skeletal | Mangiavini et al. 2014 (94) | - | - | - | - | ↑ | ↓ | - | ↑ |
| | Wang et al. 2007 (83) | - | - | Glut1 ↑ | - | ↑ | ↓ | ↑ OBs | ↑ |
| | Wan et al. 2008 (74) | - | - | - | PIM↑ | ↑ | ↓ | - | ↑ |
| | Zhang et al. 2014 (91) | - | - | - | - | ↑ | ↓ | ↑ OBs | ↑ |
| | Zuo et al. 2015 (82) | - | - | - | - | ↑ | ↓ | ↑ BMSCs | ↑ |
| | Kang et al. 2017 (90) | - | - | - | - | ↑ | ↓ | ↑ OBs | ↑ |
| | Weng et al. 2014 (85) | - | - | - | - | ↑ | ↓ | ↑ OBs | ↑ |
| | Rankin et al. 2012 (95) | - | - | - | - | ↑ | ↓ | ↑ OBs | ↑ |
| | Dirckx et al. 2018 (96) | - | - | ↑ | - | ↑ | ↓ | ↓ OBs ↑Osx | ↑ |
| | Loots et al. 2018 (89) | ↓ | - | - | - | ↑ | ↓ | ↑ OCYs | ↑ |
| | Chen et al. 2022 (97) | - | - | - | - | ↑ | ↓ | ↑ OBs | - |
| Hematopoietic | Takubo et al. 2007 (98) | ↓ | - | - | - | - | - | - | - |
| | Cho et al. 2016 (92) | - | ↓ | - | PIM↑ | - | - | - | - |
| | Xu et al. 2019 (93) | ↓ | - | ↑ | - | - | - | - | - |
| | Burrows et al. 2020 (99) | ↓ | ↓ | - | PIM↑ | - | - | - | - |
| | Chicana et al. 2022 (104) | ↓ | No Change (Chapter 2) | Glut1 ↑ (Chapter 3) | Age dependent PIM ↑ | ↑ | ↓ | Cytokines ↓ | ↑ |

## References


1. Galloway JL, Zon LI. Ontogeny of hematopoiesis: examining the emergence of hematopoietic cells in the vertebrate embryo. Curr Top Dev Biol (2003) 53:139-58. doi: 10.1016/s0070-2153(03)53004-6
2. Orkin SH, Zon LI. Hematopoiesis: an evolving paradigm for stem cell biology. Cell (2008) 132(4):631-44. doi: 10.1016/j.cell.2008.01.025
3. Palis J, Yoder MC. Yolk-sac hematopoiesis: the first blood cells of mouse and man. Exp Hematol (2001) 29(8):927-36. doi: 10.1016/s0301-472x(01)00669-5
4. Cumano A, Godin I. Ontogeny of the hematopoietic system. Annu Rev Immunol (2007) 25:745-85. doi: 10.1146/annurev.immunol.25.022106.141538
5. Yamamoto K, Miwa Y, Abe-Suzuki S, Abe S, Kirimura S, Onishi I, et al. Extramedullary hematopoiesis: Elucidating the function of the hematopoietic stem cell niche (Review). Mol Med Rep (2016) 13(1):587-91. doi: 10.3892/mmr.2015.4621
6. Henig I, Zuckerman T. Hematopoietic stem cell transplantation-50 years of evolution and future perspectives. Rambam Maimonides Med J (2014) 5(4):e0028. doi: 10.5041/RMMJ.10162
7. Yang L, Bryder D, Adolfsson J, Nygren J, Mansson R, Sigvardsson M, et al. Identification of Lin(-)Sca1(+)kit(+)CD34(+)Flt3- short-term hematopoietic stem cells capable of rapidly reconstituting and rescuing myeloablated transplant recipients. Blood (2005) 105(7):2717-23. doi: 10.1182/blood-2004-06-2159
8. Osawa M, Hanada K, Hamada H, Nakauchi H. Long-term lymphohematopoietic reconstitution by a single CD34-low/negative hematopoietic stem cell. Science (1996) 273(5272):242-5. doi: 10.1126/science.273.5272.242
9. Christensen JL, Weissman IL. Flk-2 is a marker in hematopoietic stem cell differentiation: a simple method to isolate long-term stem cells. Proc Natl Acad Sci U S A (2001) 98(25):14541-6. doi: 10.1073/pnas.261562798
10. Pietras EM, Reynaud D, Kang YA, Carlin D, Calero-Nieto FJ, Leavitt AD, et al. Functionally Distinct Subsets of Lineage-Biased Multipotent Progenitors Control Blood Production in Normal and Regenerative Conditions. Cell Stem Cell (2015) 17(1):35-46. doi: 10.1016/j.stem.2015.05.003
11. Kondo M, Wagers AJ, Manz MG, Prohaska SS, Scherer DC, Beilhack GF, et al. Biology of hematopoietic stem cells and progenitors: implications for clinical application. Annu Rev Immunol (2003) 21:759-806. doi: 10.1146/annurev.immunol.21.120601.141007
12. Kondo M. Lymphoid and myeloid lineage commitment in multipotent hematopoietic progenitors. Immunol Rev (2010) 238(1):37-46. doi: 10.1111/j.1600-065X.2010.00963.x
13. Karsunky H, Inlay MA, Serwold T, Bhattacharya D, Weissman IL. Flk2+ common lymphoid progenitors possess equivalent differentiation potential for the B and T lineages. Blood (2008) 111(12):5562-70. doi: 10.1182/blood-2007-11-126219
14. Kondo M, Weissman IL, Akashi K. Identification of clonogenic common lymphoid progenitors in mouse bone marrow. Cell (1997) 91(5):661-72. doi: 10.1016/s0092-8674(00)80453-5

15. Akashi K, Traver D, Miyamoto T, Weissman IL. A clonogenic common myeloid progenitor that gives rise to all myeloid lineages. Nature (2000) 404(6774):193-7. doi: 10.1038/35004599
16. Manz MG, Traver D, Miyamoto T, Weissman IL, Akashi K. Dendritic cell potentials of early lymphoid and myeloid progenitors. Blood (2001) 97(11):3333-41. doi: 10.1182/blood.v97.11.3333
17. Roodman GD. Advances in bone biology: the osteoclast. Endocr Rev (1996) 17(4):308-32. doi: 10.1210/edrv-17-4-308
18. Wei W, Zeve D, Wang X, Du Y, Tang W, Dechow PC, et al. Osteoclast progenitors reside in the peroxisome proliferator-activated receptor gamma-expressing bone marrow cell population. Mol Cell Biol (2011) 31(23):4692-705. doi: 10.1128/MCB.05979-11
19. Friedman AD. Transcriptional control of granulocyte and monocyte development. Oncogene (2007) 26(47):6816-28. doi: 10.1038/sj.onc.1210764
20. Zhang CC, Lodish HF. Cytokines regulating hematopoietic stem cell function. Curr Opin Hematol (2008) 15(4):307-11. doi: 10.1097/MOH.0b013e3283007db5
21. Robb L. Cytokine receptors and hematopoietic differentiation. Oncogene (2007) 26(47):6715-23. doi: 10.1038/sj.onc.1210756
22. Seita J, Weissman IL. Hematopoietic stem cell: self-renewal versus differentiation. Wiley Interdiscip Rev Syst Biol Med (2010) 2(6):640-53. doi: 10.1002/wsbm.86
23. Metcalf D. Hematopoietic cytokines. Blood (2008) 111(2):485-91. doi: 10.1182/blood-2007-03-079681
24. Zhu J, Emerson SG. Hematopoietic cytokines, transcription factors and lineage commitment. Oncogene (2002) 21(21):3295-313. doi: 10.1038/sj.onc.1205318
25. Zhang Y, Gao S, Xia J, Liu F. Hematopoietic Hierarchy - An Updated Roadmap. Trends Cell Biol (2018) 28(12):976-86. doi: 10.1016/j.tcb.2018.06.001
26. Yamamoto R, Wilkinson AC, Nakauchi H. Changing concepts in hematopoietic stem cells. Science (2018) 362(6417):895-6. doi: 10.1126/science.aat7873
27. Cheng H, Zheng Z, Cheng T. New paradigms on hematopoietic stem cell differentiation. Protein & Cell (2019) 11(1):34-44. doi: 10.1007/s13238-019-0633-0
28. Carsetti R. The development of B cells in the bone marrow is controlled by the balance between cell-autonomous mechanisms and signals from the microenvironment. J Exp Med (2000) 191(1):5-8. doi: 10.1084/jem.191.1.5
29. Hardy RR, Hayakawa K. B cell development pathways. Annu Rev Immunol (2001) 19:595-621. doi: 10.1146/annurev.immunol.19.1.595
30. Hardy RR, Kincade PW, Dorshkind K. The protean nature of cells in the B lymphocyte lineage. Immunity (2007) 26(6):703-14. doi: 10.1016/j.immuni.2007.05.013
31. Baumgarth N. A Hard(y) Look at B-1 Cell Development and Function. J Immunol (2017) 199(10):3387-94. doi: 10.4049/jimmunol.1700943
32. Owen JJ, Cooper MD, Raff MC. In vitro generation of B lymphocytes in mouse foetal liver, a mammalian 'bursa equivalent'. Nature (1974) 249(455):361-3. doi: 10.1038/249361a0
33. Baumgarth N. B-1 Cell Heterogeneity and the Regulation of Natural and Antigen-Induced IgM Production. Front Immunol (2016) 7:324. doi: 10.3389/fimmu.2016.00324
34. Montecino-Rodriguez E, Dorshkind K. B-1 B cell development in the fetus and adult. Immunity (2012) 36(1):13-21. doi: 10.1016/j.immuni.2011.11.017

35. Montecino-Rodriguez E, Leathers H, Dorshkind K. Identification of a B-1 B cell-specified progenitor. Nat Immunol (2006) 7(3):293-301. doi: 10.1038/ni1301
36. Esplin BL, Welner RS, Zhang Q, Borghesi LA, Kincade PW. A differentiation pathway for B1 cells in adult bone marrow. Proc Natl Acad Sci U S A (2009) 106(14):5773-8. doi: 10.1073/pnas.0811632106
37. Montecino-Rodriguez E, Fice M, Casero D, Berent-Maoz B, Barber CL, Dorshkind K. Distinct Genetic Networks Orchestrate the Emergence of Specific Waves of Fetal and Adult B-1 and B-2 Development. Immunity (2016) 45(3):527-39. doi: 10.1016/j.immuni.2016.07.012
38. Choi YS, Dieter JA, Rothaeusler K, Luo Z, Baumgarth N. B-1 cells in the bone marrow are a significant source of natural IgM. Eur J Immunol (2012) 42(1):120-9. doi: 10.1002/eji.201141890
39. Baumgarth N, Herman OC, Jager GC, Brown LE, Herzenberg LA, Chen J. B-1 and B-2 cell-derived immunoglobulin M antibodies are nonredundant components of the protective response to influenza virus infection. J Exp Med (2000) 192(2):271-80. doi: 10.1084/jem.192.2.271
40. Haas KM, Poe JC, Steeber DA, Tedder TF. B-1a and B-1b cells exhibit distinct developmental requirements and have unique functional roles in innate and adaptive immunity to S. pneumoniae. Immunity (2005) 23(1):7-18. doi: 10.1016/j.immuni.2005.04.011
41. De Silva NS, Klein U. Dynamics of B cells in germinal centres. Nat Rev Immunol (2015) 15(3):137-48. doi: 10.1038/nri3804
42. Hardy RR, Carmack CE, Shinton SA, Kemp JD, Hayakawa K. Resolution and characterization of pro-B and pre-pro-B cell stages in normal mouse bone marrow. J Exp Med (1991) 173(5):1213-25. doi: 10.1084/jem.173.5.1213
43. Allman DM, Ferguson SE, Lentz VM, Cancro MP. Peripheral B cell maturation. II. Heat-stable antigen(hi) splenic B cells are an immature developmental intermediate in the production of long-lived marrow-derived B cells. J Immunol (1993) 151(9):4431-44.
44. Nemazee DA, Burki K. Clonal deletion of B lymphocytes in a transgenic mouse bearing anti-MHC class I antibody genes. Nature (1989) 337(6207):562-6. doi: 10.1038/337562a0
45. Gay D, Saunders T, Camper S, Weigert M. Receptor editing: an approach by autoreactive B cells to escape tolerance. J Exp Med (1993) 177(4):999-1008. doi: 10.1084/jem.177.4.999
46. Tiegs SL, Russell DM, Nemazee D. Receptor editing in self-reactive bone marrow B cells. J Exp Med (1993) 177(4):1009-20. doi: 10.1084/jem.177.4.1009
47. Melamed D, Benschop RJ, Cambier JC, Nemazee D. Developmental regulation of B lymphocyte immune tolerance compartmentalizes clonal selection from receptor selection. Cell (1998) 92(2):173-82. doi: 10.1016/s0092-8674(00)80912-5
48. Cain CJ, Rueda R, McLelland B, Collette NM, Loots GG, Manilay JO. Absence of sclerostin adversely affects B-cell survival. J Bone Miner Res (2012) 27(7):1451-61. doi: 10.1002/jbmr.1608
49. Manilay JO, Zouali M. Tight relationships between B lymphocytes and the skeletal system. Trends Mol Med (2014) 20(7):405-12. doi: 10.1016/j.molmed.2014.03.003

50. Panaroni C, Wu JY. Interactions between B lymphocytes and the osteoblast lineage in bone marrow. Calcif Tissue Int (2013) 93(3):261-8. doi: 10.1007/s00223-013-9753-3
51. Nagasawa T. Microenvironmental niches in the bone marrow required for B-cell development. Nat Rev Immunol (2006) 6(2):107-16. doi: 10.1038/nri1780
52. Schofield R. The relationship between the spleen colony-forming cell and the haemopoietic stem cell Blood Cells (1978) (4(1-2)):7-25.
53. Kopp HG, Avecilla ST, Hooper AT, Rafii S. The bone marrow vascular niche: home of HSC differentiation and mobilization. Physiology (Bethesda) (2005) 20:349-56. doi: 10.1152/physiol.00025.2005
54. Komsany A, Pezzella F. Chapter 7 - The perivascular niche. Tumor Vascularization (2020):113-27. doi: https://doi.org/10.1016/B978-0-12-819494-2.00007-9
55. Itkin T, Gur-Cohen S, Spencer JA, Schajnovitz A, Ramasamy SK, Kusumbe AP, et al. Distinct bone marrow blood vessels differentially regulate haematopoiesis. Nature (2016) 532(7599):323-8. doi: 10.1038/nature17624
56. Greenbaum A, Hsu YM, Day RB, Schuettpelz LG, Christopher MJ, Borgerding JN, et al. CXCL12 in early mesenchymal progenitors is required for haematopoietic stem-cell maintenance. Nature (2013) 495(7440):227-30. doi: 10.1038/nature11926
57. Ding L, Saunders TL, Enikolopov G, Morrison SJ. Endothelial and perivascular cells maintain haematopoietic stem cells. Nature (2012) 481(7382):457-62. doi: 10.1038/nature10783
58. Trinh T, Broxmeyer HE. Role for Leptin and Leptin Receptors in Stem Cells During Health and Diseases. Stem Cell Rev Rep (2021) 17(2):511-22. doi: 10.1007/s12015-021-10132-y
59. Wilson A, Trumpp A. Bone-marrow haematopoietic-stem-cell niches. Nat Rev Immunol (2006) 6(2):93-106. doi: 10.1038/nri1779
60. Nilsson SK, Johnston HM, Coverdale JA. Spatial localization of transplanted hemopoietic stem cells: inferences for the localization of stem cell niches. Blood (2001) 97(8):2293-9. doi: 10.1182/blood.v97.8.2293
61. Lambertsen RH, Weiss L. A model of intramedullary hematopoietic microenvironments based on stereologic study of the distribution of endocloned marrow colonies. Blood (1984) 63(2):287-97.
62. Gong JK. Endosteal marrow: a rich source of hematopoietic stem cells. Science (1978) 199(4336):1443-5. doi: 10.1126/science.75570
63. Kiel MJ, Yilmaz OH, Iwashita T, Yilmaz OH, Terhorst C, Morrison SJ. SLAM family receptors distinguish hematopoietic stem and progenitor cells and reveal endothelial niches for stem cells. Cell (2005) 121(7):1109-21. doi: 10.1016/j.cell.2005.05.026
64. Morrison SJ, Scadden DT. The bone marrow niche for haematopoietic stem cells. Nature (2014) 505(7483):327-34. doi: 10.1038/nature12984
65. Ding L, Morrison SJ. Haematopoietic stem cells and early lymphoid progenitors occupy distinct bone marrow niches. Nature (2013) 495(7440):231-5. doi: 10.1038/nature11885
66. Cordeiro Gomes A, Hara T, Lim VY, Herndler-Brandstetter D, Nevius E, Sugiyama T, et al. Hematopoietic Stem Cell Niches Produce Lineage-Instructive Signals to Control Multipotent Progenitor Differentiation. Immunity (2016) 45(6):1219-31. doi: 10.1016/j.immuni.2016.11.004

67. Acar M, Kocherlakota KS, Murphy MM, Peyer JG, Oguro H, Inra CN, et al. Deep imaging of bone marrow shows non-dividing stem cells are mainly perisinusoidal. Nature (2015) 526(7571):126-30. doi: 10.1038/nature15250
68. Levesque JP, Helwani FM, Winkler IG. The endosteal 'osteoblastic' niche and its role in hematopoietic stem cell homing and mobilization. Leukemia (2010) 24(12):1979-92. doi: 10.1038/leu.2010.214
69. Green AC, Tjin G, Lee SC, Chalk AM, Straszkowski L, Kwang D, et al. The characterization of distinct populations of murine skeletal cells that have different roles in B lymphopoiesis. Blood (2021) 138(4):304-17. doi: 10.1182/blood.2020005865
70. Fistonich C, Zehentmeier S, Bednarski JJ, Miao R, Schjerven H, Sleckman BP, et al. Cell circuits between B cell progenitors and IL-7(+) mesenchymal progenitor cells control B cell development. J Exp Med (2018) 215(10):2586-99. doi: 10.1084/jem.20180778
71. Zehentmeier S, Pereira JP. Cell circuits and niches controlling B cell development. Immunol Rev (2019) 289(1):142-57. doi: 10.1111/imr.12749
72. Egawa T, Kawabata K, Kawamoto H, Amada K, Okamoto R, Fujii N, et al. The earliest stages of B cell development require a chemokine stromal cell-derived factor/pre-B cell growth-stimulating factor. Immunity (2001) 15(2):323-34. doi: 10.1016/s1074-7613(01)00185-6
73. Spencer JA, Ferraro F, Roussakis E, Klein A, Wu J, Runnels JM, et al. Direct measurement of local oxygen concentration in the bone marrow of live animals. Nature (2014) 508(7495):269-73. doi: 10.1038/nature13034
74. Wan C, Gilbert SR, Wang Y, Cao X, Shen X, Ramaswamy G, et al. Activation of the hypoxia-inducible factor-1alpha pathway accelerates bone regeneration. Proc Natl Acad Sci U S A (2008) 105(2):686-91. doi: 10.1073/pnas.0708474105
75. Hirao M, Hashimoto J, Yamasaki N, Ando W, Tsuboi H, Myoui A, et al. Oxygen tension is an important mediator of the transformation of osteoblasts to osteocytes. Journal of bone and mineral metabolism (2007) 25(5):266-76. doi: 10.1007/s00774-007-0765-9
76. Knowles HJ. Hypoxic regulation of osteoclast differentiation and bone resorption activity. Hypoxia (Auckland, NZ) (2015) 3:73-82. doi: 10.2147/hp.S95960
77. Komatsu DE, Hadjiargyrou M. Activation of the transcription factor HIF-1 and its target genes, VEGF, HO-1, iNOS, during fracture repair. Bone (2004) 34(4):680-8. doi: 10.1016/j.bone.2003.12.024
78. Danis A. [Mechanism of bone lengthening by the Ilizarov technique]. Bulletin et memoires de l'Academie royale de medecine de Belgique (2001) 156(1-2):107-12.
79. Zhao Q, Shen X, Zhang W, Zhu G, Qi J, Deng L. Mice with increased angiogenesis and osteogenesis due to conditional activation of HIF pathway in osteoblasts are protected from ovariectomy induced bone loss. Bone (2012) 50(3):763-70. doi: 10.1016/j.bone.2011.12.003
80. Tando T, Sato Y, Miyamoto K, Morita M, Kobayashi T, Funayama A, et al. Hif1alpha is required for osteoclast activation and bone loss in male osteoporosis. Biochemical and biophysical research communications (2016) 470(2):391-6. doi: 10.1016/j.bbrc.2016.01.033
81. Miyauchi Y, Sato Y, Kobayashi T, Yoshida S, Mori T, Kanagawa H, et al. HIF1alpha is required for osteoclast activation by estrogen deficiency in postmenopausal

osteoporosis. Proceedings of the National Academy of Sciences of the United States of America (2013) 110(41):16568-73. doi: 10.1073/pnas.1308755110
82. Zuo GL, Zhang LF, Qi J, Kang H, Jia P, Chen H, et al. Activation of HIFa pathway in mature osteoblasts disrupts the integrity of the osteocyte/canalicular network. PLoS One (2015) 10(3):e0121266. doi: 10.1371/journal.pone.0121266
83. Wang Y, Wan C, Deng L, Liu X, Cao X, Gilbert SR, et al. The hypoxia-inducible factor alpha pathway couples angiogenesis to osteogenesis during skeletal development. The Journal of clinical investigation (2007) 117(6):1616-26. doi: 10.1172/jci31581
84. Chicana B, Donham C, Millan AJ, Manilay JO. Wnt Antagonists in Hematopoietic and Immune Cell Fate: Implications for Osteoporosis Therapies. Curr Osteoporos Rep (2019) 17(2):49-58. doi: 10.1007/s11914-019-00503-3
85. Weng T, Xie Y, Huang J, Luo F, Yi L, He Q, et al. Inactivation of Vhl in osteochondral progenitor cells causes high bone mass phenotype and protects against age-related bone loss in adult mice. Journal of bone and mineral research : the official journal of the American Society for Bone and Mineral Research (2014) 29(4):820-9. doi: 10.1002/jbmr.2087
86. Riddle RC, Leslie JM, Gross TS, Clemens TL. Hypoxia-inducible factor-1alpha protein negatively regulates load-induced bone formation. J Biol Chem (2011) 286(52):44449-56. doi: 10.1074/jbc.M111.276683
87. Haase VH. The VHL tumor suppressor: master regulator of HIF. Current pharmaceutical design (2009) 15(33):3895-903.
88. Bader HL, Hsu T. Systemic VHL gene functions and the VHL disease. FEBS letters (2012) 586(11):1562-9. doi: 10.1016/j.febslet.2012.04.032
89. Loots GG, Robling AG, Chang JC, Murugesh DK, Bajwa J, Carlisle C, et al. Vhl deficiency in osteocytes produces high bone mass and hematopoietic defects. Bone (2018) 116:307-14. doi: 10.1016/j.bone.2018.08.022
90. Kang H, Yang K, Xiao L, Guo L, Guo C, Yan Y, et al. Osteoblast Hypoxia-Inducible Factor-1alpha Pathway Activation Restrains Osteoclastogenesis via the Interleukin-33-MicroRNA-34a-Notch1 Pathway. Front Immunol (2017) 8:1312. doi: 10.3389/fimmu.2017.01312
91. Zhang LF, Qi J, Zuo G, Jia P, Shen X, Shao J, et al. Osteoblast-secreted factors promote proliferation and osteogenic differentiation of bone marrow stromal cells via VEGF/heme-oxygenase-1 pathway. PLoS One (2014) 9(6):e99946. doi: 10.1371/journal.pone.0099946
92. Cho SH, Raybuck AL, Stengel K, Wei M, Beck TC, Volanakis E, et al. Germinal centre hypoxia and regulation of antibody qualities by a hypoxia response system. Nature (2016) 537(7619):234-8. doi: 10.1038/nature19334
93. Xu S, Huo J, Huang Y, Aw M, Chen S, Mak S, et al. von Hippel-Lindau Protein Maintains Metabolic Balance to Regulate the Survival of Naive B Lymphocytes. iScience (2019) 17:379-92. doi: 10.1016/j.isci.2019.07.002
94. Mangiavini L, Merceron C, Araldi E, Khatri R, Gerard-O'Riley R, Wilson TL, et al. Loss of VHL in mesenchymal progenitors of the limb bud alters multiple steps of endochondral bone development. Dev Biol (2014) 393(1):124-36. doi: 10.1016/j.ydbio.2014.06.013

95. Rankin EB, Wu C, Khatri R, Wilson TL, Andersen R, Araldi E, et al. The HIF signaling pathway in osteoblasts directly modulates erythropoiesis through the production of EPO. Cell (2012) 149(1):63-74. doi: 10.1016/j.cell.2012.01.051
96. Dirckx N, Tower RJ, Mercken EM, Vangoitsenhoven R, Moreau-Triby C, Breugelmans T, et al. Vhl deletion in osteoblasts boosts cellular glycolysis and improves global glucose metabolism. J Clin Invest (2018) 128(3):1087-105. doi: 10.1172/JCI97794
97. Chen K, Zhao J, Qiu M, Zhang L, Yang K, Chang L, et al. Osteocytic HIF-1alpha Pathway Manipulates Bone Micro-structure and Remodeling via Regulating Osteocyte Terminal Differentiation. Front Cell Dev Biol (2022) 9:721561. doi: 10.3389/fcell.2021.721561
98. Takubo K, Goda N, Yamada W, Iriuchishima H, Ikeda E, Kubota Y, et al. Regulation of the HIF-1alpha level is essential for hematopoietic stem cells. Cell Stem Cell (2010) 7(3):391-402. doi: 10.1016/j.stem.2010.06.020
99. Burrows N, Bashford-Rogers RJM, Bhute VJ, Penalver A, Ferdinand JR, Stewart BJ, et al. Dynamic regulation of hypoxia-inducible factor-1alpha activity is essential for normal B cell development. Nat Immunol (2020) 21(11):1408-20. doi: 10.1038/s41590-020-0772-8
100. Liu X, Tu Y, Zhang L, Qi J, Ma T, Deng L. Prolyl hydroxylase inhibitors protect from the bone loss in ovariectomy rats by increasing bone vascularity. Cell Biochem Biophys (2014) 69(1):141-9. doi: 10.1007/s12013-013-9780-8
101. Fan L, Li J, Yu Z, Dang X, Wang K. The hypoxia-inducible factor pathway, prolyl hydroxylase domain protein inhibitors, and their roles in bone repair and regeneration. Biomed Res Int (2014) 2014:239356. doi: 10.1155/2014/239356
102. Hulley PA, Papadimitriou-Olivgeri I, Knowles HJ. Osteoblast-Osteoclast Coculture Amplifies Inhibitory Effects of FG-4592 on Human Osteoclastogenesis and Reduces Bone Resorption. JBMR Plus (2020) 4(7):e10370. doi: 10.1002/jbm4.10370
103. Frost J, Rocha S, Ciulli A. Von Hippel-Lindau (VHL) small-molecule inhibitor binding increases stability and intracellular levels of VHL protein. J Biol Chem (2021) 297(2):100910. doi: 10.1016/j.jbc.2021.100910
104. Chicana B, Abbasizadeh N, Burns C, Taglinao H, Spencer JA, Manilay JO. Deletion of Vhl in Dmp1-expressing cells causes microenvironmental impairment of B cell lymphopoiesis. bioRxiv (2022). doi: 10.1101/2021.09.10.459794

CHAPTER 2

# Deletion of *Vhl* in Dmp1-expressing cells causes microenvironmental impairment of B cell lymphopoiesis

Publication in Frontiers in Immunology

Citation: **Chicana B,** Abbasizadeh N, Burns C, Taglinao H, Spencer JA, Manilay JO. Deletion of *Vhl* in Dmp1-expressing cells causes microenvironmental impairment of B cell lymphopoiesis. Frontiers in Immunology 2022 Feb 16. doi: 10.3389/fimmu.2022.780945**.** URL= https://www.frontiersin.org/article/10.3389/fimmu.2022.780945

## Brief Summary

In this chapter we explore how changes in bone homeostasis can impact immune development and we elaborate on possible mechanisms in which the BM microenvironment of *VhlcKO* mice does not support normal B cell development.

Published (Chicana et al. 2022) findings:

- The *Vhl*cKO bone marrow displays a block early in B cell development starting at Fractions B-C (pro-B) as early as 6-weeks-old
- Upstream hematopoietic progenitors such as LSKs (LT-HSCs, ST-HSCs, MPP2, MPP3, MPP4, CLPs) were increased in frequency in the bone marrow of *Vhl*cKO
- Fraction B-C (pro-B) show increased apoptosis and decreased cell proliferation in the bone marrow starting at 10-weeks-old
- CXCL12, a B cell supporting cytokine, is reduced in BM fluid and PB serum of *Vhl*cKO mice compared to controls
- Vascular density, volume and leakiness was increased in *Vhl*cKO mice and more severe at 6-months-old
- *Vhl*cKO LSKs and B cells display an age dependent PIM+ expression, suggesting a cellular response to hypoxia as the mice age

Unpublished findings:

- 3-week-old *Vhl*cKO mice display no defects in B cell development, proliferation, or apoptosis in the BM
- *Vhl*cKO mice at 10–14-week-old can produce antigen-specific antibodies and germinal centers, regardless of the developmental defects ongoing in the bone marrow
- We found that *Vhl*cKO spleens have increased LT-HSCs, ST-HSCs, MPP2, MPP3 and MPP4 in frequency and numbers at 10 weeks and 6-month-old mice (extramedullary hematopoiesis)
- No change of B1a cells in bone marrow and peritoneal cavity were observed, but there was a decrease in spleens; B1b cells remained unchanged in bone marrow, spleens and peritoneal cavity of *Vhl*cKO mice
- B cell development in the calvarial bone marrow and long bone (femurs and tibia) BM are similar in control and *Vhl*cKO mice
- Serial bone digests help to isolate bone cells from dense bones of *Vhl*cKO mice.

frontiers in Immunology

ORIGINAL RESEARCH
published: 16 February 2022
doi: 10.3389/fimmu.2022.780945

# Deletion of *Vhl* in *Dmp1*-Expressing Cells Causes Microenvironmental Impairment of B Cell Lymphopoiesis

*Betsabel Chicana[1,2], Nastaran Abbasizadeh[2,3], Christian Burns[2,3], Hanna Taglinao[1], Joel A. Spencer[2,3,4*†] and Jennifer O. Manilay[1,2*†]*

[1] Department of Molecular and Cell Biology, School of Natural Sciences, University of California, Merced, Merced, CA, United States, [2] Quantitative and Systems Biology Graduate Program, University of California, Merced, Merced, CA, United States, [3] Department of Bioengineering, School of Engineering, University of California, Merced, Merced, CA, United States, [4] Bioengineering Graduate Program, University of California, Merced, Merced, CA, United States

OPEN ACCESS

**Edited by:**
Rachel Maurie Gerstein, University of Massachusetts Medical School, United States

**Reviewed by:**
Encarnacion Montecino-Rodriguez, University of California, Los Angeles, United States
Dan Link, Washington University in St. Louis, United States

***Correspondence:**
Joel A. Spencer
joel.spencer@ucmerced.edu
Jennifer O. Manilay
jmanilay@ucmerced.edu

[†] These authors share senior authorship

**Specialty section:**
This article was submitted to B Cell Biology, a section of the journal Frontiers in Immunology

**Received:** 22 September 2021
**Accepted:** 11 January 2022
**Published:** 16 February 2022

**Citation:**
Chicana B, Abbasizadeh N, Burns C, Taglinao H, Spencer JA and Manilay JO (2022) Deletion of Vhl in Dmp1-Expressing Cells Causes Microenvironmental Impairment of B Cell Lymphopoiesis. Front. Immunol. 13:780945. doi: 10.3389/fimmu.2022.780945

The contributions of skeletal cells to the processes of B cell development in the bone marrow (BM) have not been completely described. The von-Hippel Lindau protein (VHL) plays a key role in cellular responses to hypoxia. Previous work showed that *Dmp1*-Cre; *Vhl* conditional knockout mice (*Vhl*cKO), which deletes *Vhl* in subsets of mesenchymal stem cells, late osteoblasts and osteocytes, display dysregulated bone growth and reduction in B cells. Here, we investigated the mechanisms underlying the B cell defects using flow cytometry and high-resolution imaging. In the *Vhl*cKO BM, B cell progenitors were increased in frequency and number, whereas Hardy Fractions B-F were decreased. *Vhl*cKO Fractions B-C cells showed increased apoptosis and quiescence. Reciprocal BM chimeras confirmed a B cell-extrinsic source of the *Vhl*cKO B cell defects. In support of this, *Vhl*cKO BM supernatant contained reduced CXCL12 and elevated EPO levels. Intravital and *ex vivo* imaging revealed *Vhl*cKO BM blood vessels with increased diameter, volume, and a diminished blood-BM barrier. Staining of *Vhl*cKO B cells with an intracellular hypoxic marker indicated the natural existence of distinct B cell microenvironments that differ in local oxygen tensions and that the B cell developmental defects in *Vhl*cKO BM are not initiated by hypoxia. Our studies identify novel mechanisms linking altered bone homeostasis with drastic BM microenvironmental changes that dysregulate B cell development.

**Keywords: B lymphocytes, osteoimmunology, hypoxia, microenvironment, bone marrow niches**

## INTRODUCTION

The mechanisms by which changes in bone homeostasis affect immune development in the bone marrow (BM) are not fully understood (1–4). A detailed understanding of how bone microenvironments affect immune cell development and function could provide strategies towards novel therapeutic approaches to immune deficiencies. B cells produce antibodies (Abs), which are crucial for a robust adaptive immune response. B cells are generated from hematopoietic stem cells (HSCs) in the liver during fetal life, and in the BM in the adult (5). B cell development in the BM occurs in a series of defined stages that rely on growth factors that are produced by several

non-hematopoietic stromal cells, including mesenchymal stem cells (MSCs) and osteoblasts (OBs) (1).

The von-Hippel Lindau protein (VHL) regulates hypoxia-inducible factor (HIF) degradation, which is involved in cellular adaptation to low oxygen environments (6). When HIF1α accumulates in normoxic conditions, it travels to the nucleus to activate over 100 hypoxia-inducible target genes (7). VHL is expressed ubiquitously in many cell types, and global deletion of the *Vhl* gene results in embryonic lethality, so conditional knockout approaches are necessary to investigate the cell-specific roles of VHL in specific microenvironments. Conditional deletion of *Vhl* in OBs and in hematopoietic progenitors have demonstrated a role for VHL in these cell types (8, 9). The role of HIF and its regulation on the immune system has been extensively reviewed (10), but the mechanisms by which cell-intrinsic and cell-extrinsic VHL regulate specific immune cell lineages has not fully been addressed.

The BM microenvironment manifests hypoxic heterogeneities in a spatio-temporal manner (11–13), however the implications of these oxygen tension ($pO_2$) differences on hematopoiesis are not well characterized. Hypoxia slows the processes of angiogenesis and osteogenesis during fracture healing and bone formation, but also promotes OB differentiation into OCYs (14), and can stimulate osteoclast formation (15). Studies have shown HIF stabilization as a therapeutic option for treating bone fractures (16, 17) and osteoporosis (18–20), but the underlying molecular mechanism remains poorly understood. *Vhl* plays an important role regulating HIF expression, and disruption of *Vhl* in bone cells leads to improper bone homeostasis (7, 8, 21, 22). *Vhl* depletion in osteochondral progenitor cells and osteocalcin-positive OBs leads to an increase in bone mass through an increase in OB number (7, 22). Furthermore, disrupting VHL in OBs induces expression of β-catenin, revealing the mechanism by which VHL/HIF pathway promotes bone formation through the Wnt pathway (7, 23, 24). Altogether, these studies of *Vhl* deletion in osteolineage cells have not examined the cell-extrinsic effects of these changes on the immune cells residing in the BM.

The BM contains specialized microenvironments that maintain blood cells and supply factors required for their development and maintenance. Perivascular stromal cells, osteoprogenitor cells, endothelial cells (ECs), MSCs, OBs and OCYs are critical B cell "niches" and are all cells that support B cell development (1, 4, 25, 26), in part through production of cytokines. Essential cytokines for B cell development include CXC-chemokine ligand 12 (CXCL12) (27–29), FLT3 ligand (FLT3L) (30), IL-7 (30–33), stem-cell factor (SCF) (31, 32) and receptor activator of nuclear factor-κB ligand (RANKL) (34). The BM contains a dense vascular network and vascular sinuses creating the perivascular region, which provides a niche where B cells are known to develop and reside (35). A model of B cell developmental niches based on CXCL12 and IL7 levels has been proposed (4) in which B cells start at the pre-pro-B cell (Fraction A) stage where they are located in the perisinusoidal niche, especially near CXCL12+ reticular cells. As B cells continue to mature to the pro-B cell stage (Fractions B-C), they also interact with IL-7 expressing cells, and then pre-B cells migrate away from the sinusoids toward galectin-1+ stromal cells that do not express IL7 (36). This model has been updated given recent reports of the four new MSC subsets, their ability to support B lymphopoiesis, and their locations within the BM (37). During aging, vascular density decreases in many tissues due to impaired angiogenesis caused by EC dysfunction (38, 39). Vascular "hyperpermeability" also increases with age, via changes in ECs lining the blood vessel wall, disrupting the blood-BM barrier (40–42). The role of the vasculature and regulation of vessel permeability in hematopoiesis, especially in B cell development, remains unknown.

To understand how changes in bone homeostasis may affect immune cell development, we previously utilized *Dmp1*-Cre;*Vhl* conditional knockout mice (*Vhl*cKO), in which *Vhl* is deleted primarily in OCYs, but also in some MSC subsets and late OBs (43). In the *Vhl*cKO bones, the number of hematopoietic cells is severely reduced, and B cell development is stunted (21). Here, we provide evidence for molecular, cellular and structural changes in the *Vhl*cKO BM niche that adversely affect B cell development in a cell-extrinsic manner, such as decreased production of B cell supporting cytokines and structural changes in the BM vasculature. We also observed an age-dependent change in hypoxia that could further contribute to the B cell defects. These studies reveal novel molecular mechanisms by which *Vhl* deletion in *Dmp1*-expressing cells affect B cell niches.

## MATERIALS AND METHODS

### Study Design

A G*Power statistical (44) power analysis (α=0.05 and power of 0.95) based on B cell developmental data and BM cellularity determined that a minimum of n=7 mice per group was needed for our studies. The total sample size for each experiment was >7 performed in three independent experiments. Age-matched mice of both sexes were used. *Vhl*cKO and control mice (C57BL/6 wild type and *Vhl*-floxed ($Vhl^{fl/fl}$, *Dmp1-Cre*-negative mice) were used and no sex-specific differences in B cell development or other relevant characteristics to our studies were detected. Student's t-test and nonparametric Bonferroni-corrected Mann-Whitney U-test was used to test differences between mean and median values with Graph-Pad Prism and were considered significant if $p<0.05$. Outlier analysis was also performed with Graph-Pad Prism and any outliers identified were not included in the data graphs.

### Experimental Animals

Mice on the C57Bl/6 background were used. Stock #023047 B6N.FVB-Tg1Jqfe/BwdJ (*Dmp1*-Cre) (45) and Stock #012933 B6.129S4(C)-Vhl tm1Jae/J ($Vhl^{fl/fl}$) (46) were purchased from The Jackson Laboratory. These two lines of mice were crossed to generate *Vhl* conditional knockouts in *Dmp1*-expressing cells (*Vhl*cKO). Genotyping was confirmed following protocols from the Jackson Laboratory. Stock #002014 B6.SJL-Ptprca Pepcb/BoyJ mice were used for reciprocal bone marrow transplantation

studies. Mice were housed under specific pathogen-free conditions in the University of California, Merced's vivarium with autoclaved feed and water, and sterile microisolator cages. The University of California Merced Institutional Animal Care and Use Committee approved all animal work.

## Bone Marrow Transplantation

Recipient mice were 10 weeks of age at the time of transplantation. Whole bone marrow B6.SJL (CD45.1+) donor cells ($1x10^6$) were injected retro-orbitally into lethally irradiated (1000 rads using a Cesium-137 source, JL Shepherd and Associates, San Fernando, CA, USA) recipient CD45.2+ *Vhl*cKO mice or control (Cre-negative; $Vhl^{fl/fl}$) littermates under isoflurane anesthesia. Reciprocal *Vhl*cKO→WT (B6.SJL, CD45.1+) chimeras were also prepared. Animals were supplemented with neomycin in the drinking water for 14 days post-transplant as described (47).

## Sample Collection: Bone Marrow, Peripheral Blood, Spleen and Serum

### Bone Marrow Collection

Mice were euthanized by the inhalation of carbon dioxide followed by cervical dislocation. Femurs and tibias were dissected, and muscles were removed. To release the BM, bones were crushed with a mortar and pestle in M199+ (M199 with 2% FBS). BM cells were collected into 15mL conical tubes after being rinsed away from bone chips with M199+, resuspended by trituration, filtered through 70-micron nylon mesh into a 50 mL conical tube, and centrifuged for 5 mins at 1500 rpm and at 4°C. Cell pellets were resuspended and treated with ACK lysis buffer to remove erythrocytes. Cells treated with ACK were washed and resuspended in M199+. Cell counts were obtained using a hemocytometer and Trypan Blue staining to exclude dead cells.

To collect BM supernatant, femurs were cleaned of any muscle tissue and the epiphyses were cut off and discarded. The bone shaft was then placed into a 0.2 mL tube in which a hole was introduced using a needle. Thirty µL of 1x phosphate buffered saline (PBS) was placed on the top end of the bone shaft, using a 25g needle, and then the tube containing the bone was placed into a 1.5 ml microcentrifuge tube and centrifuged for 30 seconds at 15,000rpm. The BM supernatant was collected and stored at -80C until analysis.

### Peripheral Blood Collection

Mice were heated under a heat lamp to increase blood circulation and then restrained. Blood collection was performed via tail bleeds by making an incision with a scalpel blade over the ventral tail vein. No more than ten drops were collected (<0.5 mL) in a 1.5 ml Eppendorf tube with 50 uL of heparin. To obtain blood serum, blood was collected in 1.5 ml tubes without heparin and allowed to clot for 30 minutes at room temperature. The samples were then centrifuged for 10 minutes at 4000 rpm at 4°C. Blood serum was collected and stored at -80°C until the day of analysis.

### Spleen Cell Collection

Dissected spleens were processed and mashed in 1 mL of ACK lysis buffer in a petri dish for no more than one minute. Five mL of M199+ were added into the dish to dilute the ACK lysis buffer and to stop red cell lysis. Spleen cells were aspirated into a 5mL syringe to create single cell suspensions by passing the cells through the syringe several times then filtering through a 70-micron nylon mesh into a 15 mL conical tube. Cells were centrifuged at 2000 rpm at 4°C for 3 minutes. Cell pellets were loosened by gently tapping the tubes by hand before resuspending the cells in 5 mL of M199+. Live cell counts were determined using a hemocytometer and Trypan Blue staining.

## Quantification of Cytokines

Cytokine measurements were performed using a customized bead-based multiplex (13-LEGENDplex assay) from Biolegend, Inc. with the analytes IL-3, IL-5, IL-6, IL-7, IL-15, IL-34, M-CSF, TPO, GM-CSF, LIF, EPO, CXCL12, SCF for the analysis of BM serum and peripheral blood serum of *Vhl*cKO and control mice. Concentrations of cytokines were determined from samples following manufacturer's instructions and software.

## Flow Cytometry Analysis and Antibodies

Cells were stained for flow cytometry and included a pre-incubation step with unconjugated anti-CD16/32 (clone 93) to block Fc receptors as previously described (47, 48). The antibody cocktails used for different sets of stains are listed in **Supplementary Table 1**. For viability staining, DAPI (Sigma-Aldrich, 0.005 µg/ml final concentration) or propidium iodide (Sigma-Aldrich, 0.025 µg/ml final concentration) was used. Single color stains were used for setting compensations and gates were determined with fluorescent-minus one controls, isotype-matched antibody controls, or historical controls. Intracellular staining of Ki67 was performed using the eBioscience™ Foxp3/Transcription Factor Staining Buffer Set following the manufacturer's instructions. For cell cycle analysis, DAPI was used at a final concentration of 0.1 µg/ml per sample. Apoptosis staining was performed using Biolegend Annexin V Apoptosis Detection Kit with 7AAD. Flow cytometry data was acquired on the BD LSR II. The data was analyzed using FlowJo Software version 10.7.1.

## Preparation of Long Bones for Imaging

To label blood vessels, mice were injected with fluorescent antibodies (**Supplementary Table 1**) through the retro-orbital venous sinus. After 20 minutes of incubation, intracardial perfusion was performed with 1X PBS following by cold and fresh 4% paraformaldehyde (PFA). Subsequently, femurs were harvested and fixed in the 4% PFA for 30 minutes, at 4°C. The bones were then washed with 1X PBS, immersed in 30% sucrose for 1 hour, frozen in optimal cutting temperature (OCT) compound and kept at – 80°C. Samples were shaved using a cryostat (LEICA CM1860) equipped with a high-profile blade (Leica; 3802121).

To optically clear long bones, a modified uDISCO clearing protocol was used (49). After intracardial perfusion as described above, long bones were immersed in 4% PFA overnight and put through a series of *tert*-butanol (Sigma-Aldrich, SHBM5332) dehydration steps at 30% (4 hours), 50% (4 hours), 70% (overnight), 80% (4 hours), 90% (4 hours), and 100%

(overnight). Next, long bones were incubated in dichloromethane (DCM; Sigma-Aldrich, SHBJ8352) for 40 minutes and then placed in Benzyl Alcohol (Sigma-Aldrich, SHBK5469) Benzyl Benzoate (Sigma-Aldrich, MKCM1445) - DL-alpha-tocopherol (Alfa Aesar, Y04D032) (BABB-D4) for 3-4 hours. BABB-D4 is prepared by mixing Benzyl Alcohol + Benzyl Benzoate at the ratio of 1:2, adding diphenyl ether (DPE; Sigma-Aldrich, SHBL5909) to the BABB solution (1:4) and ultimately DL-alpha-tocopherol (Vitamin E) with the ratio of 1:25 to decrease fluorescence quenching. Cleared femurs were mounted in a custom glass chamber filled with BABB-D4 and sealed with solvent-resistant silicone gel (DOWSIL™ 730) (49).

## Two-Photon Microscopy

Imaging was performed with a custom-built two-photon video-rate microscope (Bliq Photonics) equipped with two femtosecond lasers (Spectra Physics; Insight X3, Spectra Physics; MaiTai eHP DS). During intravital imaging, the Spectra Physics Insight X3 and Maitai laser wavelengths were tuned to 840 nm and 1040 nm, respectively, and for *ex vivo* imaging only the Insight X3 was tuned to 1220 nm. Three fluorescent channels were acquired (503-538 nm, 572-608 nm, and 659-700 nm). For all two-photon imaging, a 25x water immersion objective (Olympus; XLPLN25XWMP2) with 1.05 numerical aperture was used to image a 317 µm by 159 µm field of view. Videos were recorded at 30 frames per second and images were generated by averaging of 30 frames from the live video mode.

For *in vivo* imaging of calvarial bone marrow, mice were anesthetized with isofluorane (3-4% induction, 1.5% maintenance at 1L/min) and the top of the head shaved. The skin was cleaned with 70% alcohol wipes before surgery. The mouse was placed on a heating pad and secured in a custom head mount. An incision was made along the sagittal and lambda suture of the skull and the skin retracted to expose the calvarial bone as previously described (11, 50). The secured mouse was then placed on the microscope stage for two-photon microscopy (11, 50). In order to measure BM blood vessel permeability, leakage and flow velocity in the calvaria BM during *in vivo* imaging, 70 kDa Rhodamine-B-Dextran (ThermoFisher, D1841) was injected retro-orbitally while the mouse was on the stage.

For *ex vivo* imaging, optically cleared long bones were mounted in a chamber sealed with solvent-resistant silicone gel (DOWSIL™ 730) and shaved long bones were mounted on a wet sponge to prevent the sample from drying during imaging. Slides were imaged with similar acquisitions settings as the *in vivo* imaging.

## Image Quantification

For *in vivo* image analysis, image processing and permeability/leakage measurements were performed with Fiji (ImageJ 1.53k) and BM blood flow velocity was quantified with custom scripts in MATLAB (2020a). To measure permeability in the calvaria, live two-photon microscopy video was recorded for the first 30 seconds after Rhodamine B Dextran was injected. The blood vessel permeability was calculated based on the change in fluorescence intensity outside of blood vessels over time as previously described (51, 52). For leakage measurements, z-stacks (2 µm step size) were recorded randomly around the calvarium BM 10 minutes after injection. Leakage values were calculated by dividing the fluorescence intensity of the perivascular space adjacent to a vessel by the fluorescence intensity inside the blood vessel. Representative examples of BM leakage were generated by taking maximum intensity projections (MIPs) of BM regions with image contrast/enhancement applied. Blood flow velocity was calculated by recording 30 second videos of blood flow in the BM calvaria and then utilizing the Line Scanning Particle Image Velocimetry (LSPIV) method implemented in a custom MATLAB script to calculate blood flow velocity as previously described (53, 54). ImageJ (ImageJ 1.53k) was used to adjust video and image contrast for figure presentation.

In long bone images, as required, 3D z-stacks were rotated with the "TransformJ" plugin in ImageJ to exclude the non-relevant signals and final images were generated by taking maximum intensity projections (MIPs) of BM regions and adjusting the image contrast/enhancement. To generate a depth-dependent profile of vessel diameter in long bones, measurements were taken at 0-30 µm (shallow BM), 75-105 µm (middle BM), and 150-180 µm (deep BM) below the endosteum. To measure vascular density, image brightness/contrast was first adjusted in Fiji (ImageJ 1.53k) and then images were converted to binary. Next, noise reduction was performed *via* Despeckle, and binary Fill Hole was applied. Finally, using analytical coding developed in Python (3.7.6), the ratio of the total blood vessel pixels to total BM pixels was determined for BM vessel density measurements.

# RESULTS

## *Vhl* Deletion in Dmp1-Expressing Cells Dysregulates Hematopoiesis

Previous studies of *Vhlc*KO mice utilized mice on a mixed genetic background (21). For our studies, we required a pure C57BL/6 (B6) background and we performed a thorough comparison of our B6 *Vhlc*KO mice to previous published results. Similar to previous reports (21), we found that long bones in B6 *VhlcKO* mice display abnormally high bone mass and density and the BM cavity is severely occluded with bone (**Figure 1A**), accompanied by stunted B cell development, splenomegaly (**Supplementary Figures 1A–E**), and reduced BM cellularity compared to controls (**Figure 1B**). In the B6 *Vhlc*KO, we extended our analysis to be longitudinal, examining hematopoietic lineages at multiple ages. Analysis of specific hematopoietic cell lineages in the BM revealed a decrease in B cells, no change in T cell frequency, and an increase in CD11b+ Gr1- cells (enriched for monocytes) and CD11b+ Gr1+ cells (enriched for Ly6G+ granulocytes, but also may include CD115+ and Ly6C+ monocytes) in 6-week-old, 10-week-old and 6-month-old mice (**Figures 1C, D**). Furthermore, an overall reduction in the absolute numbers of all hematopoietic lineages in the BM of *Vhlc*KO mice was observed (**Table 1**). Lineage analysis in the spleen at 10 weeks revealed a decrease in B cells, no change in T cells, and an increase in CD11b+ Gr1+ cells that became more prominent as mice aged to 6 months. CD11b+ Gr1- cells in the *Vhlc*KO spleen at 6-weeks-old were slightly

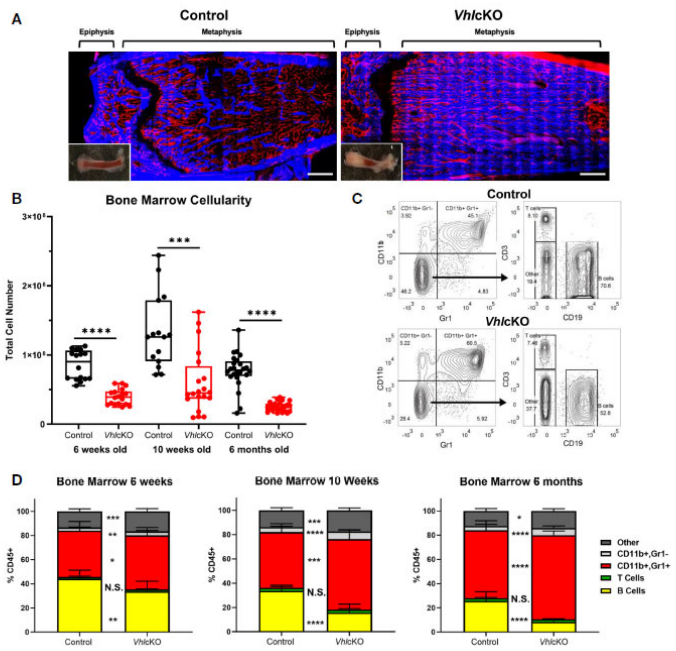


**FIGURE 1** | Bone marrow, spleen and peripheral blood lineage cell defects in the *Vhl*cKO mice. **(A)** Macroscopic and *ex vivo* imaging of the distal end of long bones revealed progressive increases in the bone mass of 10-weeks-old *Vhl*cKO femurs compared to control. Inset: photo of the femur. Red: blood vessel (AlexaFluor647 CD31, AlexaFluor647 CD144, AlexaFluor647 Sca-1), Blue: bone (SHG). Scale bar ~500μm; **(B)** bone marrow cellularity, **(C)** representative FACS plots of immune cell lineages, with the values on plots on the left representing cell frequency in total bone marrow, and the values on the plots on the right representing frequencies within the Gr-1- CD11b- gate. **(D)** frequency analysis of bone marrow lineage cells at 6-weeks of age (left), 10-weeks of age (middle) and 6-month (right). $p<0.05$*, $p<0.01$**, $p<0.001$***, $p<0.0001$**** two-tailed Student's t-test. N.S., not statistically significant.

reduced, similar to controls at 10-weeks-old, and were increased at 6-months-old (**Supplementary Figure 1E**). Peripheral blood of the *Vhl*cKO mice showed no change in B cells at 6 weeks, but B cells were decreased at 10 weeks and 6 months. In contrast, CD11b+ Gr1- cells were increased at 10-weeks-old, and CD11b+ Gr1+ cells at 6-months-old only (**Supplementary Figure 1F**).

## Increased Frequencies of Hematopoietic Progenitor Cells in the *Vhl*cKO BM

To further investigate if the defect in hematopoiesis occurred upstream of lineage-committed cells, we analyzed the hematopoietic progenitor compartments in the BM of *Vhl*cKO mice. Long-term hematopoietic stem cells (LT-HSCs: LSK, CD150+ CD48-, short term hematopoietic stem cells (ST-HSCs: LSK, CD150-, CD48-), multipotent progenitors (MPP2: LSK, CD150+, CD48+; MPP3: LSK, CD150-, CD48+; and MPP4: LSK, CD150-, Flk2+, CD48+), and common lymphoid progenitors (CLPs: Lineage-, cKit$^{int}$, Sca1$^{int}$, CD127+ Flk2+) from *Vhl*cKO and control mice were quantified using flow cytometry (**Figures 2A, B**). The results showed an increase in the frequency in LT-HSCs, ST-HSCs, MPP2, MPP3, and CLPs at 6-weeks, 10-weeks and 6-months-old (**Figure 2C**). MPPs are heterogeneous with different lineage-biased potential. MPP2/3 are myeloid-biased while MPP4 are lymphoid-primed (55, 56). In our results, MPP4 frequency was increased starting at 10-weeks-old (**Figure 2C**). These results show that deletion of *Vhl* in Dmp1-expressing cells increases progenitor frequencies and indicates that downstream differentiation of B cells may be blocked. However, examination of MPP4 absolute numbers showed decreased MPP4s in 6-week-old *Vhl*cKO, an increase at 10-weeks-old, and numbers similar to controls at 6-months old. In 6-week-old *Vhl*cKO mice, the absolute numbers of CLPs were decreased, in 10-week-old *Vhl*cKO mice, the absolute numbers of LT-HSCs and MPP3 were increased, whereas at 6-months-old, LT-HSCs and CLPs were decreased (**Figure 2D**).

## *Vhl* Deletion in *Dmp1*-Expressing Cells Dysregulates B Cell Development in the BM

To further explore the effects of *Vhl* deletion in OBs and OCYs on B cell development and to identify at which stage B cell development was stunted in the BM, we determined the frequencies of Hardy Fractions A-F (**Figures 3A, B**) using flow cytometry (1, 57). *Vhl*cKO mice regardless of age retained

**TABLE 1** | Hematopoetic lineage mean±SD and absolute number p<0.05*, p<0.01**, p<0.001***, p<0.0001**** two-tailed Student's t-test.

| | CD45+ Population (mean% ± SD) | | | | Absolute Number (mean ± SD) | | | |
|---|---|---|---|---|---|---|---|---|
| Lineage Population | Bone Marrow | | Spleen | | Bone Marrow | | Spleen | |
| **6 weeks old** | **Control** | ***Vhl* cKO** | **Control** | ***Vhl* cKO** | **Control** | ***Vhl* cKO** | **Control** | ***Vhl* cKO** |
| B cells | 44.16 ± 7.16 | 33.69 ± 8.49** | 60.71 ± 2.64 | 58.57 ± 3.51 | 2.62E+0.7 ± 7.06E+06 | 8.88E+0.6 ± 4.83E+06**** | 6.35E+0.7 ± 1.28E+07 | 5.71E+0.7 ± 9.18E+06 |
| T cells | 1.45 ± 0.79 | 1.61 ± 0.62 | 23.65 ± 3.56 | 23.49 ± 3.42 | 8.38E+0.5 ± 4.33E+05 | 3.70E+0.5 ± 1.87E+05*** | 2.49E+0.7 ± 6.57E+06 | 2.29E+0.7 ± 4.93E+06 |
| CD11b+ Gr1- | 2.58 ± 0.37 | 3.28 ± 0.74** | 2.55 ± 0.57 | 1.95 ± 0.15** | 1.53E+0.6 ± 3.92E+05 | 7.81E+0.5 ± 3.48E+05**** | 2.66E+0.6 ± 7.87E+05 | 1.90E+0.6 ± 2.96E+05* |
| CD11b+ Gr1+ | 38.46 ± 7.61 | 44.85 ± 6.47* | 2.85 ± 2.55 | 2.28 ± 0.66 | 2.42E+0.7 ± 1.12E+07 | 1.06E+0.7 ± 4.30E+06*** | 2.71E+0.6 ± 2.19E+06 | 2.17E+0.6 ± 5.06E+05 |
| **10 weeks old** | Control | *Vhl* cKO | Control | *Vhl* cKO | Control | *Vhl* cKO | Control | *Vhl* cKO |
| B cells | 33.8 ± 4.55 | 15.83 ± 7.01**** | 60.71 ± 7.63 | 46.37 ± 7.53**** | 3.32E+0.7 ± 1.47E+07 | 8.02E+0.6 ± 1.29E+07*** | 1.22E+08 ± 6.02E+07 | 1.18E+08 ± 5.98E+07 |
| T cells | 2.34 ± 1.04 | 2.35 ± 0.95 | 26.67 ± 6.15 | 29.09 ± 4.11 | 2.55E+0.6 ± 1.92E+06 | 1.05E+0.6 ± 1.35E+06* | 6.22E+07 ± 5.28E+07 | 8.10E+07 ± 5.40E+07 |
| CD11b+ Gr1- | 4.09 ± 0.67 | 6.23 ± 1.25**** | 2.50 ± 0.36 | 2.71 ± 0.38 | 4.08E+0.6 ± 2.08E+06 | 2.41E+0.6 ± 1.89E+06* | 5.49E+06 ± 4.12E+06 | 7.02E+06 ± 3.81E+06 |
| CD11b+ Gr1+ | 45.93 ± 6.89 | 58.11 ± 7.78*** | 1.15 ± 0.50 | 6.27 ± 2.93**** | 4.38E+0.7 ± 1.60E+07 | 2.22E+0.7 ± 1.50E+07** | 2.14E+06 ± 9.96E+05 | 1.66E+07 ± 1.46E+07** |
| **6 months old** | Control | *Vhl* cKO | Control | *Vhl* cKO | Control | *Vhl* cKO | Control | *Vhl* cKO |
| B cells | 25.74 ± 7.62 | 8.37 ± 1.76**** | 61.38 ± 7.09 | 42.44 ± 3.65**** | 1.48E+0.7 ± 7.35E+06 | 9.73E+0.5 ± 2.56E+05**** | 4.33E+0.7 ± 2.04E+07 | 2.77E+0.7 ± 7.48E+06** |
| T cells | 2.21 ± 0.62 | 2.23 ± 0.38 | 25.55 ± 2.81 | 25.88 ± 2.68 | 1.20E+0.6 ± 5.48E+05 | 2.58E+0.5 ± 5.65E+04**** | 1.66E+0.7 ± 6.08E+06 | 1.70E+0.7 ± 5.08E+06 |
| CD11b+ Gr1- | 3.57 ± 1.31 | 5.98 ± 1.69**** | 1.82 ± 0.47 | 2.60 ± 0.67*** | 1.94E+0.6 ± 9.20E+05 | 6.97E+0.5 ± 2.28E+05**** | 1.19E+0.6 ± 3.95E+05 | 1.74E+0.6 ± 7.95E+05* |
| CD11b+ Gr1+ | 56.01 ± 7.91 | 69.31 ± 3.49**** | 2.83 ± 4.41 | 14.33 ± 3.33**** | 3.08E+0.7 ± 1.26E+07 | 8.22E+0.6 ± 2.11E+06**** | 1.64E+0.6 ± 2.16E+06 | 9.52E+0.6 ± 3.42E+06**** |

normal frequency of Fraction A. In contrast, a decrease in the frequencies of Fractions B-C through Fraction F was observed at all ages examined (**Figure 3C**). An overall decrease in the absolute numbers of B cells across all developmental stages was observed at all three ages, with the exception of Fraction A at 10 weeks (**Figure 3D**). These results indicate an incomplete but severe block in B cell development that starts at Fractions B-C in *Vhl*cKO mice.

## Reciprocal Bone Marrow Transplantation Studies Reveal a Cell-Extrinsic Effect of the *Vhl*cKO Microenvironment on B Cell Development

We expected the cause of the B cell defect to lie within the non-hematopoietic cells, since *Dmp1* is not expressed in hematopoietic cells. To definitively determine if the effects of *Vhl* deficiency on B lymphopoiesis were due to changes in the non-hematopoietic microenvironment within the bone, we performed whole BM transplants from WT B6.SJL (CD45.1+) donors into lethally irradiated *Vhl*cKO (CD45.2+) recipients [WT→*Vhl*cKO chimeras (**Figure 4A**)]. WT (CD45.1+)→ control (Cre-negative; $Vhl^{fl/fl}$, CD45.2+) chimeras were also prepared. Donor hematopoietic chimerism was similar in controls and chimeras (**Figure 4B**). Analysis 16 weeks post-transplant showed a significant reduction in BM cellularity (**Figure 4C**) and an increase in CD11b+ Gr1+ and CD11b+ Gr1- cells and a decrease in B cells in the WT→*Vhl*cKO mice (**Figure 4D**). Analysis of B cells revealed a decrease at Fractions A through Fraction F in both frequency and absolute numbers (**Figures 4E, F**), extending the defect to include Fraction A as compared to what is observed in non-transplanted *Vhl*cKO mice (**Figure 3**). In contrast, overall hematopoiesis, including B cell development, was normal in the *Vhl*cKO→WT chimeras (**Supplementary Figure 2**). Since *Vhl* deletion in B cells can affect their function (58, 59), we confirmed that *Vhl* remained intact and was not erroneously deleted in B cells in our *Vhl*cKO mice (**Supplementary Figure 3**). These results confirm a cell-extrinsic effect of the non-hematopoietic *Vhl*cKO BM microenvironment on hematopoiesis.

## *Vhl*cKO Mice Display Patterns of Reduced B Cell Proliferation and Increased B Cell Apoptosis in the BM

We hypothesized that the observed reduction of B cells was due to increased apoptosis and diminished B cell proliferation in the BM. To test this, B cells were stained with Annexin V and 7AAD to identify cells that were live, in early stage apoptosis or late stage apoptosis (**Figure 5A**, left panels). Normally, apoptosis is the most extensive in Fraction A (pre-pro-B cells) amongst the B cell fractions (60). The frequencies of *Vhl*cKO Fraction A cells in live, early and late apoptosis stages was comparable to controls at all ages examined (**Figure 5B**). Apoptosis in Fraction B-C in *Vhl*cKOs was similar to controls at 6-weeks-old. At 10-weeks-old, the frequency of live Fraction B-C cells increased and those in early apoptosis decreased in the *Vhl*cKO. At 6-months-old, there was no difference in the frequencies of live and early stage

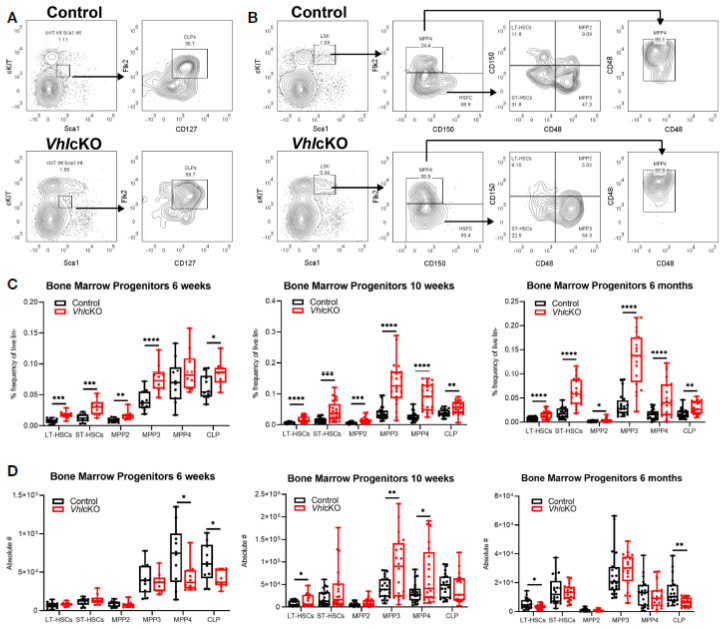


**FIGURE 2** | Increased frequency of hematopoietic progenitor cells in the *Vhl*cKO BM. **(A)** Representative FACS plots of common lymphoid progenitors (Lineage-, cKit$^{int}$, Sca1$^{int}$, CD127+ Flk2+); **(B)** representative FACS plots of hematopoietic progenitors in the bone marrow of controls (top) and *Vhl*cKOs (bottom); **(C)** frequency and **(D)** absolute number of hematopoietic progenitors in the bone marrow in 6-weeks-old (left), 10-weeks-old (middle) and 6-months-old (right) mice. $p<0.05$*, $p<0.01$**, $p<0.001$***, $p<0.0001$**** two-tailed Student's *t*-test.

apoptotic Fraction B-C cells, but their frequency in late stage apoptosis was increased (**Figure 5B**). No differences in the stages of apoptosis were observed between controls and *Vhl*cKOs for Fractions D, E and F at all ages examined, with the exception of increased Fraction F cells in late stage apoptosis at 6-months-old (**Supplementary Figure 4**).

B cell development leads to the assembly and signaling of the B cell antigen receptor (BCR). CD43+ Fraction A-C (pre-pro-B and pro-B cells) normally have higher proliferation rates compared to CD43- Fraction D-E (Pre-B cells and immature B cells) (5, 61). Proliferation is halted at Fraction D (small pre-B cell) to allow light (L) chain gene rearrangement, subsequently expressing a complete IgM surface molecule (Fraction E) (5, 62). Cell cycle analysis in *Vhl*cKO B cells was performed using Ki67 and DAPI staining (**Figure 5A**, right panels). There were no differences in the distribution of cells in G0 (quiescent, DAPI- Ki67-), G1 (DAPI- Ki67+, or S/G2/M (DAPI+ Ki67+) phases between *Vhl*cKO and control mice amongst all Hardy Fractions at 6-weeks-old (**Figure 5C** and **Supplementary Figure 5**). However, at 10-weeks-old and 6-months-old, Fractions B-C contained an increased percentage of cells in G0. At 10-weeks old, a similar frequency of Fraction B-C cells in G1 was observed between *Vhl*cKO and controls, but there was a reduced percentage of cells in S/G2/M cell cycle phases (**Figures 5A, C**). At 6-months-old, this pattern reversed, with a decreased frequency of Fraction B-C cells in G1, and similar frequency of S/G2/M cells (**Figure 5C**). Taken together, these data indicate a reduced ability of Fraction B-C cells to proliferate in a *Vhl*-deficient microenvironment as early as 10-weeks-old. No difference in proliferation of Fractions D-F was observed at any age examined, with the exception of a slight (yet statistically significant) reduction of the *Vhl*cKO Fraction F cells in G0 and increase in G1 at 6-months-old (**Supplementary Figure 5**).

B cell development at each stage requires specific signaling molecules from a variety of niche cells (5, 63). To further explore the dysregulated niche, BM supernatant was analyzed for levels of CXCL12 and SCF, which are critical for B cell development (1, 27, 28, 31). CXCL12 levels were reduced in the *Vhl*cKO BM serum, while SCF levels were unaffected (**Figure 5D**). This suggested that increased apoptosis and reduced proliferation of Fraction B-C cells are caused by reduced CXCL12 levels in the *Vhl*cKO BM.

## Increased Bone Marrow Blood Vessel Diameter and Density in *Vhl*cKO Microenvironments

We attempted to quantify MSC, OB and EC subsets using flow cytometry of collagenase-digested bones (64), but we concluded

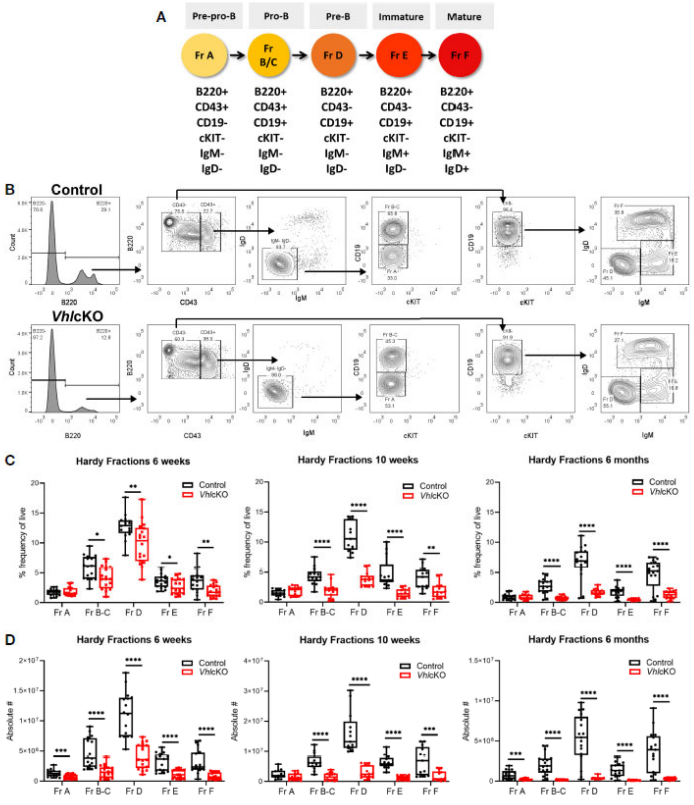


**FIGURE 3** | Dysregulated B cell development in *Vhl*cKO mice bone marrow. **(A)** Antigen markers used to identify and distinguish B cell development stages by flow cytometry. **(B)** Representative FACS plot of B cell development in the BM control (top) and *Vhl*cKO (bottom); **(C)** B cell frequency in 6-week-old (left), 10-week-old (middle), and 6-month-old (right) mice; **(D)** absolute cell numbers in 6-week-old (left), 10-week-old (middle), and 6-month-old (right). $p<0.05^{*}$, $p<0.01^{**}$, $p<0.001^{***}$, $p<0.0001^{****}$ two-tailed Student's t-test.

that the high bone mass of *Vhl*cKO mice prevented complete digestion to accurately enumerate these populations (**Supplementary Figure 6**). To more precisely examine the changes in the microenvironment of *Vhl*cKO mice, we imaged femurs that were shaved to remove cortical bone (for analysis of the metaphysis) or optically cleared with a modified uDISCO protocol (for analysis of the fully intact diaphysis) (**Supplementary Videos 1, 2**) (49). We measured the vessel diameter and frequency in the cleared long bones and found that regardless of their position in the BM, blood vessels in *Vhl*cKO mice were significantly larger in diameter than the control group (**Figures 6A–C**) while generally no difference was observed in the vessel frequency (**Supplementary Figure 7A**). Metaphyseal and diaphyseal BM and bone vessel density measurements revealed that in *Vhl*cKO, blood vessels occupy a larger volume than controls (**Figures 6D–F** and **Supplementary Figure 7B, C**). Furthermore, we observed an apparent decrease in endosteal lining arterioles in the diaphysis of 6-month-old *Vhl*cKO femurs compared to controls (**Supplementary Figure 7D**). Taken together, these data reveal a striking alteration in the overall architecture of the BM vascular network in *Vhl*cKO mice.

## *Vhl*cKO Bone Marrow Blood Vessels Display Increased Permeability

While it has been shown that the bone and vascular system undergoes significant remodeling in *Vhl*cKO mice, there has been a lack of information regarding potential functional changes to BM blood vessels. To examine changes to the BM vasculature system which could negatively impact B cell development, we sought to quantify changes to the vascular permeability, leakage and blood flow velocity *via* intravital two-photon microscopy of the calvaria. Vessel permeability reflects the rate at which small molecules exit

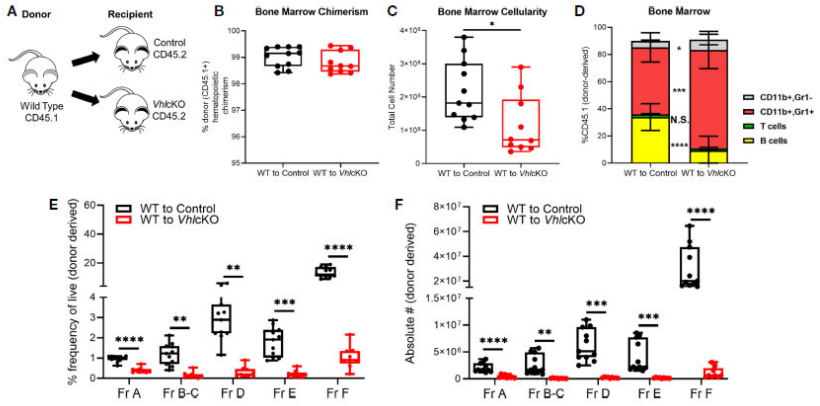


**FIGURE 4** | Altered B cell development in WT→*Vhl*cKO hematopoietic chimeras, demonstrating a cell-extrinsic effect of the *Vhl*-deleted osteolineage cells on B cell development. Mice were transplanted at 10 weeks of age and were analyzed 16 weeks post-transplantation. **(A)** experimental scheme; **(B)** donor (CD45.1) chimerism; **(C)** bone marrow cellularity; **(D)** frequency of lineage cells in bone marrow; **(E)** B cell frequency and **(F)** absolute number of B cell developmental stages at 16 weeks post-transplant. $p<0.05^{*}$, $p<0.01^{**}$, $p<0.001^{***}$, $p<0.0001^{****}$ two-tailed Student's t-test. N.S., not statistically significant.

blood vessels and fill the surrounding perivascular space, whereas leakage is the ratio of fluorescent dye in the perivascular space and vascular lumen after reaching equilibrium. Blood vessel leakage and permeability was calculated by administering Rhodamine B Dextran (70kDa) *via* a retro-orbital injection. We found that *Vhl*cKO mice displayed greater vascular leakage overall, and that vascular leakage increased in both control and *Vhl*cKO mice with age (**Figures 7A, B** and **Supplementary Videos 3–8**). Similarly, we observed an increase in vascular permeability in *Vhl*cKO mice, which significantly increased with age (**Figure 7C** and **Supplementary Videos 9, 10**). We observed a decrease in blood flow velocity in *Vhl*cKO mice compared to controls for 6-week-old and 10-week-old mice (**Figure 7D**). Lastly, we observed an age-related reduction in blood flow in both *Vhl*cKO and control mice (**Figure 7D**), which is consistent with previously published changes in BM vascular flow rate with age (65).

## Evidence for Age-Related Reduction in Oxygen Levels Within Local Niches in the *Vhl*cKO Bone Marrow

Hypoxic niches in the BM microenvironment are crucial for hematopoietic development but BM oxygenation can be altered through changes in vascular supply and/or cellular consumption (11). Dynamic regulation of HIF-1α levels is required for normal B cell development such that HIF activity is high in B cell precursors and must decrease in the immature B cell stage in the BM (66). In wild type mice at 10-16 weeks of age, studies using the hypoxic marker pimonidazole (PIM) revealed that HSCs in the BM stain positively with PIM, indicating a hypoxic niche (67). In contrast, low PIM staining in BM B220+ cells was observed in 6-12 week old mice, indicating a relatively normoxic niche for B220+ cells in wild type mice (68). To evaluate hypoxia in distinct B cell developmental stages, *Vhl*cKO and control mice were injected with PBS or 120 mg/kg PIM. PIM staining of LSKs in the BM was positive, as previously reported (67), but this staining was more intense in LSKs of control and *Vhl*cKO mice at 6 months of age (**Figure 8A** top panels). Remarkably, PIM staining in *Vhl*cKO LSKs was significantly higher than control LSKs at 6 months (**Figure 8B**). CD45+ B220+ cells [which include all Hardy Fractions, in addition to other hematopoietic progenitors, natural killer cells, dendritic cells and T cells (69–73)] displayed negative or low staining with PIM in both control or *Vhl*cKO mice at 10 weeks old, but the PIM staining in B220+ cells in *Vhl*cKO mice at 6 months was significantly elevated compared to controls (**Figure 8A**, bottom panels and **Figure 8B**). Next, we performed PIM staining in order to determine if specific Hardy Fractions were experiencing hypoxia in the *Vhl*cKO bone marrow. This analysis revealed that in general, the Fraction A cells stain with PIM at a higher level than the Fractions B through Fraction F cells (**Figure 8C**), but that the intensity of PIM staining on Fraction A cells in the *Vhl*cKO mice at 6 months of age was significantly higher than controls (**Figures 8B, C** and **Table 2**). This reveals that in wild-type mice, Fraction A cells might reside in a hypoxic niche, similar to LSKs. It also indicates that as B cells mature, they may move away to a less hypoxic niche. Our results also indicate that the oxygen levels in the microenvironment of Fraction A cells in the *Vhl*cKO BM is similar to controls at 10-weeks-old, but at 6-months-old, the microenvironment for Fraction A cells is relatively hypoxic compared to the microenvironments for Fraction B through Fraction F.

## DISCUSSION

Here, we report that deletion of the *Vhl* gene in *Dmp1*-expressing cells results in cell-extrinsic changes in the bone marrow microenvironment that deleteriously affect B cell development

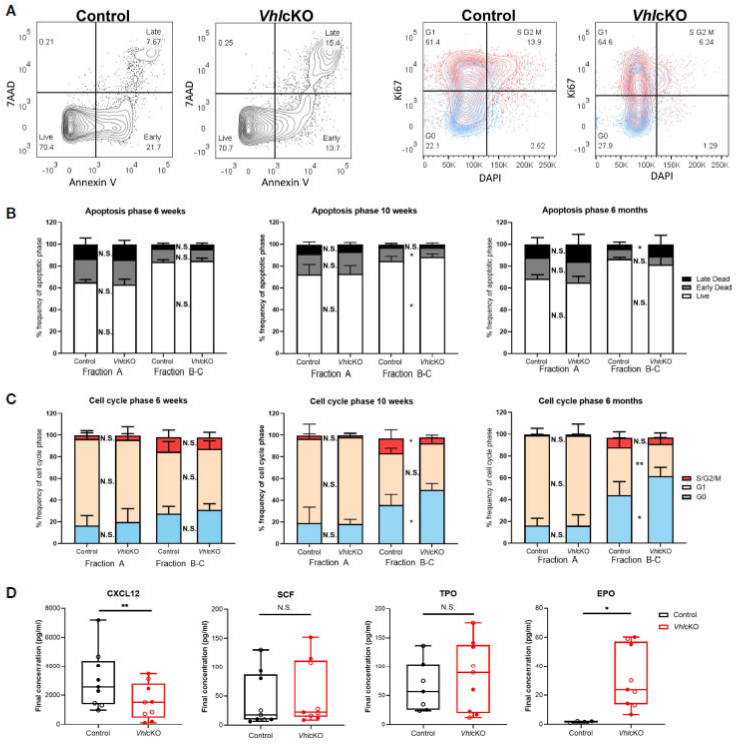


**FIGURE 5** | *Vhlc*KO mice display increase apoptosis and reduced cell proliferation during early B cell development. **(A)** Representative FACS plots of apoptotic phases (live, early apoptosis, and late apoptosis) in B220+ cells (left) and cell cycle phases (G0 (quiescent), G1, and S/G2/M) in B220+ cells (red:CD43+ blue: CD43-) (right) in 10-weeks-old mice; **(B)** frequency of apoptotic phases in Fractions A and B-C in 6-weeks-old, 10-weeks-old and 6-month-old mice; **(C)** frequency of cells in each cell cycle phase within Fractions A and B-C at 6-weeks-old, 10-weeks-old old and 6-month-old mice. Our cell cycle analysis antibody panel (**Supplementary Table 1**) did not include anti-IgM and anti-IgD, so we could not remove these cells from the CD43+ population. However, these cells are very low in frequency in the *Vhlc*KO (**Figure 3**) and do not significantly change the proliferation results in controls (data not shown); **(D)** CXCL12, SCF, TPO, and EPO cytokine level measurements in bone marrow supernatant of combined 10-weeks-old (filled) and 6-months-old (open) control or *Vhlc*KO mice. $p<0.05$*, $p<0.01$** two-tailed Student's t-test. N.S., not statistically significant.

as early as 6 weeks of age. Specifically, we observed reduced CXCL12 levels in the bone marrow, which could result in the inability of Fraction B-C to proliferate. We also observed elevated levels of EPO, and an increase in the blood vessel diameters and vessel density in the *Vhlc*KO at all ages examined, consistent with a response to hypoxia. To our knowledge, our report is the first to show pimonidazole binding on Fraction A cells in wild type mice, indicating that in general, Fraction A cells reside in hypoxic niches of the BM, similar to LSKs. Burrows et al., 2020 utilized EF5, a hypoxia probe similar to pimonidazole (66), and reported high EF5 staining of "pro-B/pre-B" (B220+ IgM- IgD-) cells, which includes Hardy Fractions A-D, but they did not distinguish EF5 staining on clearly delineated Hardy Fractions, as we have in our current study. In addition, our staining of Hardy Fraction cell subsets with pimonidazole revealed that Fraction A cells in the *Vhlc*KO experienced more extreme hypoxia at 6 months of age. Collectively, our analyses demonstrate that the B cell developmental defects in the *Vhlc*KO bone marrow microenvironment observed at younger ages (6 weeks and 10 weeks) are not due to dysregulation of oxygen levels in their local niches. However, the B cell defects could be exacerbated by hypoxia as the mice age to 6 months.

Evidence from several groups, including our own (2, 47, 74) supports that distinct BM cell subsets, including perisinusoidal cells (which are a subset of MSCs), osteoprogenitor cells (OBPs), OBs and OCYs support different stages of B cell maturation by providing CXCL12 (75, 76) and IL7 (1), both of which are important for proliferation and survival of Hardy Fractions A, B and C (a.k.a. pre-pro-B and pro-B cells) (4). Hematopoietic stem cells and progenitors are localized in the relatively hypoxic sinusoidal regions of the marrow (11, 12) which are anatomically and physically separate from the endosteal niches. Osteolineage cells

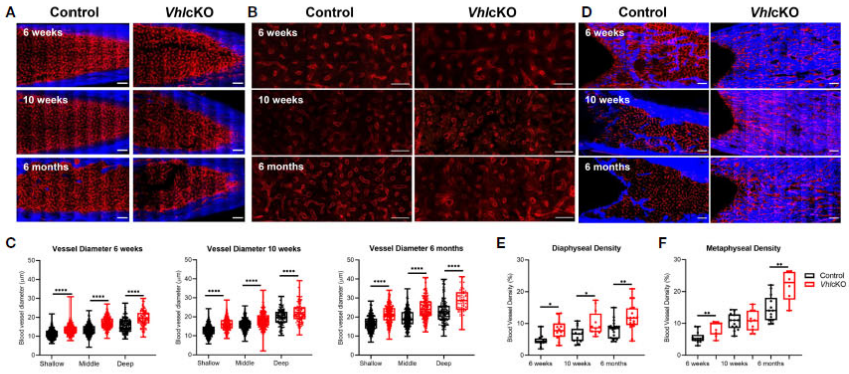


**FIGURE 6** | | *Ex vivo* two-photon imaging of long bones in *Vhl*cKO and controls. **(A)** Representative macroscopic images of the femur diaphyseal BM (scale bars: ~200 µm), **(B)** magnified z-stacks (scale bars: ~100 µm), and **(C)** statistical analysis after uDISCO clearing show an increase in the *Vhl*cKO vascular diameter relative to the controls; **(D)** *ex vivo* images of femur metaphyseal BM after max intensity projection reveal bone replacement and vascular alteration in *Vhl*cKO; **(E, F)** quantification of the metaphyseal and diaphyseal vascular density (scale bars: ~200 µm). Red: blood vessels (labeled with Alexa647 conjugated antibodies against CD31, CD144, and Sca-1), Blue: bone (SHG: Second harmonic generation). *p<0.05, **p<0.01, ****p<0.0001, two-tailed Student's t-test.

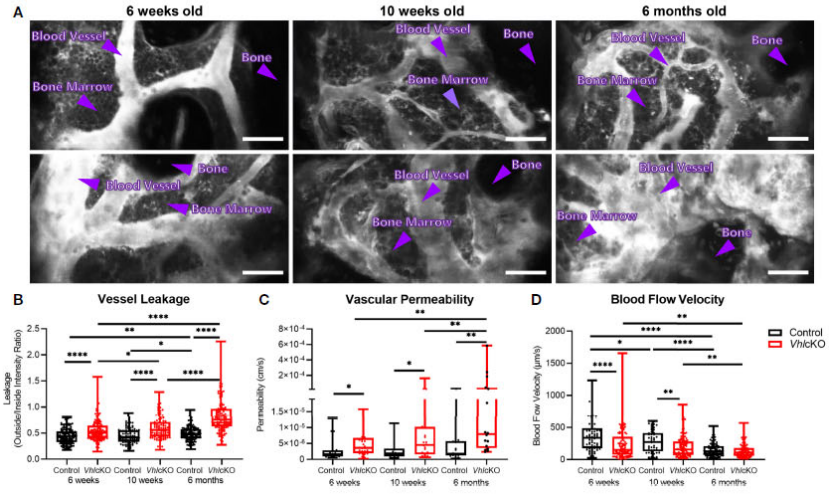


**FIGURE 7** | Disruption in blood-bone marrow barrier revealed by intravital microscopy. Blood vessel microenvironment comparisons of control and *Vhl*cKO mice at 6-week (n=4), 10-week (n=4) and 6-month (n=5) timepoints. **(A)** Representative contrast adjusted max intensity projections of the calvarial BM in control and *Vhl*cKO mice by age; White: blood vessel (Rhodamine B Dextran, 70 kDa); scale bar: 50 µm; quantification of calvarial BM **(B)** blood vessel leakage, **(C)** vascular permeability, and **(D)** blood flow velocity. *p<0.05, **p<0.01, ****p<0.0001, Mann-Whitney test.

originate from MSCs, which then differentiate to OBPs, early OBs, late OBs and mature OCYs. MSCs and HSCs are found in close proximity to each other (77) and might also be located within the BM cavity in direct contact with B cell progenitors (1). Osteoblast depletion studies *in vivo* demonstrated OBs as a key regulator of B cell development (78) and this was later supported later by independent studies in mice, in which OBs that lack expression of Gsα (79) and that OBs defective in the mTORC1 signaling pathway (80) could not support full B cell development. The role of MSCs in the regulation of B cell proliferation, survival, and

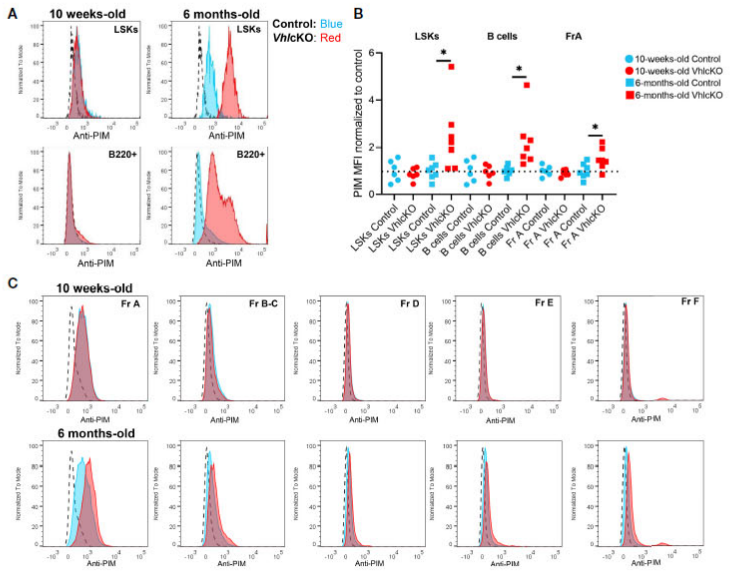


**FIGURE 8** | Hypoxia cell marker pimonidazole indicates difference by age and amongst B cell fractions in control and VhlcKO mice. *Vhl*cKO and control mice were injected with PBS or 120 mg/kg pimonidazole (PIM). PIM staining of **(A)** Live, Lin-, CD45+, Sca1+, cKit+ (LSKs) (top) and Live, B220+ cells (bottom) in the BM of 10-weeks-old and 6-months-old mice; dashed line: isotype control; blue line: anti-PIM staining in controls; red: anti-PIM staining in *Vhl*cKO; **(B)** summary of PIM staining in *Vhl*cKOs (red) normalized to the mean fluorescence intensity (MFI) in controls (blue); results from 4 independent experiments are shown; **(C)** representative anti-PIM staining plots of individual B cell Fractions **(A–F)** from a control (blue) and a *Vhl*cKO mouse (red) at 10-weeks-old (top) and at 6-months-old (bottom). *p<0.05, two-tailed student's t-test.

differentiation appears to be highly context-dependent (81–83), and new reports of novel CD51+ MSC subsets and their differential ability to support B lymphopoiesis in the BM (25, 37) will require further scrutiny in the context of altered bone homeostasis.

One caveat to the identification of the "true" niche cells that support B cell development is new information on off-target gene deletion in *Dmp1*-Cre mice. We utilized *Dmp1*-Cre for our *Vhl* deletion studies as they are the main model currently available to target osteocytes. However, despite its widespread use, *Dmp1-Cre* displays off-target expression (43, 84, 85). Broad MSC targeting of *Vhl* in *Prx-Cre;Vhl*$^{fl/fl}$ mice resulted in delays in BM cavity development, increases in trabecular bone with dilated BM vessels and few hematopoietic cells in perinatal mice (86). Similar phenotypes were observed in *Osx-Cre;Vhl*$^{fl/fl}$ mice (87), perhaps because *Osx* and *Prx* expression overlap at an early osteoprogenitor stage. *Ocn-Cre;Vhl*$^{fl/fl}$ mice, which targets mainly mature OBs, displayed similar bone and hematopoietic phenotypes plus angiogenesis in the long bones and changes in OCY morphology with fewer dendrite connections (23). Taken together, these studies indicate that deletion of *Vhl* at the MSC, OBs and OCY phases from ontogeny results in physical changes in bone microenvironment and altered hematopoiesis, and implies that the phenotypes observed could have been generated at an early osteoprogenitor stage and erroneously attributed to more mature osteolineages. Single cell RNA-Seq data on bone marrow stromal cells (88–90) could provide information on non-overlapping mRNAs between MSCs, early OBs, late OBs, in order to create new mouse models for studies of HSC and B cell bone marrow niches, and permit discovery of the specific contributions of MSCs and OBPs to B cell development.

Our studies show an effect of *Vhl*-deletion in *Dmp1*-expressing cells on ECs. Our imaging results suggest that there is an increase in bone ECs, which is consistent with previous studies in *Osx*-Cre; *Vhl*$^{fl/fl}$ mice where endomucin staining showed that *Vhl* deletion increased bone vasculature with dilated blood vessels (21). We also observed larger vessels in the BM across all ages and an increase in BM blood volume. These changes, along with the observed decrease in endosteal arterioles in the long bones of 6 month old mice and an increase in PIM staining, suggests that oxygenation of the *Vhl*cKO marrow may be lower than normal, which may play a role in dysregulation of B cell development in older mice. Future studies will be needed to clarify this and to identify other changes in specific types or locations of blood vessels in the *Vhl*cKO model as a function of age.

Given the connection between *Vhl* and hypoxia response, it was interesting that EPO levels were high in the BM supernatant of the *Vhl*cKO mice. High *Epo* mRNA was also observed in the bones of *Osx*-Cre;*Vhl*$^{fl/fl}$ (8) mice. Deletion of *Vhl* at the mature

**TABLE 2** | Mode Fluorescence Intensity of PIM staining on B cell fractions in control and *Vhl*cKO mice.

| Age | Genotype | Treatment | MFI (mode) | | | | |
|---|---|---|---|---|---|---|---|
| | | | Fr A | Fr B-C | Fr D | Fr E | Fr F |
| **10-weeks-old** | *Vhl* cKO | Isotype | 336 | 187 | 146 | 125 | 146 |
| | *Vhl* cKO | Isotype | 358 | 166 | 146 | 166 | 208 |
| | Control | PIM | 3561 | 1177 | 638 | 638 | 613 |
| | Control | PIM | 3678 | 1501 | 689 | 638 | 689 |
| | Control | PIM | 2940 | 742 | 470 | 493 | 402 |
| | Control | PIM | 3926 | 1547 | 715 | 824 | 663 |
| | Control | PIM | 1371 | 293 | 229 | 229 | 229 |
| | Control | PIM | 715 | 250 | 187 | 187 | 187 |
| | *Vhl* cKO | PIM | 2514 | 796 | 380 | 402 | 424 |
| | *Vhl* cKO | PIM | 3034 | 912 | 493 | 540 | 588 |
| | *Vhl* cKO | PIM | 3132 | 1371 | 493 | 564 | 564 |
| | *Vhl* cKO | PIM | 3561 | 943 | 540 | 564 | 516 |
| | *Vhl* cKO | PIM | 1106 | 424 | 336 | 336 | 358 |
| | *Vhl* cKO | PIM | 882 | 271 | 208 | 187 | 208 |
| **6-months-old** | Control | PIM | 293 | 146 | 104 | 125 | 125 |
| | *Vhl* cKO | PIM | 293 | 83.5 | 83.5 | 125 | 146 |
| | Control | PIM | 4057 | 1290 | 613 | 689 | 613 |
| | Control | PIM | 1413 | 470 | 358 | 380 | 358 |
| | Control | PIM | 1744 | 516 | 336 | 358 | 336 |
| | Control | PIM | 2292 | 447 | 336 | 336 | 358 |
| | Control | PIM | 1413 | 493 | 314 | 358 | 314 |
| | Control | PIM | 882 | 293 | 208 | 229 | 229 |
| | Control | PIM | 1006 | 336 | 229 | 250 | 229 |
| | *Vhl* cKO | PIM | 3800 | 1106 | 824 | 742 | 882 |
| | *Vhl* cKO | PIM | 2292 | 742 | 424 | 564 | 613 |
| | *Vhl* cKO | PIM | 4481 | 1594 | 769 | 1038 | 974 |
| | *Vhl* cKO | PIM | 3926 | 1106 | 824 | 796 | 974 |
| | *Vhl* cKO | PIM | 1594 | 493 | 271 | 271 | 336 |
| | *Vhl* cKO | PIM | 1594 | 516 | 293 | 336 | 424 |
| | *Vhl* cKO | PIM | 1330 | 271 | 293 | 271 | 380 |

OB stage using the *Osx*-Cre (8) and *Ocn*-Cre (22) (targeting osteoprogenitors) and in MSCs, OBs and OCYs using *Dmp1*-Cre (23), increased bone mass and angiogenesis, likely through HIF1α-regulated expression of VEGF and EPO. If elevated EPO levels directly affect B cell development in the *Vhl*cKO BM has not yet been verified. However, it has been reported that ECs in the BM suppress levels of CXCL12 expression in response to increased EPO levels (91). We also observed decreased CXCL12 in the BM supernatant of *Vhl*cKO mice. CXCL12 is required for proper development and retention of B cells in the BM (29, 76). This suggests that altered vascular components in the *Vhl*cKO bone and BM microenvironments impair B cell development possibly through the effects of EPO on EC function.

Permeability of the BM vasculature in the *Vhl*cKO mice was also compromised. We found an increased vascular leakage and permeability in the *Vhl*cKO BM compared to controls regardless of age. In addition, vascular permeability appeared to increase with age, with the highest vascular permeability and leakage being observed in 6-month-old *Vhl*cKO mice when compared with 6-week-old mice. Interestingly, it was observed that vascular blood flow velocity decreased in 6-week-old and 10-week-old *Vhl*cKO mice but was not affected in 6-month-old *Vhl*cKO mice. An increase in blood flow velocity would normally explain an increase in permeability and leakage, but that is not evident in our data. Instead, the more likely explanation is that the blood-bone marrow barrier is compromised, increasing the exposure of the BM to plasma components.

Deletion of *Vhl* in B cells stabilizes *Hif1α* levels and affects mature B cell function by impairing cell proliferation, antibody class-switching, generation of high affinity antibodies, antibody responses, and impairs metabolic balance essential for naive B cell survival and development (58, 59, 92). Dynamic regulation of HIF-1α levels was also found to be a crucial step in B cell development in the BM (66). Burrows et al. found decreased *Hif*1α activity at the immature B cell stage in the BM and that HIF-1α suppression was required for normal B cell development (66). This dynamic regulation of HIF-1α activity during B cell development is consistent with our results, which revealed that Fraction A cells stain highly with PIM, and PIM staining was reduced as B cell development progressed to Fraction F. Together, our findings and that of Burrows et al. suggest that the earliest B cell stages (e.g. pre-pro B, Fraction A) might prefer a more hypoxic niche compared to the later B cell stages. Although *Vhl* is deleted in *Dmp1*-expressing cells in our model, we cannot yet rule out if this deletion is artificially causing changes that would be found in a true hypoxic state through *Hif1* stabilization, when in fact the oxygenation of the BM of the *Vhl*cKO is not altered. In addition, PIM cannot provide true quantification of dissolved oxygen concentration in tissue. PIM adduct staining results could reflect inadequate oxygen supply to the BM, faulty rates of intracellular oxygen consumption, or both. Direct *in vivo* measurement of oxygen tension using two-photon phosphorescence lifetime microscopy would help answer this question (11).

The information generated in this study helps define the role of *Vhl* and altered bone homeostasis on immune cell development. Our results suggest the following working model of the interactions in the BM microenvironment that controls B cell development (**Figure 9**): *Vhl* in *Dmp1*-expressing MSCs, OBs and OCYs plays a significant role in the BM microenvironment, indirectly regulating B cell development through a decrease in CXCL12, an increase in EPO, increased vasculature and vascular permeability. However, the oxygen levels in the *Vhl*cKO appear to be dynamic, such that developing Fraction A cells experience hypoxia in older, but not younger mice. We conclude that the B cell developmental defects in the BM of *Vhl*cKO mice are not initiated by dysregulated oxygen levels in the BM. However, direct measures of oxygen tension in the local niches of each Hardy B cell Fraction is yet to be performed (and is a goal for our future studies). Our results demonstrate the significant changes of the physical niche in *Vhl*cKO mice and their effects on B cell development. Whether the physical space, niche cells, or molecular signals all play a direct or indirect role on B cell development remains to be explored and defined, with the possibility that these events are completely independent of each other. The results of this work could contribute to the development of new therapies or new targets for exogenous CXCL12 and EPO antagonists, to preserve and improve bone marrow function during microenvironmental niche changes or stress.

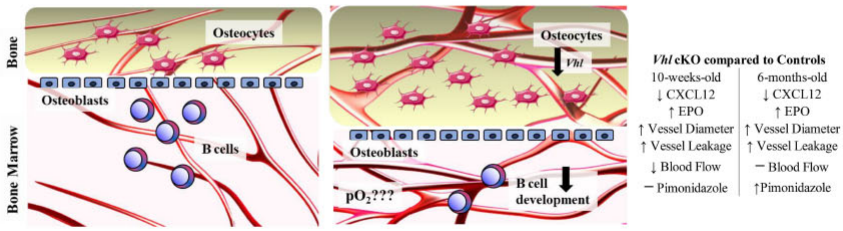


**FIGURE 9** | Working model describing the changes in the bone marrow microenvironment in *Vhl*cKO mice. Left panel: Schematic of healthy control bone marrow where VHL/HIF signaling is intact, the transition from osteoblasts to osteocytes is homeostatically balanced and interactions of developing B cells and stromal cells within their niches promotes their differentiation, maturation and proliferation. Right panel: Lack of *Vhl* in late osteoblasts and osteocytes has a severe effect on hematopoiesis in the bone marrow, changing the B cell niche and indirectly regulating B cell development through decrease of CXCL12, increase of EPO and changes to the BM microenvironment vasculature and permeability. Changes in the oxygen levels in the local niches for Fraction A cells do not occur until later ages, as shown by pimonidazole staining. Direct measurement of $pO_2$ in the BM is necessary to determine if the BM oxygenation landscape is altered compared to controls.

## DATA AVAILABILITY STATEMENT

The raw data supporting the conclusions of this article will be made available by the authors, without undue reservation.

## ETHICS STATEMENT

The animal study was reviewed and approved by University of California, Merced IACUC.

## AUTHOR CONTRIBUTIONS

BC, NA, CB, JS, and JM contributed to experimental design, data collection, analysis, and manuscript writing. HT contributed to data collection and analysis. JS and JM approved the final manuscript and are joint senior authors.

## FUNDING

This work was funded by the University of California, NIH grants R15 AI154245-01 (JM and JS) and NIH F31 AI154815 (BC), and through support of the NSF-CREST: Center for Cellular and Biomolecular Machines at the University of California, Merced (NSF-HRD-1547848; NA, CB, and JS).

## ACKNOWLEDGMENTS

We thank the staff of the Department of Animal Research Services (DARS) and the Stem Cell Instrumentation Foundry (SCIF) at UC Merced for the excellent animal care and technical support. We also acknowledge Hawa Padmore and William Pratcher for their early contributions to protocol setup. The authors also thank the staff of the Health Sciences Research Institute (HSRI) at UC Merced for their administrative support. A preprint of this manuscript was submitted to *BioRxiv* before peer-review (93).

## SUPPLEMENTARY MATERIAL

The Supplementary Material for this article can be found online at: https://www.frontiersin.org/articles/10.3389/fimmu.2022.780945/full#supplementary-material

**Supplementary Videos 1, 2** | Representative ex vivo Videos recorded in the uDISCO cleared long bone BM.

**Supplementary Video 1** | Representative 10-week-old Control uDISCO cleared long bone Z stack (scale bar ~200 µm).

**Supplementary Video 2** | Representative 10-week-old Control uDISCO cleared long bone 3D view (scale bar ~100 µm).

**Supplementary Videos 3-8** | Representative Leakage Videos recorded in the calvaria BM. Representative zstacks of the calvaria BM recorded 10 minutes after Rhodamine B Dextran injection. Z step size is 2 µm and scale bars ~50 µm. Green Channel = bone (SHG), Blue = Rhodamine-B-Dextran (70 kDa). Brightness/Contrast adjusted for display only.

**Supplementary Video 3** | Representative 6-week-old Control Leakage Zstack.

**Supplementary Video 4** | Representative 6-week-old VhlcKO Leakage Zstack.

**Supplementary Video 5** | Representative 10-week-old Control Leakage Zstack.

**Supplementary Video 6** | Representative 10-week-old VhlcKO Leakage Zstack.

**Supplementary Video 7** | Representative 6-month-old Control Leakage Zstack.

**Supplementary Video 8** | Representative 6-month-old VhlcKO Leakage Zstack.

**Supplementary Videos 9, 10** | Representative permeability videos recorded in the calvaria BM. Representative video of the calvaria BM permeability recorded immediately after Rhodamine-B-Dextran injection. Scale bars ~50 µm. Brightness/Contrast adjusted for display only.

**Supplementary Video 9** | Representative 6-week-old Control Permeability Video.

**Supplementary Video 10** | Representative 6-week-old VhlcKO Permeability Video.

## REFERENCES


1. Nagasawa T. Microenvironmental Niches in the Bone Marrow Required for B-Cell Development. *Nat Rev Immunol* (2006) 6:107–16. doi: 10.1038/nri1780
2. Manilay JO, Zouali M. Tight Relationships Between B Lymphocytes and the Skeletal System. *Trends Mol Med* (2014) 20:405–12. doi: 10.1016/j.molmed.2014.03.003
3. Panaroni C, Wu JY. Interactions Between B Lymphocytes and the Osteoblast Lineage in Bone Marrow. *Calcif Tissue Int* (2013) 93:261–8. doi: 10.1007/s00223-013-9753-3
4. Aurrand-Lions M, Mancini SJC. Murine Bone Marrow Niches From Hematopoietic Stem Cells to B Cells. *Int J Mol Sci* (2018) 19(8):2353. doi: 10.3390/ijms19082353
5. Carsetti R. The Development of B Cells in the Bone Marrow is Controlled by the Balance Between Cell-Autonomous Mechanisms and Signals From the Microenvironment. *J Exp Med* (2000) 191:5–8. doi: 10.1084/jem.191.1.5
6. Haase VH. The VHL Tumor Suppressor: Master Regulator of HIF. *Curr Pharm Des* (2009) 15:3895–903. doi: 10.2174/138161209789649394
7. Wang Y, Wan C, Deng L, Liu X, Cao X, Gilbert SR, et al. The Hypoxia-Inducible Factor Alpha Pathway Couples Angiogenesis to Osteogenesis During Skeletal Development. *J Clin Invest* (2007) 117:1616–26. doi: 10.1172/JCI31581
8. Dirckx N, Tower RJ, Mercken EM, Vangoitsenhoven R, Moreau-Triby C, Breugelmans T, et al. Vhl Deletion in Osteoblasts Boosts Cellular Glycolysis and Improves Global Glucose Metabolism. *J Clin Invest* (2018) 128:1087–105. doi: 10.1172/JCI97794
9. Takubo K, Goda N, Yamada W, Iriuchishima H, Ikeda E, Kubota Y, et al. Regulation of the HIF-1alpha Level is Essential for Hematopoietic Stem Cells. *Cell Stem Cell* (2010) 7:391–402. doi: 10.1016/j.stem.2010.06.020
10. Bader HL, Hsu T. Systemic VHL Gene Functions and the VHL Disease. *FEBS Lett* (2012) 586:1562–9. doi: 10.1016/j.febslet.2012.04.032
11. Spencer JA, Ferraro F, Roussakis E, Klein A, Wu J, Runnels JM, et al. Direct Measurement of Local Oxygen Concentration in the Bone Marrow of Live Animals. *Nature* (2014) 508:269–73. doi: 10.1038/nature13034
12. Christodoulou C, Spencer JA, Yeh SA, Turcotte R, Kokkaliaris KD, Panero R, et al. Live-Animal Imaging of Native Haematopoietic Stem and Progenitor Cells. *Nature* (2020) 578:278–83. doi: 10.1038/s41586-020-1971-z
13. Rytelewski M, Harutyunyan K, Baran N, Mallampati S, Zal MA, Cavazos A, et al. Inhibition of Oxidative Phosphorylation Reverses Bone Marrow Hypoxia Visualized in Imageable Syngeneic B-ALL Mouse Model. *Front Oncol* (2020) 10:991. doi: 10.3389/fonc.2020.00991
14. Hirao M, Hashimoto J, Yamasaki N, Ando W, Tsuboi H, Myoui A, et al. Oxygen Tension is an Important Mediator of the Transformation of Osteoblasts to Osteocytes. *J Bone Miner Metab* (2007) 25:266–76. doi: 10.1007/s00774-007-0765-9
15. Knowles HJ. Hypoxic Regulation of Osteoclast Differentiation and Bone Resorption Activity. *Hypoxia (Auckl)* (2015) 3:73–82. doi: 10.2147/HP.S95960
16. Komatsu DE, Hadjiargyrou M. Activation of the Transcription Factor HIF-1 and its Target Genes, VEGF, HO-1, iNOS, During Fracture Repair. *Bone* (2004) 34:680–8. doi: 10.1016/j.bone.2003.12.024
17. Danis A. [Mechanism of Bone Lengthening by the Ilizarov Technique]. *Bull Mem Acad R Med Belg* (2001) 156:107–12. doi: 10.1155/2014/239356
18. Zhao Q, Shen X, Zhang W, Zhu G, Qi J, Deng L. Mice With Increased Angiogenesis and Osteogenesis Due to Conditional Activation of HIF Pathway in Osteoblasts are Protected From Ovariectomy Induced Bone Loss. *Bone* (2012) 50:763–70. doi: 10.1016/j.bone.2011.12.003
19. Tando T, Sato Y, Miyamoto K, Morita M, Kobayashi T, Funayama A, et al. Hif1alpha is Required for Osteoclast Activation and Bone Loss in Male Osteoporosis. *Biochem Biophys Res Commun* (2016) 470:391–6. doi: 10.1016/j.bbrc.2016.01.033
20. Miyauchi Y, Sato Y, Kobayashi T, Yoshida S, Mori T, Kanagawa H, et al. HIF1alpha is Required for Osteoclast Activation by Estrogen Deficiency in Postmenopausal Osteoporosis. *Proc Natl Acad Sci USA* (2013) 110:16568–73. doi: 10.1073/pnas.1308755110
21. Loots GG, Robling AG, Chang JC, Murugesh DK, Bajwa J, Carlisle C, et al. Vhl Deficiency in Osteocytes Produces High Bone Mass and Hematopoietic Defects. *Bone* (2018) 116:307–14. doi: 10.1016/j.bone.2018.08.022
22. Weng T, Xie Y, Huang J, Luo F, Yi L, He Q, et al. Inactivation of Vhl in Osteochondral Progenitor Cells Causes High Bone Mass Phenotype and Protects Against Age-Related Bone Loss in Adult Mice. *J Bone Miner Res* (2014) 29:820–9. doi: 10.1002/jbmr.2087
23. Zuo GL, Zhang LF, Qi J, Kang H, Jia P, Chen H, et al. Activation of HIFa Pathway in Mature Osteoblasts Disrupts the Integrity of the Osteocyte/Canalicular Network. *PloS One* (2015) 10:e0121266. doi: 10.1371/journal.pone.0121266
24. Wan C, Gilbert SR, Wang Y, Cao X, Shen X, Ramaswamy G, et al. Activation of the Hypoxia-Inducible Factor-1alpha Pathway Accelerates Bone Regeneration. *Proc Natl Acad Sci USA* (2008) 105:686–91. doi: 10.1073/pnas.0708474105
25. Silberstein L. B Cells: Fed and Grown in the Bone. *Blood* (2021) 138:286–7. doi: 10.1182/blood.2021011855
26. Kwang D, Tjin G, Purton LE. Regulation of Murine B Lymphopoiesis by Stromal Cells. *Immunol Rev* (2021) 302:47–67. doi: 10.1111/imr.12973
27. Egawa T, Kawabata K, Kawamoto H, Amada K, Okamoto R, Fujii N, et al. The Earliest Stages of B Cell Development Require a Chemokine Stromal Cell-Derived Factor/Pre-B Cell Growth-Stimulating Factor. *Immunity* (2001) 15:323–34. doi: 10.1016/S1074-7613(01)00185-6
28. Nagasawa T, Hirota S, Tachibana K, Takakura N, Nishikawa S, Kitamura Y, et al. Defects of B-Cell Lymphopoiesis and Bone-Marrow Myelopoiesis in Mice Lacking the CXC Chemokine PBSF/SDF-1. *Nature* (1996) 382:635–8. doi: 10.1038/382635a0
29. Tokoyoda K, Egawa T, Sugiyama T, Choi BI, Nagasawa T. Cellular Niches Controlling B Lymphocyte Behavior Within Bone Marrow During Development. *Immunity* (2004) 20:707–18. doi: 10.1016/j.immuni.2004.05.001
30. Sitnicka E, Brakebusch C, Martensson IL, Svensson M, Agace WW, Sigvardsson M, et al. Complementary Signaling Through Flt3 and Interleukin-7 Receptor Alpha is Indispensable for Fetal and Adult B Cell Genesis. *J Exp Med* (2003) 198:1495–506. doi: 10.1084/jem.20031152
31. McNiece IK, Langley KE, Zsebo KM. The Role of Recombinant Stem Cell Factor in Early B Cell Development. Synergistic Interaction With IL-7. *J Immunol* (1991) 146:3785–90.
32. von Freeden-Jeffry U, Vieira P, Lucian LA, McNeil T, Burdach SE, Murray R. Lymphopenia in Interleukin (IL)-7 Gene-Deleted Mice Identifies IL-7 as a Nonredundant Cytokine. *J Exp Med* (1995) 181:1519–26. doi: 10.1084/jem.181.4.1519
33. Dias S, Silva H Jr, Cumano A, Vieira P. Interleukin-7 is Necessary to Maintain the B Cell Potential in Common Lymphoid Progenitors. *J Exp Med* (2005) 201:971–9. doi: 10.1084/jem.20042393
34. Dougall WC, Glaccum M, Charrier K, Rohrbach K, Brasel K, De Smedt T, et al. RANK is Essential for Osteoclast and Lymph Node Development. *Genes Dev* (1999) 13:2412–24. doi: 10.1101/gad.13.18.2412
35. Cariappa A, Mazo IB, Chase C, Shi HN, Liu H, Li Q, et al. Perisinusoidal B Cells in the Bone Marrow Participate in T-Independent Responses to Blood-Borne Microbes. *Immunity* (2005) 23:397–407. doi: 10.1016/j.immuni.2005.09.004
36. Mourcin F, Breton C, Tellier J, Narang P, Chasson L, Jorquera A, et al. Galectin-1-Expressing Stromal Cells Constitute a Specific Niche for Pre-BII Cell Development in Mouse Bone Marrow. *Blood* (2011) 117:6552–61. doi: 10.1182/blood-2010-12-323113
37. Green AC, Tjin G, Lee SC, Chalk AM, Straszkowski L, Kwang D, et al. The Characterization of Distinct Populations of Murine Skeletal Cells That Have Different Roles in B Lymphopoiesis. *Blood* (2021) 138(4):304–17. doi: 10.1182/blood.2020005865
38. Xu X, Wang B, Ren C, Hu J, Greenberg DA, Chen T, et al. Age-Related Impairment of Vascular Structure and Functions. *Aging Dis* (2017) 8:590–610. doi: 10.14336/AD.2017.0430
39. Kusumbe AP, Ramasamy SK, Itkin T, Mae MA, Langen UH, Betsholtz C, et al. Age-Dependent Modulation of Vascular Niches for Haematopoietic Stem Cells. *Nature* (2016) 532:380–4. doi: 10.1038/nature17638
40. Alberts B, Johnson A, Lewis J, Raff M, Roberts K, Walter P, et al. Blood Vessels and Endothelial Cells. In: *Molecular Biology of the Cell, 4th edition*. New York: Garland Science (2002).
41. Ungvari Z, Tarantini S, Kiss T, Wren JD, Giles CB, Griffin CT, et al. Endothelial Dysfunction and Angiogenesis Impairment in the Ageing Vasculature. *Nat Rev Cardiol* (2018) 15:555–65. doi: 10.1038/s41569-018-0030-z
42. Oakley R, Tharakan B. Vascular Hyperpermeability and Aging. *Aging Dis* (2014) 5:114–25. doi: 10.14336/ad.2014.0500114

43. Dallas SL, Xie Y, Shiflett LA, Ueki Y. Mouse Cre Models for the Study of Bone Diseases. *Curr Osteoporos Rep* (2018) 16:466–77. doi: 10.1007/s11914-018-0455-7
44. Faul F, Erdfelder E, Lang AG, Buchner A. G*Power 3: A Flexible Statistical Power Analysis Program for the Social, Behavioral, and Biomedical Sciences. *Behav Res Methods* (2007) 39:175–91. doi: 10.3758/BF03193146
45. Lu Y, Xie Y, Zhang S, Dusevich V, Bonewald LF, Feng JQ. DMP1-Targeted Cre Expression in Odontoblasts and Osteocytes. *J Dent Res* (2007) 86:320–5. doi: 10.1177/154405910708600404
46. Haase VH, Glickman JN, Socolovsky M, Jaenisch R. Vascular Tumors in Livers With Targeted Inactivation of the Von Hippel-Lindau Tumor Suppressor. *Proc Natl Acad Sci USA* (2001) 98:1583–8. doi: 10.1073/pnas.98.4.1583
47. Cain CJ, Rueda R, McLelland B, Collette NM, Loots GG, Manilay JO. Absence of Sclerostin Adversely Affects B-Cell Survival. *J Bone Miner Res* (2012) 27:1451–61. doi: 10.1002/jbmr.1608
48. Gravano DM, Manilay JO. Inhibition of Proteolysis of Delta-Like-1 Does Not Promote or Reduce T-Cell Developmental Potential. *Immunol Cell Biol* (2010) 88:746–53. doi: 10.1038/icb.2010.30
49. Pan C, Cai R, Quacquarelli FP, Ghasemigharagoz A, Lourbopoulos A, Matryba P, et al. Shrinkage-Mediated Imaging of Entire Organs and Organisms Using uDISCO. *Nat Methods* (2016) 13:859–67. doi: 10.1038/nmeth.3964
50. Sipkins DA, Wei X, Wu JW, Runnels JM, Cote D, Means TK, et al. *In Vivo* Imaging of Specialized Bone Marrow Endothelial Microdomains for Tumour Engraftment. *Nature* (2005) 435:969–73. doi: 10.1038/nature03703
51. Itkin T, Gur-Cohen S, Spencer JA, Schajnovitz A, Ramasamy SK, Kusumbe AP, et al. Distinct Bone Marrow Blood Vessels Differentially Regulate Haematopoiesis. *Nature* (2016) 532:323–8. doi: 10.1038/nature17624
52. Jung Y, Spencer JA, Raphael AP, Wu JW, Alt C, Runnels JR, et al. Intravital Imaging of Mouse Bone Marrow: Hemodynamics and Vascular Permeability. *Methods Mol Biol* (2018) 1763:11–22. doi: 10.1007/978-1-4939-7762-8_2
53. Kim TN, Goodwill PW, Chen Y, Conolly SM, Schaffer CB, Liepmann D, et al. Line-Scanning Particle Image Velocimetry: An Optical Approach for Quantifying a Wide Range of Blood Flow Speeds in Live Animals. *PloS One* (2012) 7:e38590. doi: 10.1371/journal.pone.0038590
54. Wu JW, Jung Y, Yeh SA, Seo Y, Runnels JM, Burns CS, et al. Intravital Fluorescence Microscopy With Negative Contrast. *PloS One* (2021) 16: e0255204. doi: 10.1371/journal.pone.0255204
55. Pietras EM, Reynaud D, Kang YA, Carlin D, Calero-Nieto FJ, Leavitt AD, et al. Functionally Distinct Subsets of Lineage-Biased Multipotent Progenitors Control Blood Production in Normal and Regenerative Conditions. *Cell Stem Cell* (2015) 17:35–46. doi: 10.1016/j.stem.2015.05.003
56. Cheng H, Zheng Z, Cheng T. New Paradigms on Hematopoietic Stem Cell Differentiation. *Protein Cell* (2019) 11:34–44. doi: 10.1007/s13238-019-0633-0
57. Hardy RR, Carmack CE, Shinton SA, Kemp JD, Hayakawa K. Resolution and Characterization of Pro-B and Pre-Pro-B Cell Stages in Normal Mouse Bone Marrow. *J Exp Med* (1991) 173:1213–25. doi: 10.1084/jem.173.5.1213
58. Cho SH, Raybuck AL, Stengel K, Wei M, Beck TC, Volanakis E, et al. Germinal Centre Hypoxia and Regulation of Antibody Qualities by a Hypoxia Response System. *Nature* (2016) 537:234–8. doi: 10.1038/nature19334
59. Xu S, Huo J, Huang Y, Aw M, Chen S, Mak S, et al. Von Hippel-Lindau Protein Maintains Metabolic Balance to Regulate the Survival of Naive B Lymphocytes. *iScience* (2019) 17:379–92. doi: 10.1016/j.isci.2019.07.002
60. Lu LW, Osmond DG. Apoptosis and its Modulation During B Lymphopoiesis in Mouse Bone Marrow. *Immunol Rev* (2000) 175:158–74. doi: 10.1111/j.1600-065X.2000.imr017506.x
61. Markus Werner HJ. Chapter 6 - Proliferation and Differentiation Programs of Developing B Cells. In: *Molecular Biology of B Cells, 2nd ed*. London: Academic Press (2015). p. 75–97. doi: 10.1016/B978-0-12-397933-9.00006-0
62. Rolink A, Haasner D, Melchers F, Andersson J. The Surrogate Light Chain in Mouse B-Cell Development. *Int Rev Immunol* (1996) 13:341–56. doi: 10.3109/08830189609061757
63. Melchers F. Checkpoints That Control B Cell Development. *J Clin Invest* (2015) 125:2203–10. doi: 10.1172/JCI78083
64. Schepers K, Hsiao EC, Garg T, Scott MJ, Passegue E. Activated Gs Signaling in Osteoblastic Cells Alters the Hematopoietic Stem Cell Niche in Mice. *Blood* (2012) 120:3425–35. doi: 10.1182/blood-2011-11-395418
65. Kita K, Kawai K, Hirohata K. Changes in Bone Marrow Blood Flow With Aging. *J Orthop Res* (1987) 5:569–75. doi: 10.1002/jor.1100050412
66. Burrows N, Bashford-Rogers RJM, Bhute VJ, Penalver A, Ferdinand JR, Stewart BJ, et al. Dynamic Regulation of Hypoxia-Inducible Factor-1alpha Activity Is Essential for Normal B Cell Development. *Nat Immunol* (2020) 21:1408–20. doi: 10.1038/s41590-020-0772-8
67. Parmar K, Mauch P, Vergilio JA, Sackstein R, Down JD. Distribution of Hematopoietic Stem Cells in the Bone Marrow According to Regional Hypoxia. *Proc Natl Acad Sci USA* (2007) 104:5431–6. doi: 10.1073/pnas.0701152104
68. Nombela-Arrieta C, Pivarnik G, Winkel B, Canty KJ, Harley B, Mahoney JE, et al. Quantitative Imaging of Haematopoietic Stem and Progenitor Cell Localization and Hypoxic Status in the Bone Marrow Microenvironment. *Nat Cell Biol* (2013) 15:533–43. doi: 10.1038/ncb2730
69. Rolink A, ten Boekel E, Melchers F, Fearon DT, Krop I, Andersson J. A Subpopulation of B220+ Cells in Murine Bone Marrow Does Not Express CD19 and Contains Natural Killer Cell Progenitors. *J Exp Med* (1996) 183:187–94. doi: 10.1084/jem.183.1.187
70. Balciunaite G, Ceredig R, Massa S, Rolink AG. A B220+ CD117+ CD19- Hematopoietic Progenitor With Potent Lymphoid and Myeloid Developmental Potential. *Eur J Immunol* (2005) 35:2019–30. doi: 10.1002/eji.200526318
71. Nikolic T, Dingjan GM, Leenen PJM, Hendriks RW. A Subfraction of B220+ Cells in Murine Bone Marrow and Spleen Does Not Belong to the B Cell Lineage But has Dendritic Cell Characteristics. *Eur J Immunol* (2002) 32 (3):686–92. doi: 10.1002/1521-4141(200203)32:3<686::AID-IMMU686>3.0.CO;2-I
72. Blasius AL, Barchet W, Cella M, Colonna M. Development and Function of Murine B220+CD11c+NK1.1+ Cells Identify Them as a Subset of NK Cells. *J Exp Med* (2007) 204:2561–8. doi: 10.1084/jem.20070991
73. Hardy RR, Kincade PW, Dorshkind K. The Protean Nature of Cells in the B Lymphocyte Lineage. *Immunity* (2007) 26:703–14. doi: 10.1016/j.immuni.2007.05.013
74. Yee CS, Manilay JO, Chang JC, Hum NR, Murugesh DK, Bajwa J, et al. Conditional Deletion of Sost in MSC-Derived Lineages Identifies Specific Cell Type Contributions to Bone Mass and B Cell Development. *J Bone Miner Res* (2018) 33(10):1748–59. doi: 10.1002/jbmr.3467
75. Ding L, Morrison SJ. Haematopoietic Stem Cells and Early Lymphoid Progenitors Occupy Distinct Bone Marrow Niches. *Nature* (2013) 495:231–5. doi: 10.1038/nature11885
76. Greenbaum A, Hsu YM, Day RB, Schuettpelz LG, Christopher MJ, Borgerding JN, et al. CXCL12 in Early Mesenchymal Progenitors is Required for Haematopoietic Stem-Cell Maintenance. *Nature* (2013) 495:227–30. doi: 10.1038/nature11926
77. Méndez-Ferrer S, Michurina TV, Ferraro F, Mazloom AR, Macarthur BD, Lira SA, et al. Mesenchymal and Haematopoietic Stem Cells Form a Unique Bone Marrow Niche. *Nature* (2010) 466:829–34. doi: 10.1038/nature09262
78. Zhu J, Garrett R, Jung Y, Zhang Y, Kim N, Wang J, et al. Osteoblasts Support B-Lymphocyte Commitment and Differentiation From Hematopoietic Stem Cells. *Blood* (2007) 109:3706–12. doi: 10.1182/blood-2006-08-041384
79. Wu JY, Purton LE, Rodda SJ, Chen M, Weinstein LS, McMahon AP, et al. Osteoblastic Regulation of B Lymphopoiesis is Mediated by Gs{alpha}-Dependent Signaling Pathways. *Proc Natl Acad Sci USA* (2008) 105:16976–81. doi: 10.1073/pnas.0802898105
80. Martin SK, Fitter S, Khawanky N, Grose RH, Walkley CR, Purton LE, et al. Mtorc1 Plays an Important Role in Osteoblastic Regulation of B-Lymphopoiesis. *Sci Rep* (2018) 8:14501. doi: 10.1038/s41598-018-32858-5
81. Asari S, Itakura S, Ferreri K, Liu CP, Kuroda Y, Kandeel F, et al. Mesenchymal Stem Cells Suppress B-Cell Terminal Differentiation. *Exp Hematol* (2009) 37:604–15. doi: 10.1016/j.exphem.2009.01.005
82. Tabera S, Pérez-Simón JA, Diez-Campelo M, Sánchez-Abarca LI, Blanco B, López A, et al. The Effect of Mesenchymal Stem Cells on the Viability, Proliferation and Differentiation of B-Lymphocytes. *Haematologica* (2008) 93:1301–9. doi: 10.3324/haematol.12857
83. Traggiai E, Volpi S, Schena F, Gattorno M, Ferlito F, Moretta L, et al. Bone Marrow-Derived Mesenchymal Stem Cells Induce Both Polyclonal Expansion and Differentiation of B Cells Isolated From Healthy Donors and Systemic Lupus Erythematosus Patients. *Stem Cells* (2008) 26:562–9. doi: 10.1634/stemcells.2007-0528

84. Dasgupta K, Lessard S, Hann S, Fowler ME, Robling AG, Warman ML. Sensitive Detection of Cre-Mediated Recombination Using Droplet Digital PCR Reveals Tg(BGLAP-Cre) and Tg(DMP1-Cre) are Active in Multiple non-Skeletal Tissues. *Bone* (2020) 142:115674. doi: 10.1016/j.bone.2020.115674
85. Lim J, Burclaff J, He G, Mills JC, Long F. Unintended Targeting of Dmp1-Cre Reveals a Critical Role for Bmpr1a Signaling in the Gastrointestinal Mesenchyme of Adult Mice. *Bone Res* (2017) 5:16049. doi: 10.1038/boneres.2016.49
86. Mangiavini L, Merceron C, Araldi E, Khatri R, Gerard-O'Riley R, Wilson TL, et al. Loss of VHL in Mesenchymal Progenitors of the Limb Bud Alters Multiple Steps of Endochondral Bone Development. *Dev Biol* (2014) 393:124–36. doi: 10.1016/j.ydbio.2014.06.013
87. Rankin EB, Wu C, Khatri R, Wilson TL, Andersen R, Araldi E, et al. The HIF Signaling Pathway in Osteoblasts Directly Modulates Erythropoiesis Through the Production of EPO. *Cell* (2012) 149:63–74. doi: 10.1016/j.cell.2012.01.051
88. Tikhonova AN, Dolgalev I, Hu H, Sivaraj KK, Hoxha E, Cuesta-Dominguez A, et al. The Bone Marrow Microenvironment at Single-Cell Resolution. *Nature* (2019) 569:222–8. doi: 10.1038/s41586-019-1104-8
89. Baryawno N, Przybylski D, Kowalczyk MS, Kfoury Y, Severe N, Gustafsson K, et al. A Cellular Taxonomy of the Bone Marrow Stroma in Homeostasis and Leukemia. *Cell* (2019) 177:1915–32.e1916. doi: 10.1016/j.cell.2019.04.040
90. Wolock SL, Krishnan I, Tenen DE, Matkins V, Camacho V, Patel S, et al. Mapping Distinct Bone Marrow Niche Populations and Their Differentiation Paths. *Cell Rep* (2019) 28:302–11.e305. doi: 10.1016/j.celrep.2019.06.031
91. Ito T, Hamazaki Y, Takaori-Kondo A, Minato N. Bone Marrow Endothelial Cells Induce Immature and Mature B Cell Egress in Response to Erythropoietin. *Cell Struct Funct* (2017) 42:149–57. doi: 10.1247/csf.17018
92. Kojima H, Kobayashi A, Sakurai D, Kanno Y, Hase H, Takahashi R, et al. Differentiation Stage-Specific Requirement in Hypoxia-Inducible Factor-1alpha-Regulated Glycolytic Pathway During Murine B Cell Development in Bone Marrow. *J Immunol* (2010) 184:154–63. doi: 10.4049/jimmunol.0800167
93. Chicana B, Abbasizadeh N, Burns C, Taglinao H, Spencer JA, Manilay JO. Deletion of Vhl in Dmp1-Expressing Cells Causes Microenvironmental Impairment of B Cell Lymphopoiesis. *bioRxiv* (2021). doi: 10.1101/2021.09.10.459794

**Conflict of Interest:** The authors declare that the research was conducted in the absence of any commercial or financial relationships that could be construed as a potential conflict of interest.

**Publisher's Note:** All claims expressed in this article are solely those of the authors and do not necessarily represent those of their affiliated organizations, or those of the publisher, the editors and the reviewers. Any product that may be evaluated in this article, or claim that may be made by its manufacturer, is not guaranteed or endorsed by the publisher.

*Copyright © 2022 Chicana, Abbasizadeh, Burns, Taglinao, Spencer and Manilay. This is an open-access article distributed under the terms of the Creative Commons Attribution License (CC BY). The use, distribution or reproduction in other forums is permitted, provided the original author(s) and the copyright owner(s) are credited and that the original publication in this journal is cited, in accordance with accepted academic practice. No use, distribution or reproduction is permitted which does not comply with these terms.*

# Supplemental figures of Chicana et al. 2022

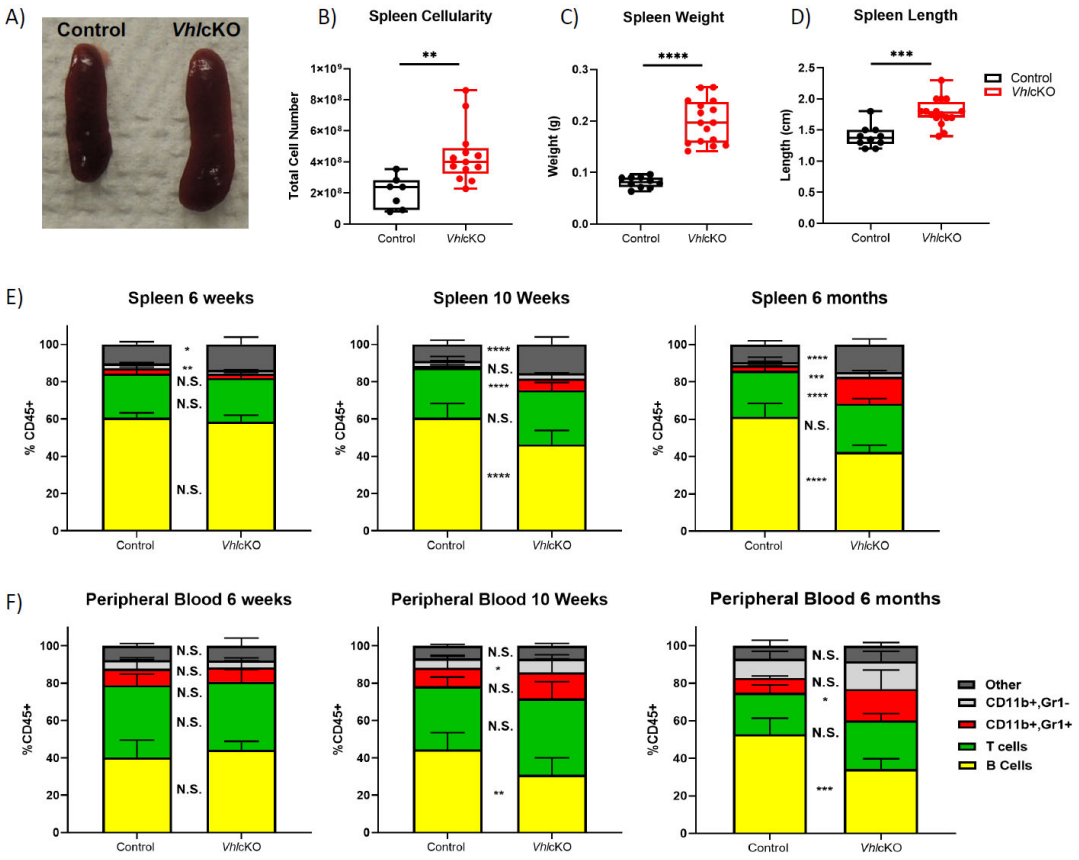


**Supplemental Figure 1. Analysis of hematopoietic lineages and cellularity in the spleen of *Vhlc*KO mice.** A) White light image of spleens, scale bar: 1cm; B) spleen cellularity; C) spleen weights; D) spleen length; E) spleen and F) peripheral blood lineage frequency at 6-weeks-old (left), 10-weeks-old (middle), and 6-months-old (right). *p<0.05, **p<0.01,***p<0.001, ****p<0.0001, two-tailed Student's t-test.

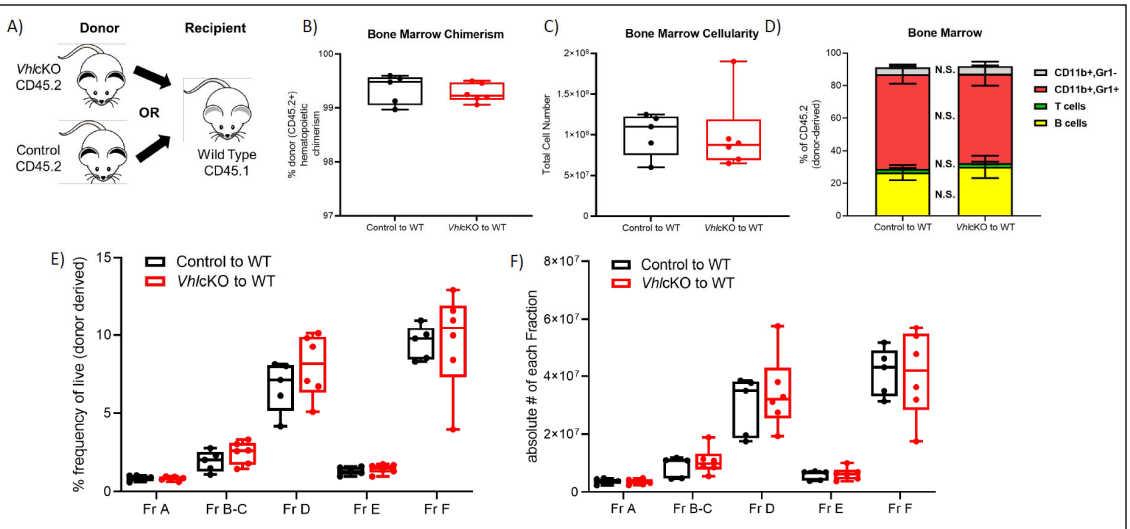


**Supplemental Figure 2. Evidence against cell-intrinsic effects of *Vhl* deletion on B cell development in *Vhl*cKO mice.** A) Experimental scheme. Mice were transplanted at 10 weeks of age and were 26 weeks old at time of analysis. B) donor (CD45.2+) chimerism; C) bone marrow cellularity; D) frequency of lineage cells in bone marrow; E) frequency and F) absolute numbers of B cell developmental stages in chimeras 16 weeks post-transplant. N.S. not statistically significant; two-tailed Student's t-test.

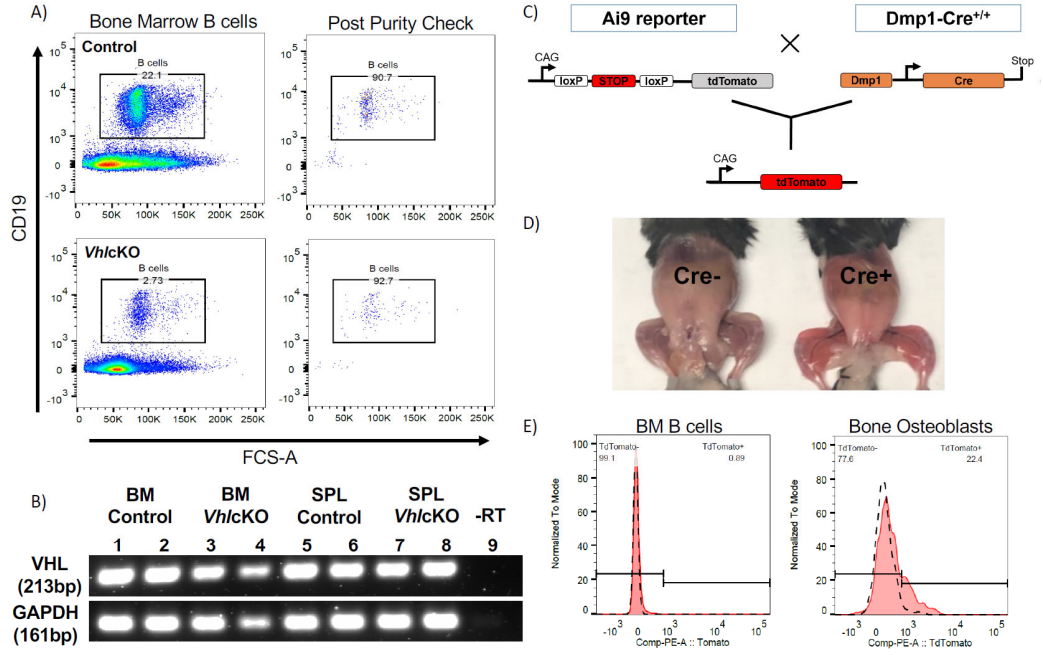


**Supplemental Figure 3. Validation of *Vhl* expression in B cells in *Vhl*cKO mice and expression of *Dmp1*-Cre using Ai9 reporter mice** A) Bone marrow CD19+ B lymphocyte percentages pre- and post- sorting from control and *Vhl*cKO mice and B) PCR validation of *Vhl* and *Gapdh* gene expression in DNA of sorted B cells (Live, CD19+), demonstrating *Vhl* is intact in B cells in the *Vhl*cKO; C) reporter cross of *Dmp1*-Cre mice with Ai9 (tdTomato) mice; D) tdTomato expression in *Dmp1*-Cre;Ai9 mice; E) flow cytometry measurement of tdTomato on BM B cells and osteoblasts (Lin-, CD45-, CD31-, Sca1-, CD51+) in *Dmp1*-Cre;Ai9 mice.

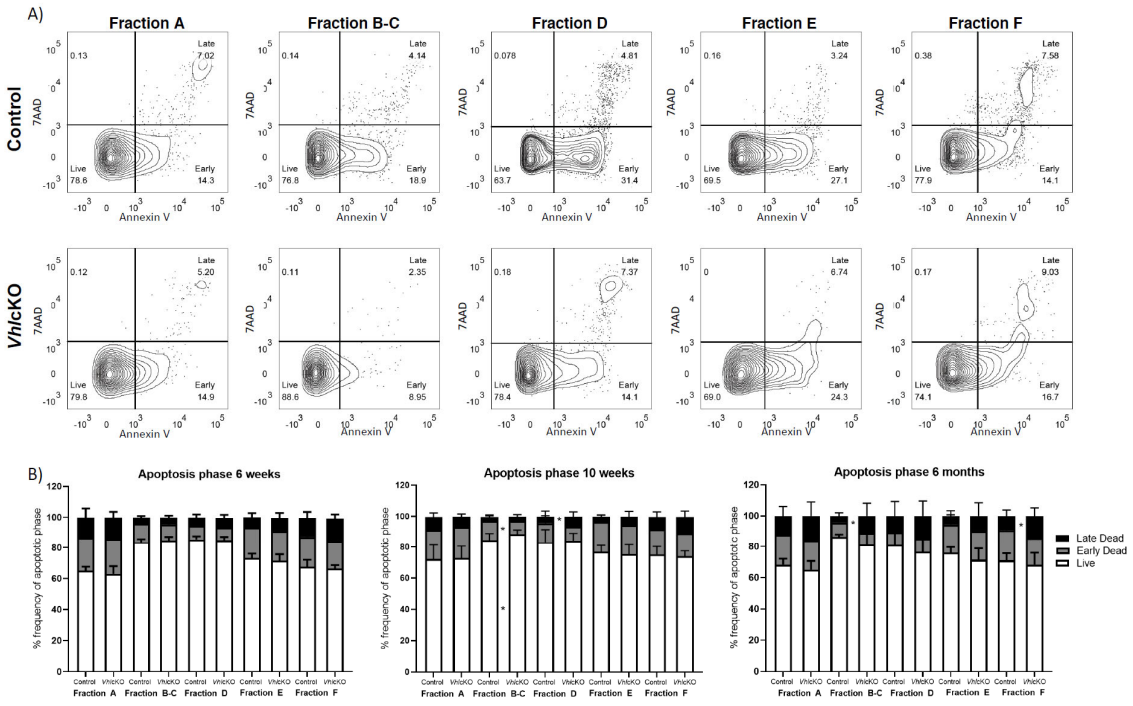


**Supplemental Figure 4. Apoptosis analysis of B cell Fractions A-F** A) Representative FACS plot of apoptotic phases in control (top) and *Vhl*cKO (bottom) at 10-weeks-old; B) frequency of apoptotic phase in Fractions A-F in 6-weeks-old, 10-weeks-old and 6-month-old mice; $p<0.05$*; two-tailed Student's t-test.

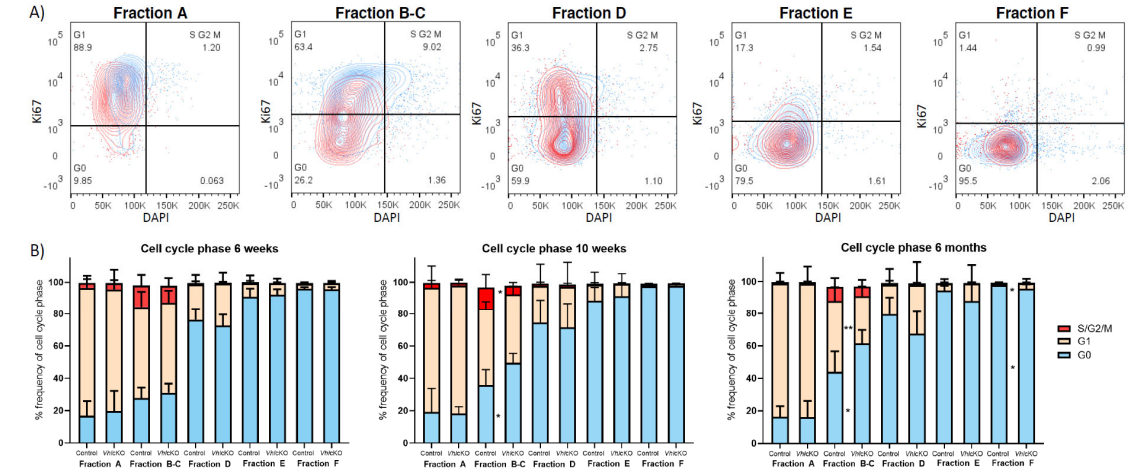


**Supplemental Figure 5. Proliferation analysis of B cell Fractions A-F** A) Representative FACS plot of cell cycle analysis in Fractions A-F cells (red: *Vhl*cKO blue: control) in 10-weeks-old mice; B) frequency of cells in each cell cycle phase within Fractions A-F at 6-weeks-old, 10-weeks-old old and 6-month-old mice. $p<0.05$*, $p<0.01$**; two-tailed Student's t-test.

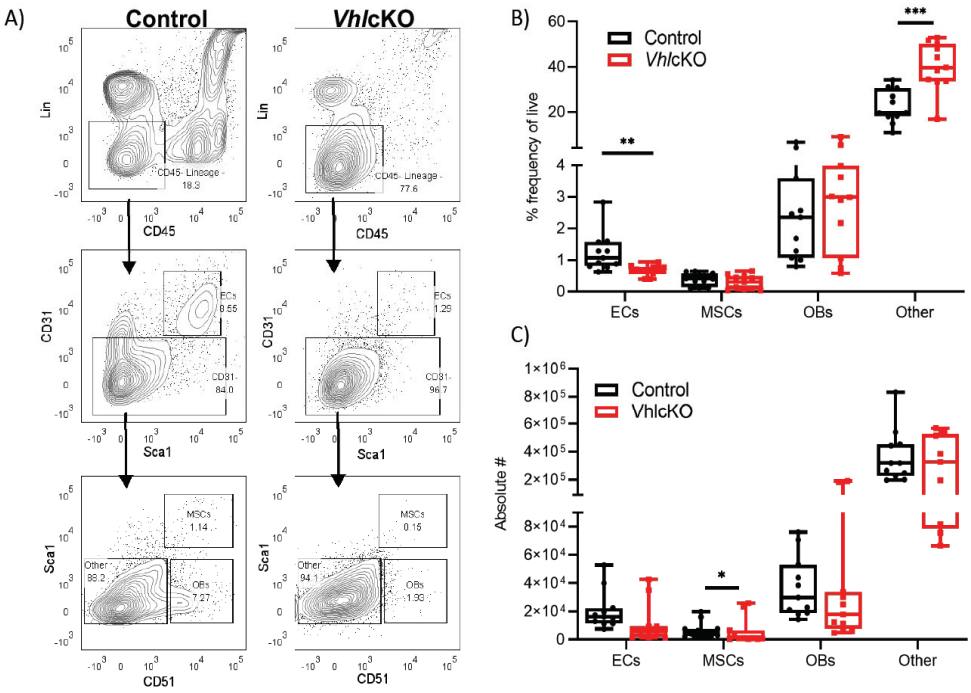


**Supplemental Figure 6. Flow cytometric analysis of *Vhl*cKO bones**. A) Flow cytometry gating strategy for bone niche cells (ECs, MSCs, OBs) after 2hr bone digest; B) frequencies and C) absolute numbers of each cell subset out of the live cell gate (not shown). $p<0.05$*, $p<0.01$**, $p<0.001$*** two-tailed Student's t-test.

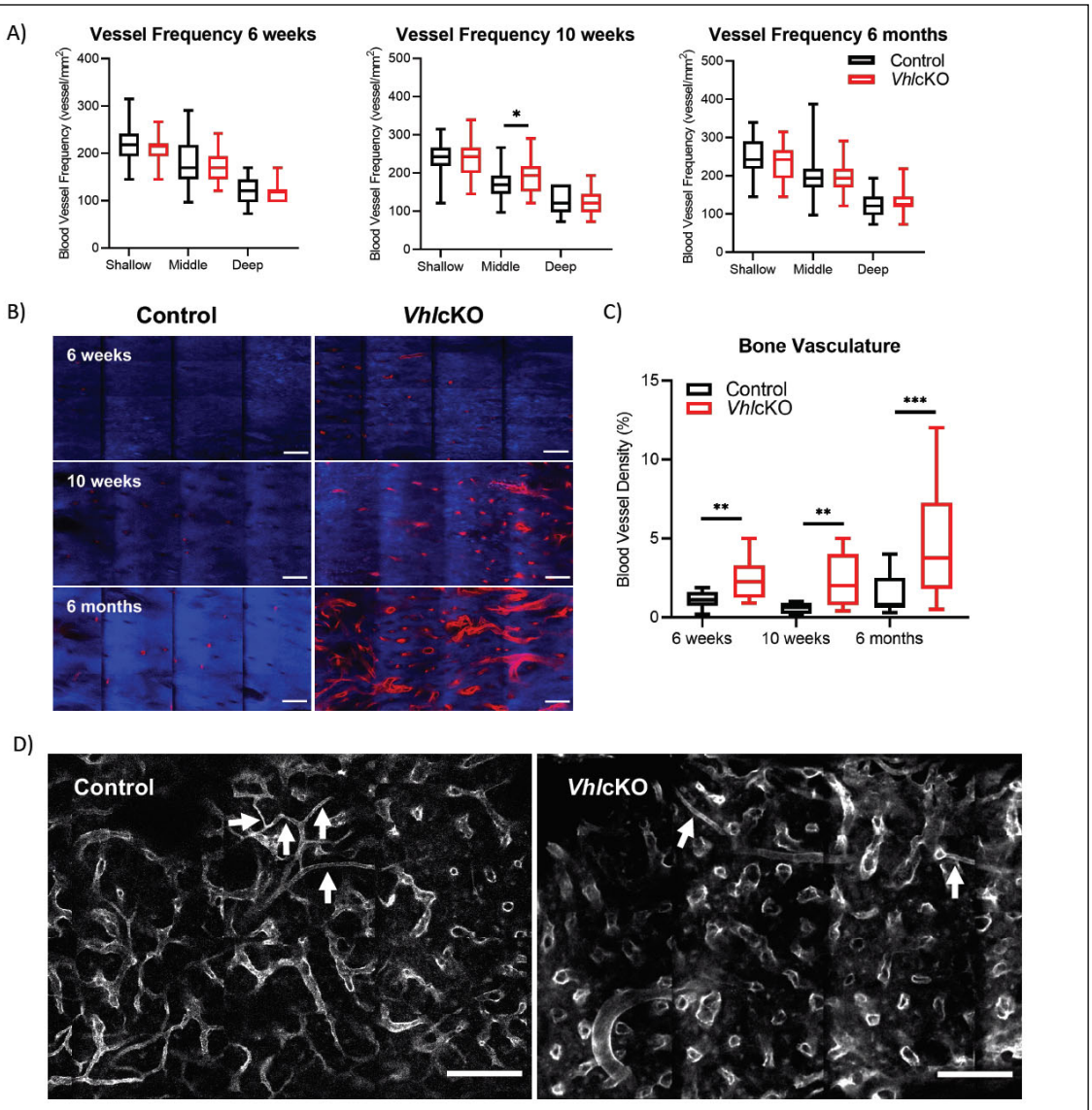


**Supplemental Figure 7. Ex vivo imaging of bone and bone marrow vasculature in *Vhl*cKO and control mice.** A) Quantification of age dependent vessel frequency in the diaphyseal BM of uDISCO cleared femurs at different depths (0-30 µm (shallow BM), 75-105 µm (middle BM), and 150-180 µm (deep BM) below the endosteum; B) maximum intensity projection images of cortical bone vascularization and C) quantification of cortical vessel density. Red: blood vessels (labeled with Alexa647 conjugated antibodies against CD31, CD144, and Sca-1), Blue: bone (SHG); D) maximum intensity projections of BM blood vessels within 50 µm of the endosteum in femurs of control (left) and *Vhl*cKO (right) mice; Grayscale: blood vessels (labeled with Alexa647 conjugated antibodies against CD31, CD144, and Sca-1). White arrows point to small diameter arterioles. Scale bars ~100 $\mu m$. *p<0.05, **p<0.01,***p<0.001, two-tailed Student's t-test.

**Supplemental Table 1.** List of the fluorochrome-labeled monoclonal antibodies used for flow cytometry and vessel staining sorted by experimental cocktail

| Cocktail | Antigen | Clone | Fluorochrome | Source |
|---|---|---|---|---|
| Lineage Stain | CD45 | 30F11 | FITC | Biolegend |
| | CD19 | 6D5 | PE | Biolegend |
| | Gr1 | RB6-8C5 | PE-Cy7 | Biolegend |
| | CD3 | 145-2C11 | APC | Biolegend |
| | CD11b | M1/70 | APC-Cy7 | Biolegend |
| | Propidium iodide (PI) | | Viability Dye | Sigma-Aldrich |
| Hematopoietic Progenitor | CD3 | 145-2C11 | biotin | Biolegend |
| | CD4 | Gk1.5 | biotin | Biolegend |
| | CD8 | 53.6.7 | biotin | Biolegend |
| | CD11b | M1/70 | biotin | Biolegend |
| | CD19 | 6D5 | biotin | Biolegend |
| | Nk1.1 | PK136 | biotin | Biolegend |
| | Ter119 | TER119 | biotin | Biolegend |
| | Gr1 | RB6-8C5 | biotin | Biolegend |
| | CD150 | mShad150 | FITC | eBioscience |
| | CD135 (Flk2) | A2F10 | PE | eBioscience |
| | CD48 | HM48-1 | PE-Cy7 | Biolegend |
| | CD127 | IL-7Ra | APC | Biolegend |
| | CD117 (cKit) | 2B8 | APC-Cy7 | Biolegend |
| | Sca1 (Ly-6A/E) | D7 | BV510 | Biolegend |
| | CD45 | 30-F11 | PerCP Cy5.5 | Biolegend |
| | Streptavidin | - | Pacific Blue | Life Technologies |
| | DAPI (4′,6-diamidino-2-phenylindole) | | Viability Dye | Sigma-Aldrich |
| B cell Development | CD19 | 6D5 | FITC | Biolegend |
| | CD43 | 1B11 | PE | Biolegend |
| | B220 | RA3-6B2 | PE-Cy7 | Biolegend |
| | IgD | 12-26c.2a | BV510 | Biolegend |
| | IgM | RMM-1 | BV421 | Biolegend |
| | CD117 (cKit) | 2B8 | APC-Cy7 | Biolegend |
| | Propidium iodide (PI) | | Viability Dye | Sigma-Aldrich |
| Transplant Lineage Stain | CD19 | 6D5 | PE | Biolegend |
| | Gr1 | RB6-8C5 | PE-Cy7 | Biolegend |
| | CD3 | 145-2C11 | APC | Biolegend |
| | CD11b | M1/70 | biotin | Biolegend |
| | Streptavidin | - | Pacific Blue | Life Technologies |
| | CD45.1 | A20 | FITC | Biolegend |
| | CD45.2 | 104 | APC-Cy7 | Biolegend |
| | Propidium iodide (PI) | | Viability Dye | Sigma-Aldrich |
| Trasplant B cell development | CD19 | 6D5 | FITC | Biolegend |
| | CD43 | 1B11 | PE | Biolegend |
| | B220 | RA3-6B2 | PE-Cy7 | Biolegend |
| | IgD | 12-26c.2a | BV510 | Biolegend |
| | IgM | RMM-1 | BV421 | Biolegend |
| | CD117 (cKit) | 2B8 | APC-Cy7 | Biolegend |
| | CD45.1 | A20 | BUV395 | BD Horizon |
| | CD45.2 | 104 | APC | Biolegend |
| | Propidium iodide (PI) | | Viability Dye | Sigma-Aldrich |
| Apoptosis in B cell development | CD43 | 1B11 | PE | Biolegend |
| | B220 | RA3-6B2 | PE-Cy7 | Biolegend |
| | IgD | 12-26c.2a | BV510 | Biolegend |
| | IgM | RMM-1 | BV421 | Biolegend |
| | CD117 (cKit) | 2B8 | APC-Cy7 | Biolegend |
| | CD19 | 6D5 | APC | Biolegend |
| | CD45 | 30-F11 | BUV395 | BD Horizon |
| | 7AAD | - | 7AAD | Biolegend |
| | Annexin V | - | FITC | Biolegend |

| | | | | |
|---|---|---|---|---|
| | IgG1, κ (Isotype Control) | MOPC-21 | FITC | Biolegend |
| Proliferation Stain Fractions A-C | CD19 | 6D5 | FITC | Biolegend |
| | CD43 | 1B11 | PE | Biolegend |
| | B220 | RA3-6B2 | PE-Cy7 | Biolegend |
| | CD117 (cKit) | 2B8 | APC-Cy7 | Biolegend |
| | CD45 | 30-F11 | PerCP Cy5.5 | Biolegend |
| | Ki67 | 16A8 | APC | Biolegend |
| | IgG2a,k (Isotype Control) | RTK2758 | APC | Biolegend |
| | DAPI (4′,6-diamidino-2-phenylindole) | | Viability Dye | Sigma-Aldrich |
| Proliferation Stain Fractions D-F | IgD | 11-26c.2a | FITC | Biolegend |
| | CD43 | 1B11 | PE | Biolegend |
| | IgM | RMM-1 | PE-Cy7 | Biolegend |
| | B220 | RA3-6B2 | APC-Cy7 | Biolegend |
| | CD45 | 30-F11 | PerCP Cy5.5 | Biolegend |
| | Ki67 | 16A8 | APC | Biolegend |
| | IgG2a,k (Isotype Control) | RTK2758 | APC | Biolegend |
| | DAPI (4′,6-diamidino-2-phenylindole) | | Viability Dye | Sigma-Aldrich |
| Pimonidazole analysis of LSKs | CD3 | 145-2C11 | biotin | Biolegend |
| | CD4 | Gk1.5 | biotin | Biolegend |
| | CD8 | 53.6.7 | biotin | Biolegend |
| | CD11b | M1/70 | biotin | Biolegend |
| | CD19 | 6D5 | biotin | Biolegend |
| | Nk1.1 | PK136 | biotin | Biolegend |
| | Ter119 | TER119 | biotin | Biolegend |
| | Gr1 | RB6-8C5 | biotin | Biolegend |
| | Streptavidin | - | Pacific Blue | Life Technologies |
| | CD45 | 30-F11 | PE | eBioscience |
| | CD117 (cKit) | 2B8 | APC | Biolegend |
| | Sca1 (Ly-6A/E) | D7 | BV510 | Biolegend |
| | B220 | RA3-6B2 | PE-Cy7 | Biolegend |
| | Fixable viability | - | e780 | eBioscience |
| | anti-PIM | - | FITC | HypoxyProbe |
| | IgG1, κ (Isotype Control) | MOPC-21 | FITC | Biolegend |
| Pimonidazole analysis of B cell development | CD19 | 6D5 | PECy5 | Biolegend |
| | CD43 | 1B11 | PE | Biolegend |
| | B220 | RA3-6B2 | PE-Cy7 | Biolegend |
| | IgD | 12-26c.2a | BV510 | Biolegend |
| | IgM | RMM-1 | BV421 | Biolegend |
| | CD117 (cKit) | 2B8 | APC-Cy7 | Biolegend |
| | anti-PIM | - | FITC | HypoxyProbe |
| | IgG1, κ (Isotype Control) | MOPC-21 | FITC | Biolegend |
| Imaging antibodies | CD144 | BV13 | Alexa647 | Biolegend |
| | CD31 | MEC13.3 | Alexa647 | Biolegend |
| | Sca1 (Ly-6A/E) | D7 | Alexa647 | Biolegend |
| Bone digest stain | CD3 | 145-2C11 | PE-Cy7 | Biolegend |
| | CD4 | Gk1.5 | PE-Cy7 | Biolegend |
| | CD8 | 53.6.7 | PE-Cy7 | Biolegend |
| | CD11b | M1/70 | PE-Cy7 | Biolegend |
| | CD19 | 6D5 | PE-Cy7 | Biolegend |
| | Gr1 | RB6-8C5 | PE-Cy7 | Biolegend |
| | Nk1.1 | PK136 | PE-Cy7 | Biolegend |
| | Ter119 | TER119 | PE-Cy7 | Biolegend |
| | CD45 | 30F11 | BV421 | Biolegend |
| | CD31 | 390 | APC | Biolegend |
| | Sca1 (Ly-6A/E) | D7 | BV510 | Biolegend |
| | CD51 | RMV-7 | Biotin | Biolegend |
| | IgG1,k (Isotype Control) | RTK2071 | Biotin | Biolegend |
| | Streptavidin | - | PE | eBioscience |
| | Propidium iodide (PI) | | Viability Dye | Sigma-Aldrich |

## Unpublished Findings

In this section, I present unpublished results we accumulated during my Ph.D. thesis. These results did not fit the scope of our published story, but nonetheless provide crucial information to understand, validate, and further extend on the *Vhl*cKO changes in bone and effects on immune development.

### Dosage of *Vhl* deletion in Dmp1-expressing cells effects on B cell development

To determine the best control for our *Vhl*cKO ($Vhl^{fl/fl}$;Dmp1-$Cre^{+}$) mice, we first compared *Dmp1*-$Cre^{+}$ ($Vhl^{+/+}$) with $Vhl^{fl/fl}$ ($Cre^{-}$) mice and found that the frequencies of B cells were comparable between both strains, here on out will refer to $Vhl^{fl/fl}$ ($Cre^{-}$) as "control" (**Figure 4**). We also determined that 2 copies of the *Vhl* gene had to be floxed, as we found that 1 copy alone (or partial deletion) was more comparable to controls in terms of % frequency of B cells (**Figure 5**), suggesting that 1 copy of the Vhl gene is sufficient for proper oxygen sensing and B cell development. To best fit litter mates and aged matched mice, we decided to use $Vhl^{fl/fl}$ ($Cre^{-}$) mice as controls and homozygous flox/flox for our target deletion. We were able to generate a 1:1 ratio of *Vhl*cKOs and $Vhl^{fl/fl}$ ($Cre^{-}$) controls by crossing *Vhl*cKO ($Vhl^{fl/fl}$;*Dmp1*-$Cre^{+}$) males with $Vhl^{fl/fl}$;*Dmp1*-$Cre^{-}$ females (**Figure 6**). This cross also allowed for males to carry the $Cre^{+}$ to avoid potential germline deletion of the *Vhl* flox allele. Jackson Labs website states that "For many cre strains, but not all, using cre-positive males for breeding avoids potential germline deletion of your loxP-flanked allele" (https://www.jax.org/news-and-insights/jax-blog/2016/may/are-your-cre-lox-mice-deleting-what-you-think-they-are).

### 3-week-old mice analysis of B cell development, proliferation and apoptosis

To observe B cell development defects in the *Vhl*cKO mice prior to fully bone development, we added 3-week-old mice to our longitudinal study. *Vhl*cKO mice at 3-weeks-old were collected, processed, and analyzed in the same manner as Chicana et al. 2022 (104). We found that 3-week-old mice *Vhl*cKO are very similar to controls, with two minor exceptions, a small reduction of B cells in spleens of *Vhl*cKO, as well as a decrease of apoptosis in Fraction A cells (**Figure 7**). Otherwise, T cells, granulocytes, monocytes, and B cells from a lineage panel analysis remained comparable to controls. Progenitor cells (LT-HSCs, ST-HSCs, MPP2, MPP3 MPP4 and CLPs) also remained comparable to control. B cell hardy fractions development, proliferation and apoptosis were also similar between controls and *Vhl*cKO mice. These results suggest that the defects we observed in B cell development starting at 6-week-old *Vhl*cKO mice, as published, is driven by bone development as the mice ages.

### B cell development in calvaria was found to be similar to hindlimbs

Live imaging of vessel leakage presented in Chicana et al. 2022 was recorded from calvaria bones. To confirm that B cell development was consistent in flat vs long bones, we analyzed a comparison of B cell development at 10 weeks of age. Calvaria bones were

isolated following Bellido and Delgado-Calle 2020 protocol (105). Isolated calvarias were carefully dissected to include frontal, parietal, interparietal and occipital bones as much as possible. Calvaria was processed it in the same way as long bones (104). We found that calvaria bone marrow have very similar B cell development as long bones (hindlimbs) (**Figure 8**). These results support calvaria bone marrow as a site to study aberrant B cell development using live imaging in *Vhl*cKO mice.

**NK cell frequency reduced in *Vhl*cKO bone marrow**

In our initial studies we focused on T cells and B cells (104), leaving out NK cells which represents ~4% of live bone marrow cells (106). Natural killer cells differentiate primarily in the BM from common lymphoid precursors (CLP), same precursors that give rise to T cells and B cells. The question remained whether in the *Vhl*cKO mice NK cells were affected. Considering the CLP frequency was high in mice at 6 months of age, but T cells remained unchanged, and B cells were decrease, I hypothesized that NK cells remain unchanged or decreased as well. We observed that at 6-months-old NK cell frequency was reduced in the *Vhl*cKO bone marrow (**Figure 9**). This would indicate that although there is a progenitor increase, there is still a developmental blockage to the lymphoid branch (NK cells, T cells, and B cells) and could further explain the increase in myelopoiesis we observe in the *Vhl*cKO mice (more myeloid details in Chapter 3).

In this analysis we also observed that our *Vhl*cKO mice do not express CD161 (NK1.1) (**Figure 9c**). The NK1.1 receptor is expressed in strain C57BL/6 (B6) and other few mouse strains such as B6.SJL (107). Our *Vhl*cKO mice were backcrossed to substrains C57BL/6N and C57BL/6J for 10 generations but seems to have not gained back the NK1.1 receptor. These results support that to analyze NK cells in our *Vhl*cKO mice we need markers such as CD49b (DX5) and/or CD335 (NKp46) that's expressed in a wider range of mice strains (108, 109).

**Bone and bone marrow digests for studying the stromal niche that support hematopoiesis**

There are current limitations to studying stromal cells from bones and bone marrow, one being the lack of markers to distinguish populations, and another the dense bones from the *Vhl*cKO mice. One possible solution is the usage of a reporter mouse model. Reporter mouse models that carry a reporter gene allows for lineage tracing studies (110). Reporter genes encode proteins that can be easily distinguished such as green fluorescent protein (GFP) or red fluorescence proteins (RFP). We utilized the B6.Cg-Gt(ROSA)26Sortm9(CAG-tdTomato)Hze/J Cre reporter line also known as "Ai9", to identify any off-target expression. The Ai9 strain is designed to have a flox-flanked STOP cassette preventing transcription of the red fluorescent protein (tdTomato). We used the Ai9 reporter mice for validation of Dmp1-Cre$^{+}$ expression in bone cells and not in B cell lineages as shown in Chicana et al. 2022 supplemental figure 3. Using a reporter like Dmp1-Cre$^{+}$;Ai9 mice can also help confirm isolation of osteoblasts and osteocytes (Dmp1-

Cre$^+$, tdTomato$^+$) from bones (**Figure 10**). To isolate bone cells, an enzymatic digest is required to break down bone and release bone cells (111-113). In our lab we have used a bone digest protocol published by Schepers et al. 2012, digesting bone fragments with 3 mg/mL type I collagenase (Worthington) for 1-2 hours (114), and Winkler et al. 2010 stromal cell isolation and flow cytometry analysis (115). We found that longer digestion times were required for isolation of stromal cells from dense bones, but longer incubation was increasing apoptosis of cells and compromising RNA quality (data not shown). We adapted the osteocyte culture methods protocol from Stern and Bonewald (116, 117) serial digests, to isolate stromal populations (mesenchymal stem cells, osteoblasts, and osteocytes) for flow cytometry measurement. The serial digests consist of 9 digestion steps in collagenase solution at 300 active U/mL collagenase type-IA (Sigma-Aldrich, St. Louis, MO, USA) dissolved in Hank's balanced salt solution (HBSS) **or** EDTA tetrasodium salt dehydrate (EDTA) solution (5 mM, pH = 7.4; Sigma-Aldrich) prepared in magnesium and calcium-free Dulbecco's phosphate-buffered solution (DPBS; Mediatech) with 1% BSA (Sigma-Aldrich). All digestions took place in 8mL solution in 50ml conical tube on a rotating shaker set to 150rpm at 37°C. Each digest was 25 minutes long for a total of 3.75hr digestion of bones. Digest 1 primarily consists of fibroblastic cells, digests 2-3 are a mixture of fibroblasts and osteoblasts, digest 4-6 contains mainly osteoblasts, digest 8 contains osteoblasts and osteocytes, and digest 9 are primarily osteocytes (117). Mice bone fragments at 10-weeks-old (n=3) were pooled and digested, we found that serial digests of bones was successful at releasing *Dmp1*-Cre$^+$;Ai9 cells from bones with the highest expression of tdTomato (70%) in osteoblasts at digest 8 (**Figure 10**). We also found that sorting of these populations resulted in successful isolation of tdTomato+ cells, but it required pooling of digest1-3, digest 4-6 and digest 7-9 to get 3000-5000 cells (**Table 3**), so a higher mouse pooling n=5 might be beneficial. We tested *Dmp1* expression by PCR from digest 5 through 9, from n=3 pooled 10-week-old wild-type (B6) mice and found expression starting at digest 7 (corresponding to 2.75 hours of total digest), and the highest *Dmp1* expression in digest 9 (data not shown), these results suggest that serial bone digests would help isolate Dmp1$^+$ cells from bones. We have also tested serial digestion in *Vhl*cKO mice bones and found that it was successful at releasing cells from bones based on cellularity results (data not shown). We are waiting to generate a reporter *Vhl*cKO to be able to sort isolated *Dmp1*-Cre$^+$ cells from serial digested bones.

To further characterize the bone marrow niche, we also performed enzymatic digestion of bone marrow tissues which allows the extraction of large stromal cells enabling their identification by flow cytometry and prospective isolation via cell sorting. We found that 20-minute incubation at 37°C in collagenase Type I at 3mg/ml as stated by other labs was best at releasing stromal cells from bone marrow (118-120). Green et al. 2021 observed an osteoblast population (Lin- CD31- Sca1- CD51+) expressing PDGFRα and PDGFRβ (they call "AB"), which was also high in LeptinR gene expression, supported pre-B lymphopoiesis in culture assays (69). Our preliminary results show evidence of lower expression of MSCs, but higher frequency of LepR$^+$ PDGFRα$^+$ osteoblast population in

*Vhl*cKO digested bone marrow. Bone digests had a higher % frequency of osteoblasts, but normal expression of $LepR^+$ $PDGFR\alpha^+$ osteoblast in *Vhl*cKO compared to controls (**Figure 11**). These results start to elucidate the status of stromal populations in the *Vhl*cKO bone marrow and bones.

### *Vhl*cKO whole bone marrow have normal levels of *Hif1α* and low levels of *Il7* measured by qPCR

Based on the pimonidazole (hypoxic marker) results we published in Chicana et al. 2022, we hypothesized that 10-week-old *Vhl*cKO B cells would have high levels of HIF1α in Fraction A cells, while the other B cell fractions would have lower levels. We also expected overall similar levels between *Vhl*cKO and controls. We attempted to measure HIF1α levels in different B cell Hardy fractions by flow cytometry using anti-HIF1α. HIF1α degrades quickly, with a reported half-life of HIF-1α protein, as determined by standard immunoblotting method is of about 5–8 min under normal oxygenated conditions (121). MG132, a proteasome inhibitor, has been shown to prevent HIF-1α protein degradation in cell lines (121-123). I was unsuccessful at measuring HIF1α levels, regardless of fixation, incubation temperature, antibody titers, or incubation with MG132 (10 μM for 3 h) (**Figure 12**). We think is an issue of the assay, as we also measured *Hif1α* levels from whole bone marrow of controls and *Vhl*cKO mice by using a TaqMan qPCR assay. By qPCR, we found slightly elevated *Hif1α* levels in 6-month-old *Vhl*cKO mice but overall similar levels as controls (**Figure 13a)**. The slight elevation confirms our findings of age dependent hypoxic stress in 6-month-old mice, we published.

We have measured cytokines from bone marrow serum and published these results in Chicana et al. 2022, where we found reduced CXCL12 levels in the *Vhl*cKO BM, but IL7 was not detectable using a custom built LegendPlex assay (104). We wanted to measure levels of IL7 in the *Vhl*cKO bone marrow, because IL7 is crucial for early B cell development in the BM (124, 125). We used a TaqMan qPCR assay to measure *Cxcl12* and *Il7* gene expression from whole bone marrow of control and *Vhl*cKO mice. We found a slight reduction of *Cxcl12* levels in whole BM of *Vhl*cKO mice, we need a bigger sample size for significance, but the overall trend is aligns with the results presented in our publication (**Figure 13b**). We did observe a significant decrease of *Il7* levels in *Vhl*cKO whole bone marrow cells (**Figure 13c**). These result confirms that the microenvironment of *Vhl*cKO mice lacks IL7 and CXCL12 supporting cytokines for proper B cell development.

### Spleens of *Vhl*cKO mice have lower % frequency of B cells, but comparable absolute numbers to controls

Outside of the bone marrow and bone, we also had an interest in spleens, as the site for B cells to finish maturation. We initially observed splenomegaly in the *Vhl*cKO mice, with significant higher weight, length, and cellularity at 10-weeks-old (Supplemental Figure 1 from Chicana et al. 2022). The *Vhl*cKO mice have decrease B cell frequency in

the bone marrow, so we expected possible B cell defects also present in spleens. Analysis of B cells (Live Lin-, $B220^+$ $CD19^+$) revealed a decreased frequency in *Vhl*cKO spleens, but overall normal B cell absolute numbers (**Figure 14**). The increased spleen size and cellularity could explain why regardless of the lower frequency of B cells in the *Vhl*cKO compared to controls, we still observe B cell numbers comparable to controls. Additionally, spleens of mice 16 weeks after transplantation of whole WT bone marrow into lethally irradiated *Vhl*cKO revealed a decrease of $IgM^{+/-}$ $IgD^+$ B cells, which corresponds to follicular B cells in the spleen (**Figure 15**). These results suggest that after transplantation, follicular B cells remain decreased in *Vhl*cKO compared to non-transplanted controls.

### *Vhl*cKO mice display normal antibody production and germinal centers

Due to the decrease of B cell frequency in bone marrow and spleens, we wanted to test if B cell functionality was also affected. Mice were used at 10 weeks old for initial immunizations and analyzed 1-4 weeks after, depending on the assay. We immunized mice with 4-Hydroxy-3-nitrophenylacetyl hapten conjugated to OVAL (ovalbumin) protein through lysine by amide bonds (NP-OVA, 50 ug/100ul) to test for a T-dependent (TD) immune response (48). For NP-OVA, the adjuvant used was alum for T-helper type 2 (Th2) responses (Alhydrogel 2%). A booster shot of NP-OVA (50 ug/100ul) was administered 21 days after initial injection, with no adjuvant added. PB was analyzed 28 days after initial injection (7 days after booster). We also injected *Vhl*cKO mice with 4-Hydroxy-3-nitrophenylacetic hapten conjugated to AminoEthylCarboxyMethyl-FICOLL (NP-FICOLL, 25ug/100ul), a high molecular weight polysaccharide, to measure a T-independent (TI) immune response (126). No adjuvant was used with NP-Ficoll. PB was analyzed 8 days after initial injection. Due to the decrease of mature B cells in the *Vhl*cKO mice, I hypothesized that the *Vhl*cKO mice would have lower levels of antigen-specific antibodies compared to control mice. TI activation of B cells does not require T cell help and leads to the production of IgM and IgG3, while TD activation of B cells requires $CD4^+$ helper T cells, and leads to the production of IgM and IgG1 antibodies. We tested for IgM, IgG1 and IgG3 responses by ELISA (absorbance at 450nm) using high valency NP-BSA (Bovine Serum Albumin), Ratio >20 (127). We observed that the *Vhl*cKO mice injected with NP-OVA (TD response) produced similar levels of IgM andIgG1 as controls (**Figure 16**). *Vhl*cKO mice injected with NP-Ficoll (TI response) produced similar levels of IgM and IgG3 as controls (**Figure 18**). We also tested NP-OVA immunized mice with a low valency NP-BSA (Bovine Serum Albumin), Ratio 1-4. This was done in an attempt to restrict binding to the high-affinity antibodies. Similarly, we observed comparable concentrations of IgM and IgG1 antibodies in *Vhl*cKO and control mice (**Figure 18**). Spleens of 10-week-old *Vhl*cKO mice after NP-OVA immunized mice (as stated above) were collected 28 days after initial injection and frozen for immunohistochemistry analysis. Results revealed that the *Vhl*cKO spleens produce normal germinal centers (**Figure 19**). These results suggest that 10–14-week-old *Vhl*cKO mice can produce antigen-specific antibodies and germinal centers, regardless of the developmental defects ongoing in the bone marrow.

**Progenitors founds in spleens of *Vhl*cKO mice revealing extramedullary hematopoiesis**

We suspected extramedullary hematopoiesis was occurring in the enlarged spleens in the *Vhl*cKO mice, so we examined hematopoietic progenitors in the spleen by flow cytometry. Due to the decreased bone marrow space in the *Vhl*cKO mice we hypothesized that there would be progenitors present in the spleens. We found that *Vhl*cKO mice had increased LT-HSCs, ST-HSCs, MPP2, MPP3 and MPP4 in frequency and numbers in 10-week-old and 6-month-old mice (**Figure 20**). After transplantation of *Vhl*cKO whole bone marrow to lethally irradiated WT (CD45.1) recipients, spleens were analyzed 16 weeks post for presence of progenitors, and there was little to none LSKs (0-0.0228% frequency) present, (data not shown). These results provide evidence of extramedullary hematopoiesis and possibly suggests an attempt at compensation for the lack of bone marrow.

**Unaffected B1a and B1b cells in bone marrow of *Vhl*cKO mice**

Another important B cell population to consider are B-1 cells. Studies have revealed that B1 cells can be present in the bone marrow, and they contribute to IgM antibody production (38). Although initially B1 cells were believed to only originate from fetal progenitors (neonatal livers)(32), there have been newer reports that show that bone marrow progenitors can also produce B1 cells, but a much lower rate than conventional B2 cells (33-36). We wanted to rule out any B1 cell defect in our *Vhl*cKO model, so we measured frequency and cellularity of B1 cells in bone marrow, spleens and peritoneal cavity (PerC). We hypothesize that there would be no change or a possible decrease in B1 cells in *Vhl*cKO mice. We measured B1a (Live, Lin-, IgM+, CD11b+, CD5+) and B1b (Live, Lin-, IgM+, CD11b+, CD5-) cells from 10–19-week-old mice (38, 128, 129). We found that there was no change of B1a cells in bone marrow and peritoneal cavity, but there was a decrease in spleens; while B1b cells remained unchanged in bone marrow, spleens and peritoneal cavity (**Figure 21**).

## Conclusions

In Chapter 2, we explored the BM microenvironment in the *VhlcKO* mice that does not support normal B cell development. To determine the mechanisms that affect B cell output from the *VhlcKO* BM, we recorded B cell apoptosis and proliferation stages during B cell development. We observed reduction of B cells is due to altered B cell proliferation and apoptosis in the BM. We next determined if the effects on proliferation and apoptosis were caused by insufficient production of cytokines by specific osteolineage subsets. We observed that the *VhlcKO* microenvironment contains altered proportions of specific niche cells, and insufficient levels of cytokines that cannot support normal B cell development. We perform bead-based immunoassays to measure expression of cytokines that support the maintenance of B cells, such as CXCL12, SCF, and IL7. We found that CXCL12 levels were reduced in the *Vhl*cKO bone serum compared to controls, while SCF levels remained the same. By qPCR we found reduced levels of IL7 from whole BM of *VhlcKO* mice. Additionally, we observed diminished B cell development in the BM of *Vhl*cKO mice extended to the peripheral blood and spleen, where *Vhl* is not deleted. Localized hypoxia and HIF stabilization are normal features of germinal centers. Development of robust antibody responses from conventional B lymphocytes is diminished by the relatively low oxygen levels in the germinal centers of the spleen and lymph nodes (92). Deletion of *Vhl* in B cells stabilizes *Hif1α* levels and affects B cell function by impairing cell proliferation, antibody class-switching, generation of high affinity antibodies, antibody responses, and impairs metabolic balance is essential for naive B cell survival (92, 93). We confirmed that *Vhl* remained intact and not erroneously deleted in B cells in our *Vhlc*KO mice. Studies of the function of B cells in the periphery of the *Vhl*cKO reveals normal production of IgG1 and IgM antibodies after injection with NP specific antigens (Figure 16-18). These studies helped identify the signaling changes in the microenvironment that contribute to the defect in B cell development in the *VhlcKO* mice. Taken together, this study helps provide novel information on the cellular and molecular mechanisms in the bone microenvironment that regulate B cell development, which can be applied to other models of altered bone homeostasis.

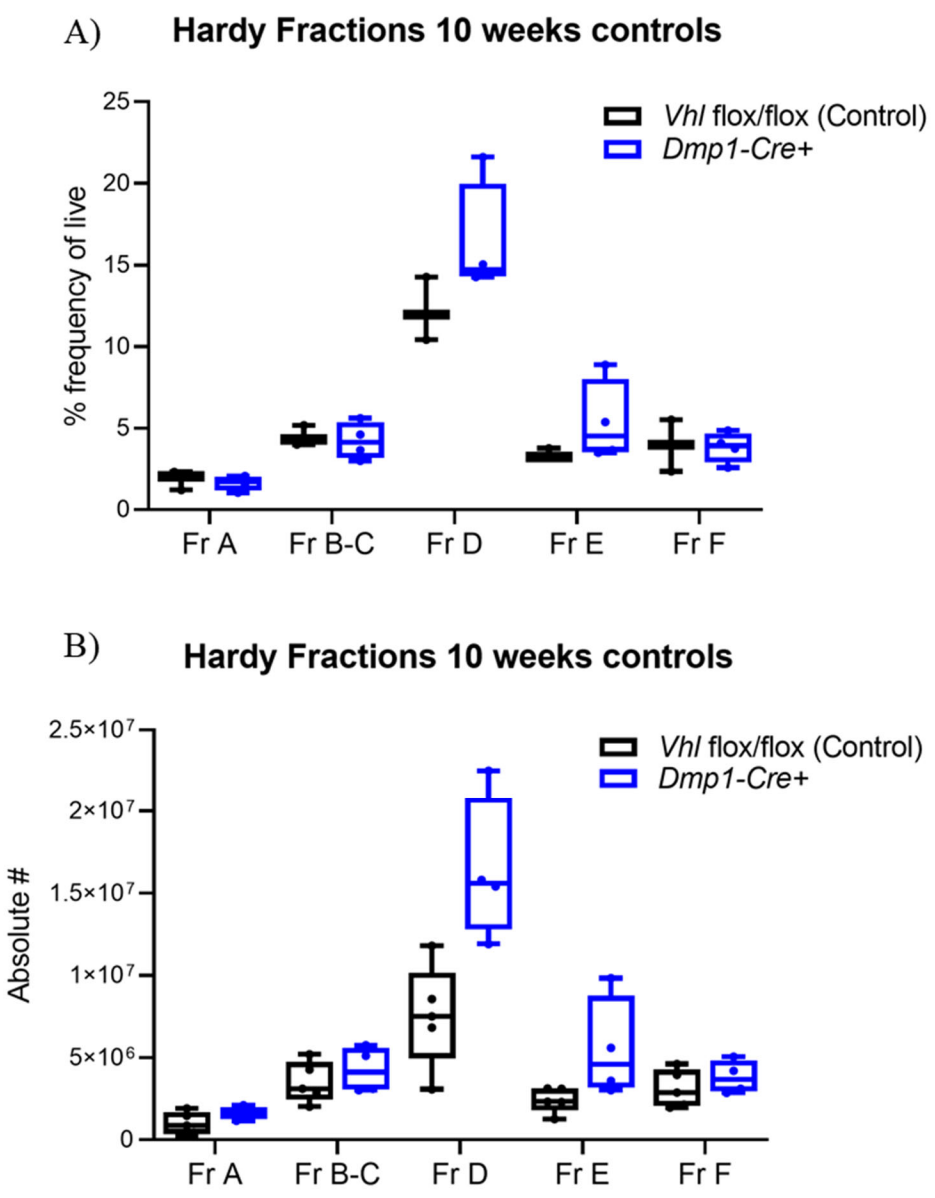


**Figure 4. Control comparison between *Vhl*$^{fl/fl}$ (Cre$^{-}$) and *Dmp1*-Cre$^{+}$ (*Vhl*$^{+/+}$).** Comparison of B cell hardy fractions at 10 weeks old revealed a similar trend of A) % frequency live and B) absolute numbers. The *Dmp1*-Cre$^{+}$ (blue) seems to have a higher absolute number of Fraction D (p= 0.053), but overall similar to *Vhl*$^{flox/flox}$ (Cre$^{-}$).

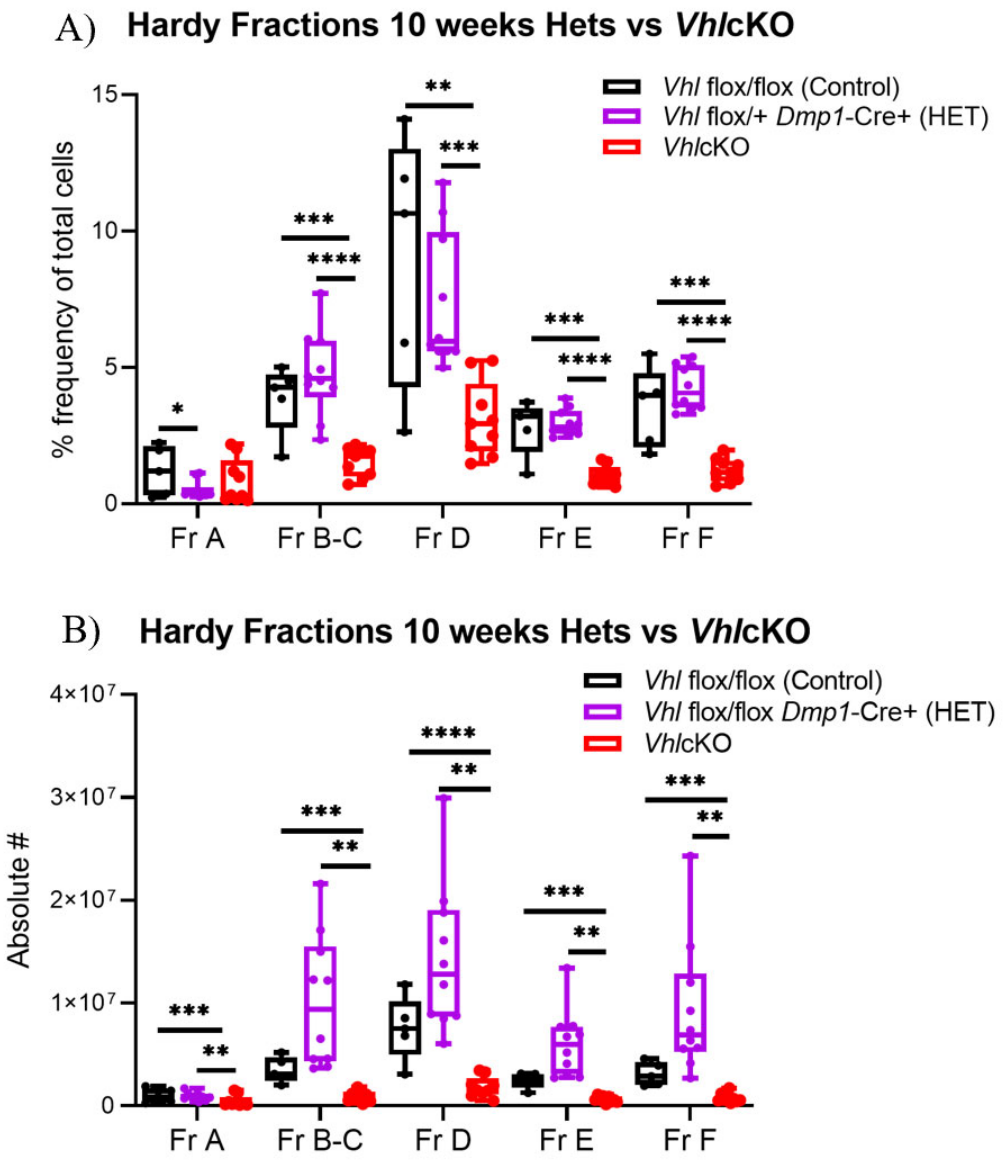


**Figure 5. Comparison between *Vhl*$^{fl/+}$;*Dmp1*-Cre$^{+}$ (HET) vs *Vhl*$^{fl/fl}$;*Dmp1*-Cre$^{+}$ (*Vhl*cKO).** Mice at 10 weeks old were analyzed for B cell hardy fraction A) frequency of total cells and B) absolute numbers in bone marrow. Results reveals a similar % frequency between controls and HETs, but absolute numbers are much higher in HET mice compared to both controls and *Vhl*cKOs. p<0.05*, p<0.01**, p<0.001***, p<0.0001**** two-tailed Student's t-test.

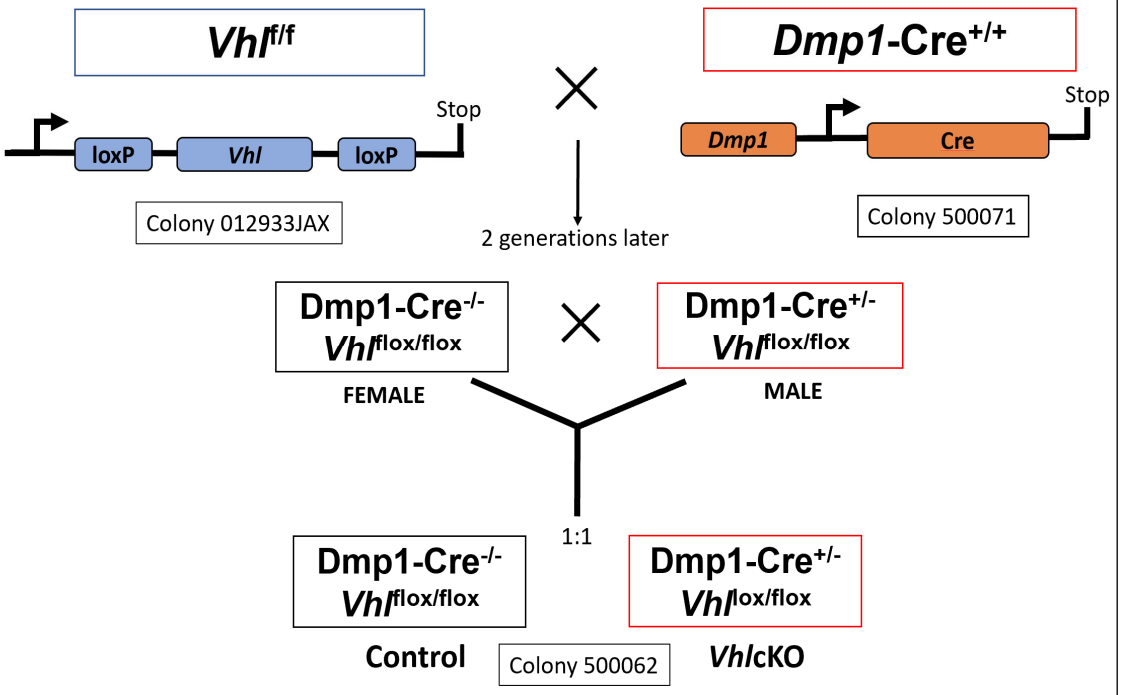


**Figure 6. Schematic of mice breeding generation of *Vhl*cKO mice.** We ordered *Vhl*$^{flox/flox}$ (B6.129S4(C)-Vhl$^{tm1Jae}$/J) Strain #:012933 and *Dmp1*-Cre$^{+}$ (B6N.FVB-Tg(Dmp1-cre)1Jqfe/BwdJ) Strain #:023047 from The Jackson Laboratory. We crossed for two generations to achieve homozygosity of the flox genes. From there we kept using Cre$^{+}$ males for breeding to avoid potential germline deletion of the loxP-flanked allele. This specific cross allowed for a 1:1 ratio of Cre$^{-}$/Cre$^{+}$ mice (controls and *Vhl*cKOs)

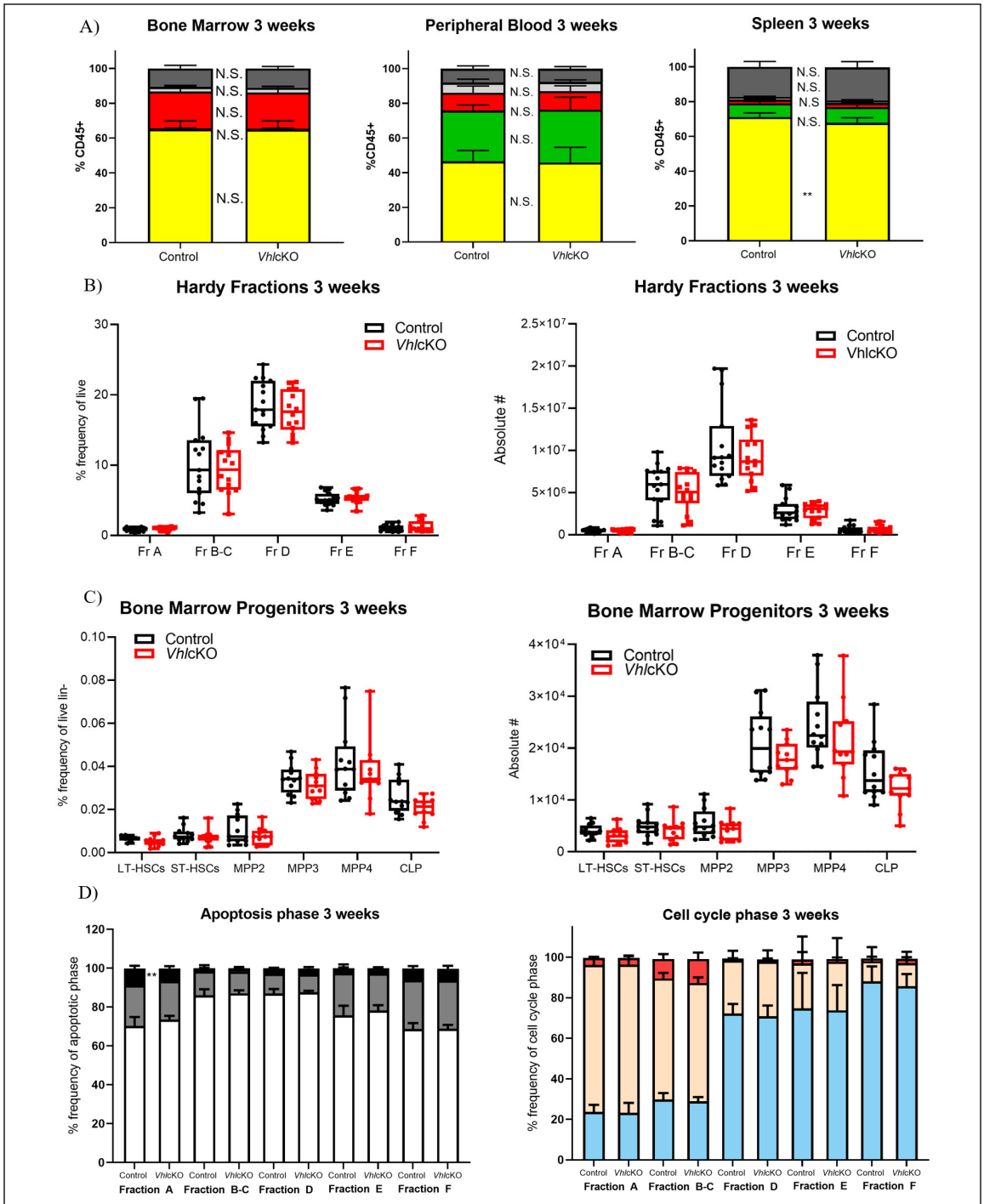


**Figure 7. Analysis of *Vhl*cKO 3-week-old mice reveals no B cell defects prior to bone development.** Same collection, processing, staining, and analysis as Chicana et al. 2022 was performed at 3 weeks old. A) lineage analysis of bone marrow, peripheral blood and spleens; B) Hardy fractions; C) % frequency of live (left) and absolute numbers (right); D) apoptosis (left) and proliferation (right) at different Hardy fractions of 3-week-old *Vhl*cKO mice.

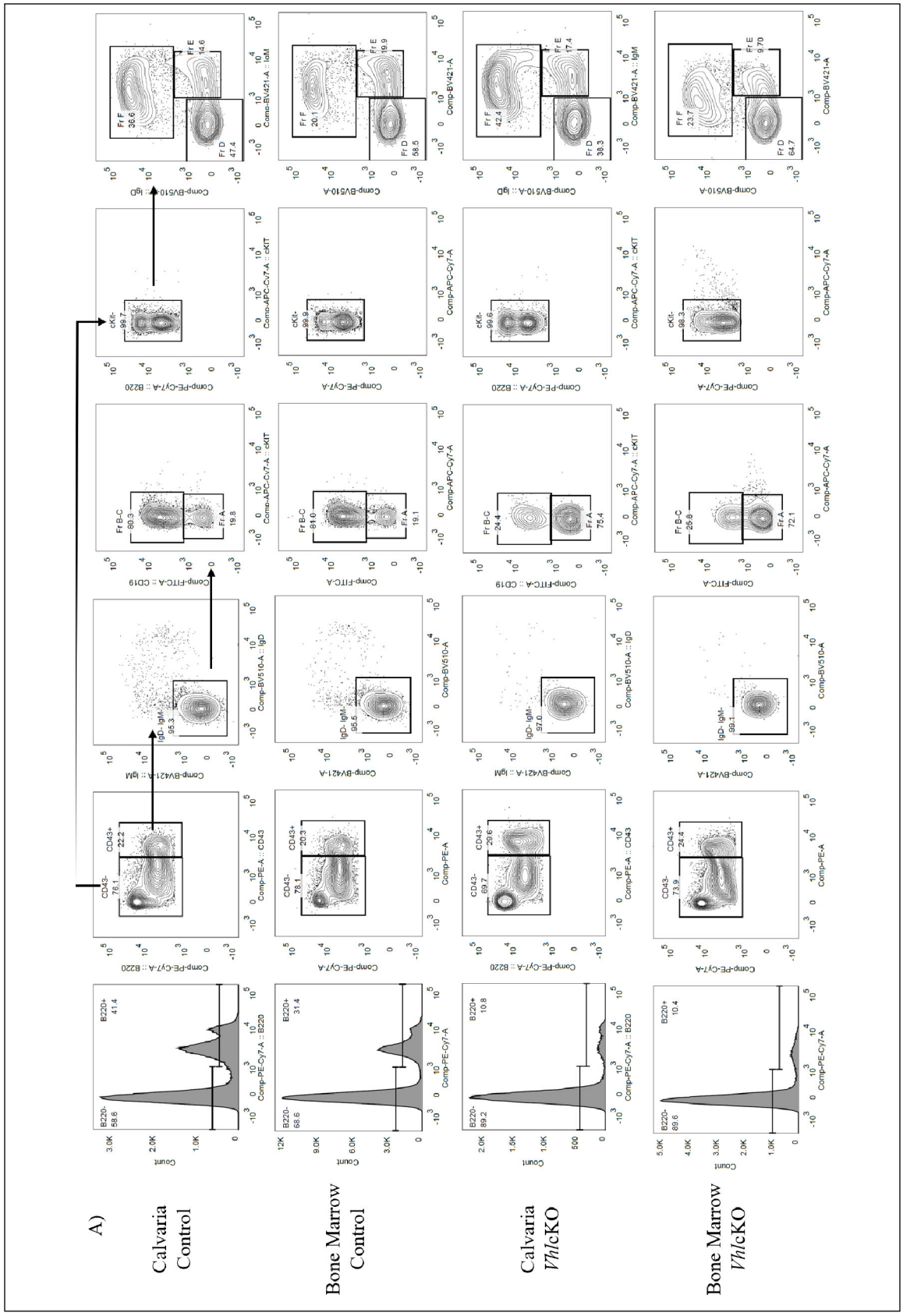
A)
Calvaria Control
Bone Marrow Control
Calvaria VhlcKO
Bone Marrow VhlcKO

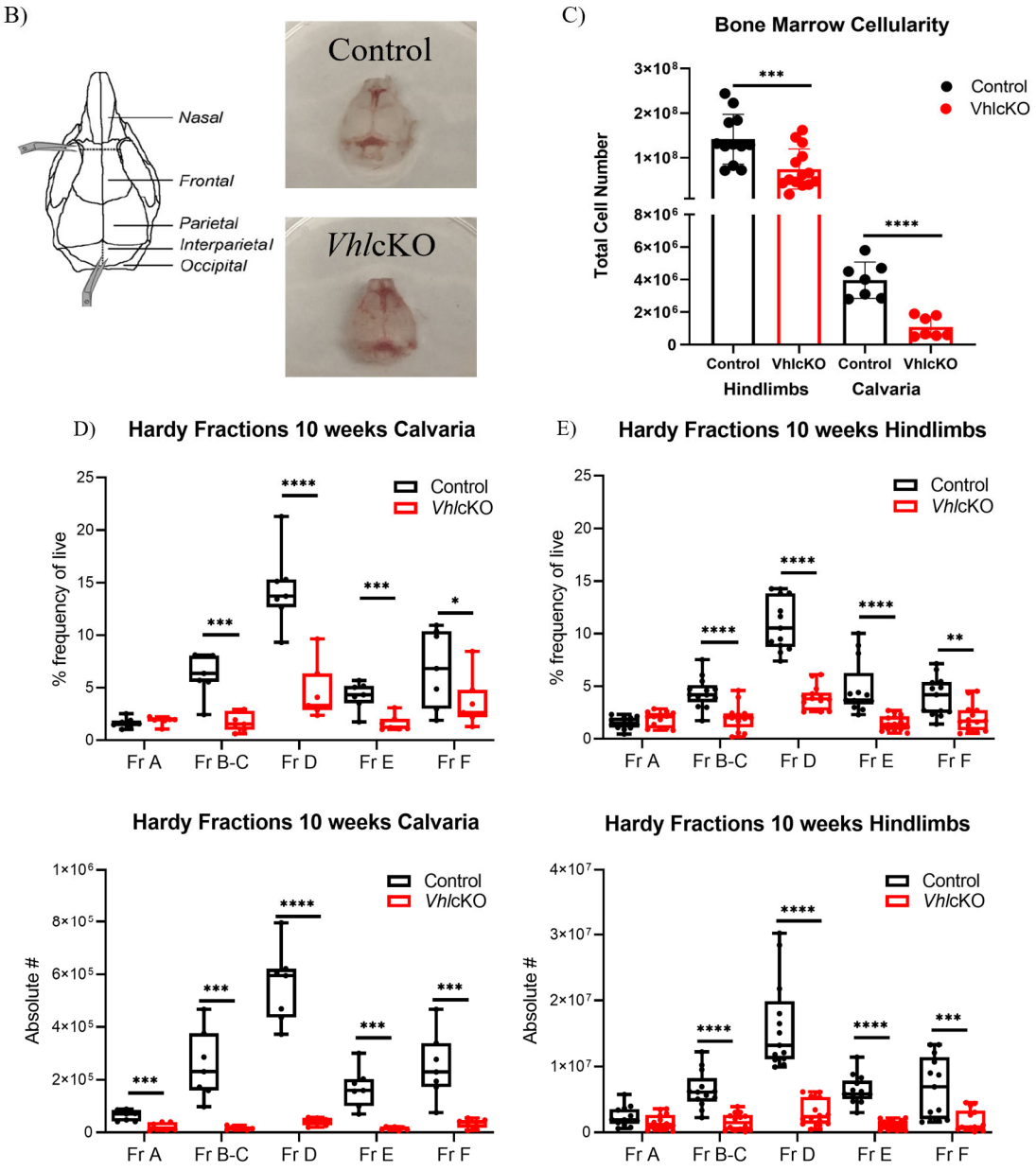


**Figure 8. Calvaria vs Hindlimbs B cell development in *Vhl*cKO mice.** Calvaria isolation, processed it the same way as long bones (104). A) flow cytometry gating example from calvaria and hindlimbs of 10 week old VhlcKO mice; B) schematic from Spijker et al. (130), and white light image of isolated calvaria from control and *Vhl*cKO mice; C) total cellularity comparison of hindlimbs vs calvaria; quantitative analysis of B cell development from D) calvaria and E) hindlimbs, %frequency of live (top) and absolute numbers (bottom). $p<0.05$*, $p<0.01$**, $p<0.001$***, $p<0.0001$**** two-tailed Student's t-test.

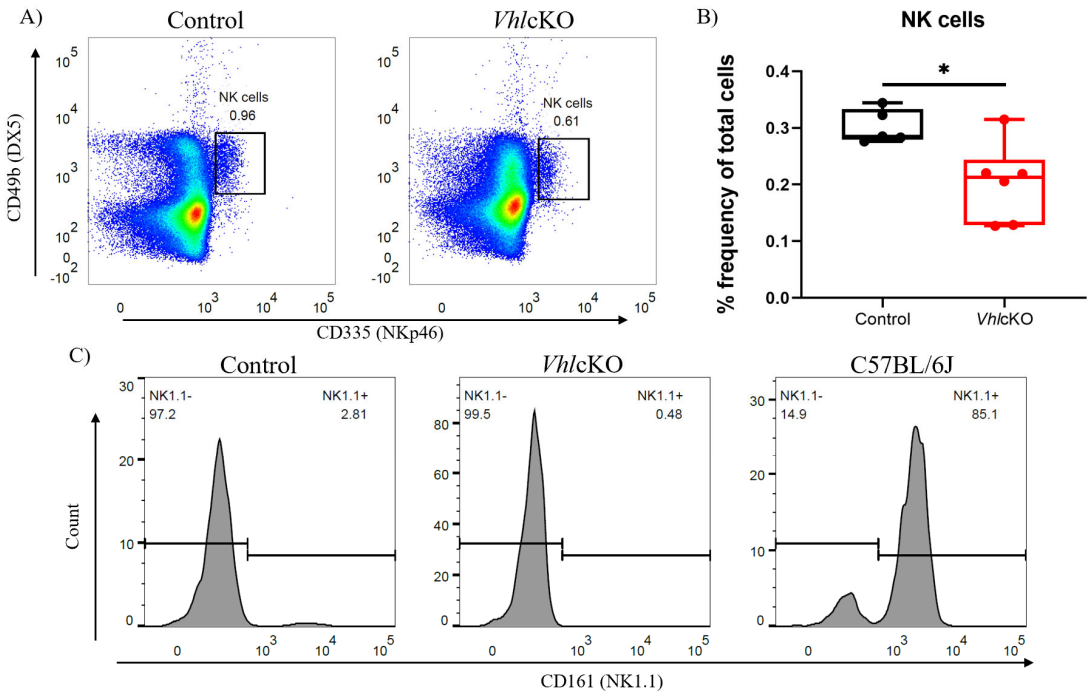


**Figure 9. Decreased NK cell frequency in bone marrow of *Vhl*cKO mice.** Bone marrow of 6-month-old mice was analyzed. A) flow cytometry gating strategy for NK cells, gated: Live, Lin-; B) % frequency of NK cells in total bone marrow cells; C) lack of expression of NK1.1 in control (C57BL/6J background), VhlcKO (C57BL/6J and C57BL/6N background) compared to wildtype C57BL/6J bone marrow NK cells.

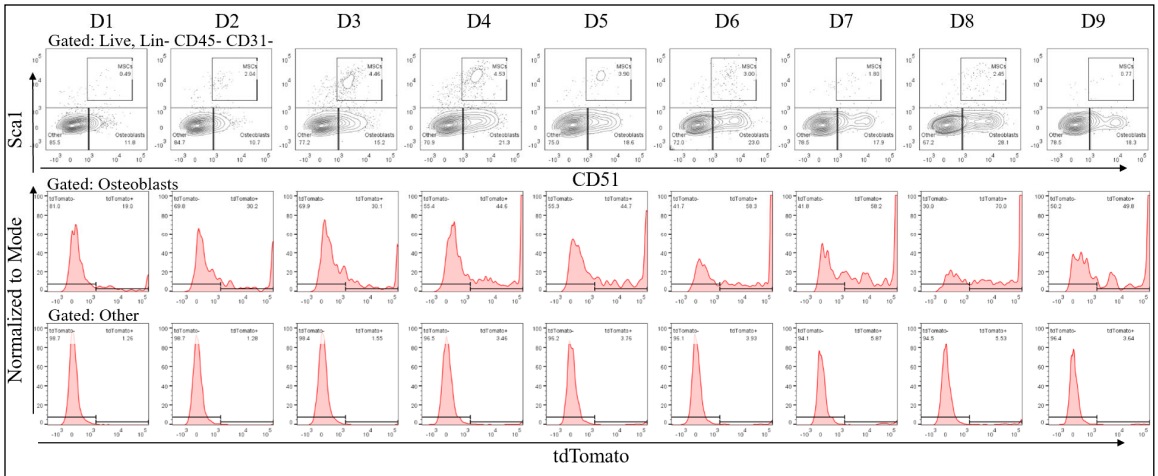


**Figure 10. Serial bone digest of Dmp1-Cre$^{+}$;Ai9 mice.** Mice bone fragments at 10-weeks-old were pooled n=3 and serial digest was performed. Gating strategy to measure stromal cells from digest 1 through 9 is shown above gated: Live, Lin$^{-}$CD45$^{-}$CD31$^{-}$ (top) and tdTomato levels (bottom) from each digest comparing osteoblast expression by digest.

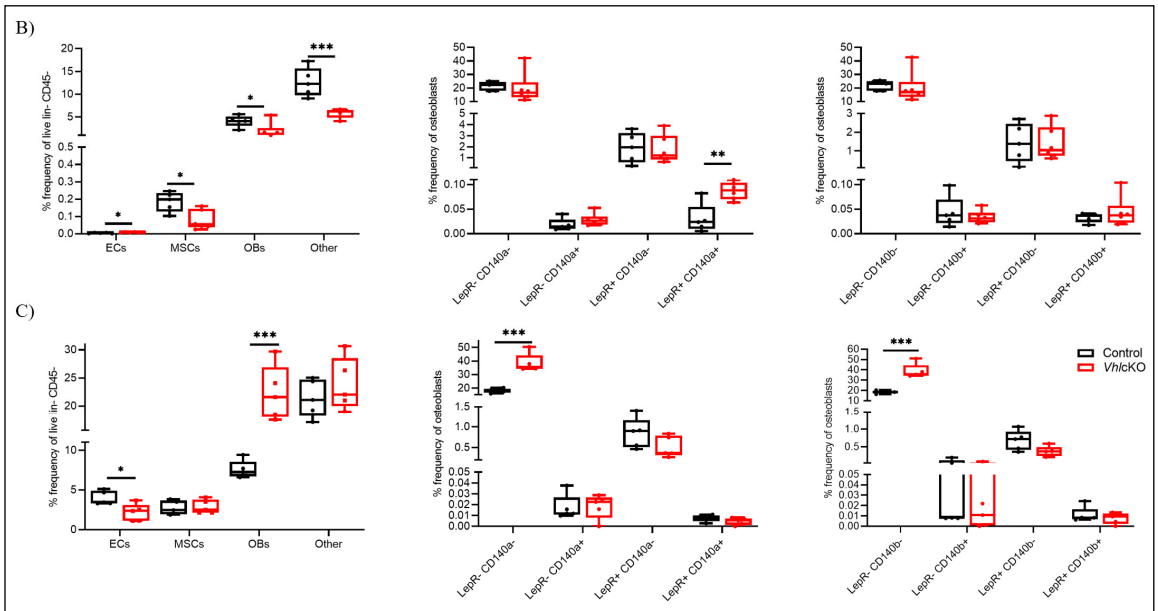


**Figure 11. Isolating bone marrow stromal niche cells by enzymatic digest**. Bone marrow from mice at 6-months-old was isolated and treated with Collagenase Type I for 20 minutes at 37°C, while bone fragments were digested in Collagenase Type I for 2 hours. A) Flow cytometry gating strategy; % frequency results of MSCs, ECs, and OBs, frequency of LeptinR and PDGFRα and PDGFRβ in B) bone marrow digests and C) bone digest. $p<0.05$*, $p<0.01$**, $p<0.001$***, $p<0.0001$**** two-tailed Student's t-test.

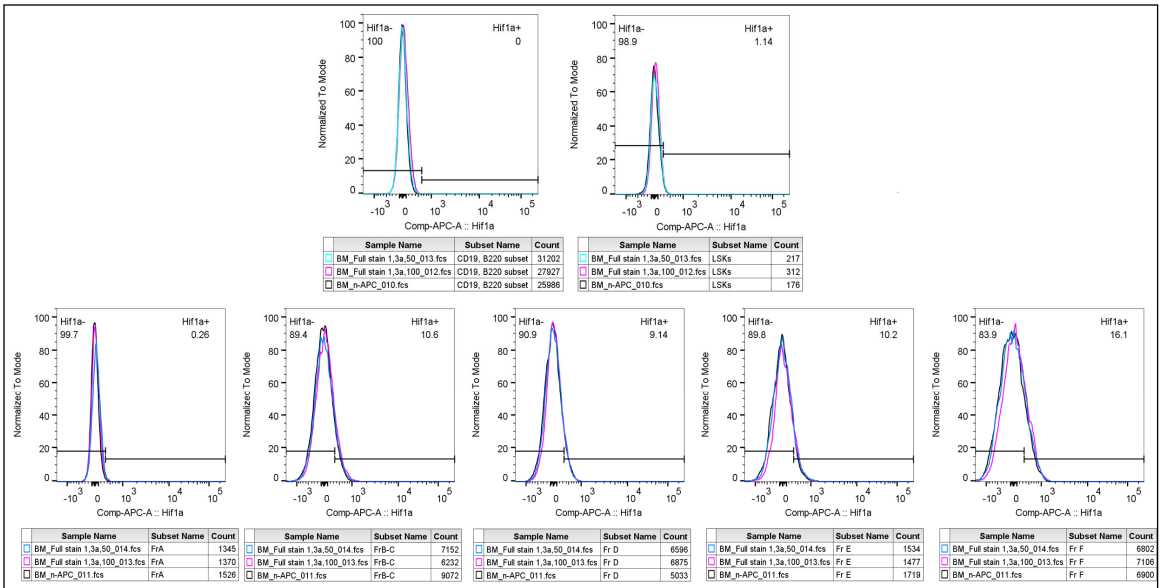


| Sample Name | Subset Name | Count |
|---|---|---|
| BM_Full stain 1,3a,50_013.fcs | CD19, B220 subset | 31202 |
| BM_Full stain 1,3a,100_012.fcs | CD19, B220 subset | 27927 |
| BM_n-APC_010.fcs | CD19, B220 subset | 25986 |

| Sample Name | Subset Name | Count |
|---|---|---|
| BM_Full stain 1,3a,50_013.fcs | LSKs | 217 |
| BM_Full stain 1,3a,100_012.fcs | LSKs | 312 |
| BM_n-APC_010.fcs | LSKs | 176 |

| Sample Name | Subset Name | Count |
|---|---|---|
| BM_Full stain 1,3a,50_014.fcs | FrA | 1345 |
| BM_Full stain 1,3a,100_013.fcs | FrA | 1370 |
| BM_n-APC_011.fcs | FrA | 1526 |

| Sample Name | Subset Name | Count |
|---|---|---|
| BM_Full stain 1,3a,50_014.fcs | FrB-C | 7152 |
| BM_Full stain 1,3a,100_013.fcs | FrB-C | 6232 |
| BM_n-APC_011.fcs | FrB-C | 9072 |

| Sample Name | Subset Name | Count |
|---|---|---|
| BM_Full stain 1,3a,50_014.fcs | Fr D | 6596 |
| BM_Full stain 1,3a,100_013.fcs | Fr D | 6875 |
| BM_n-APC_011.fcs | Fr D | 5033 |

| Sample Name | Subset Name | Count |
|---|---|---|
| BM_Full stain 1,3a,50_014.fcs | Fr E | 1534 |
| BM_Full stain 1,3a,100_013.fcs | Fr E | 1477 |
| BM_n-APC_011.fcs | Fr E | 1719 |

| Sample Name | Subset Name | Count |
|---|---|---|
| BM_Full stain 1,3a,50_014.fcs | Fr F | 6802 |
| BM_Full stain 1,3a,100_013.fcs | Fr F | 7106 |
| BM_n-APC_011.fcs | Fr F | 6900 |

**Figure 12. Unsuccessful measurement of HIF1α protein from sorted B cell Hardy fractions**. Bone marrow cells from 6-month-old controls were collected and incubated with MG132 (10 μM for 3 h), then the cells were fixated with Foxp3 transcription factor staining kit prior to staining with 1:50 or 1:100 anti-HIF1α. B cells, LSKs (top) and hardy fractions (bottom) were compared for HIF1α levels.

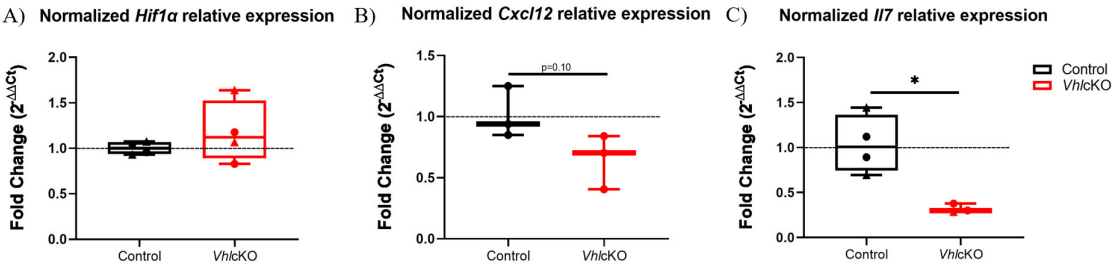


**Figure 13. Gene expression of *Hif1α*, *Cxcl12* and *Il7* from *Vhl*cKO mice.** Whole bone marrow cells were collected from 6-month-old (triangles) and 10-weeks-old (circles) and analyzed by TaqMan qPCR assay normalized by relative expression; *Hif1α*; B) *Cxcl12* (data collected by Shawn Ignacio); and C) *Il7*. $p<0.05$ two-tailed Student's t-test.

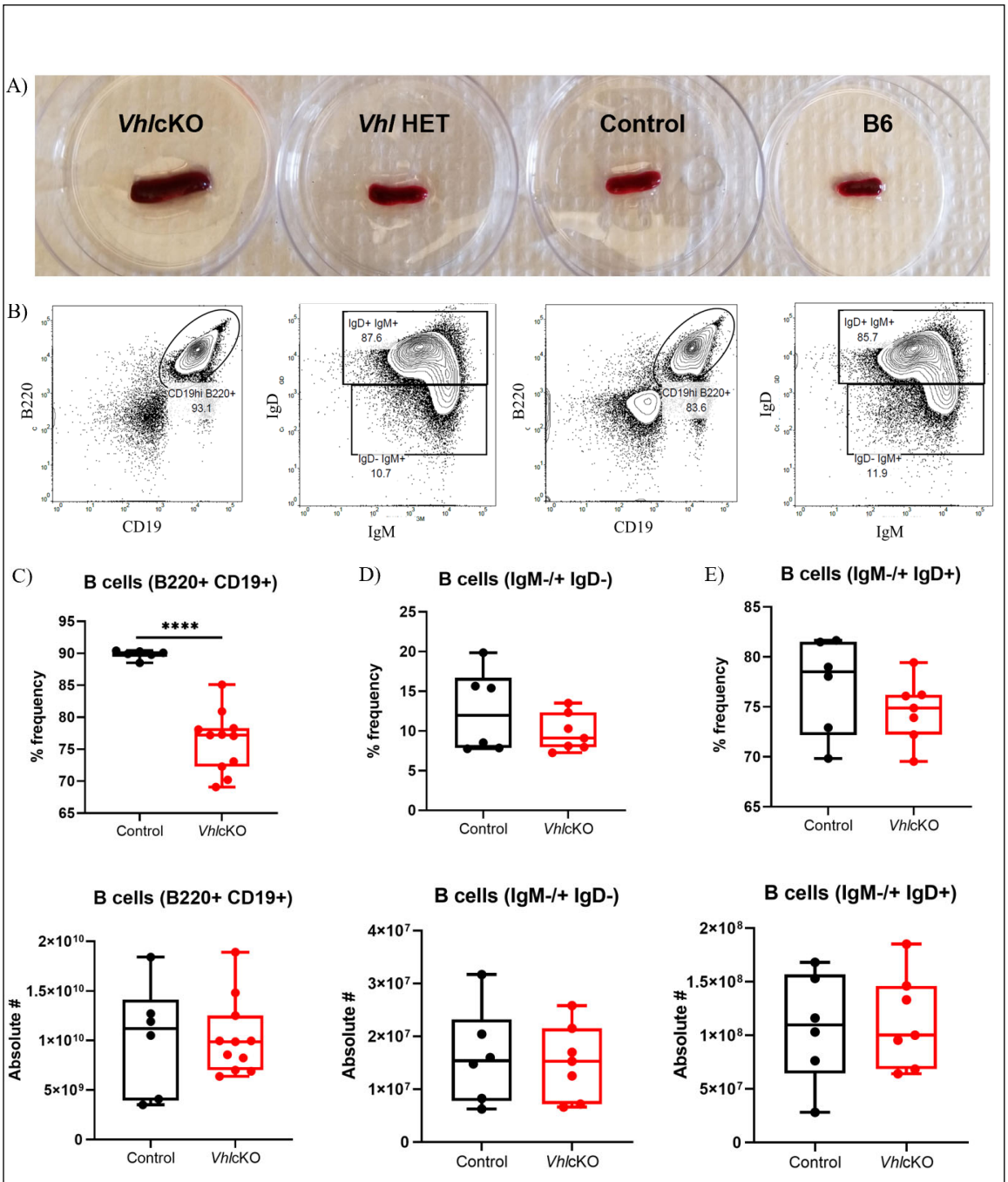


**Figure 14. *Vhl*cKO mice have reduced B cell frequency, but normal cellularity in spleens.** 10-week-old mice A) spleen white light images; B) flow cytometry gating strategy; C) frequency (top) and absolute numbers (bottom) of splenic B cells ($B220^{+}$ $CD19^{+}$); D) $IgM^{-/+}$ $IgD^{-}$ B cells corresponding to marginal zone B cells and B1 cells; and E) $IgM^{+/-}$ $IgD^{+}$ cells corresponding to follicular B cells. $p<0.0001$**** two-tailed Student's t-test.

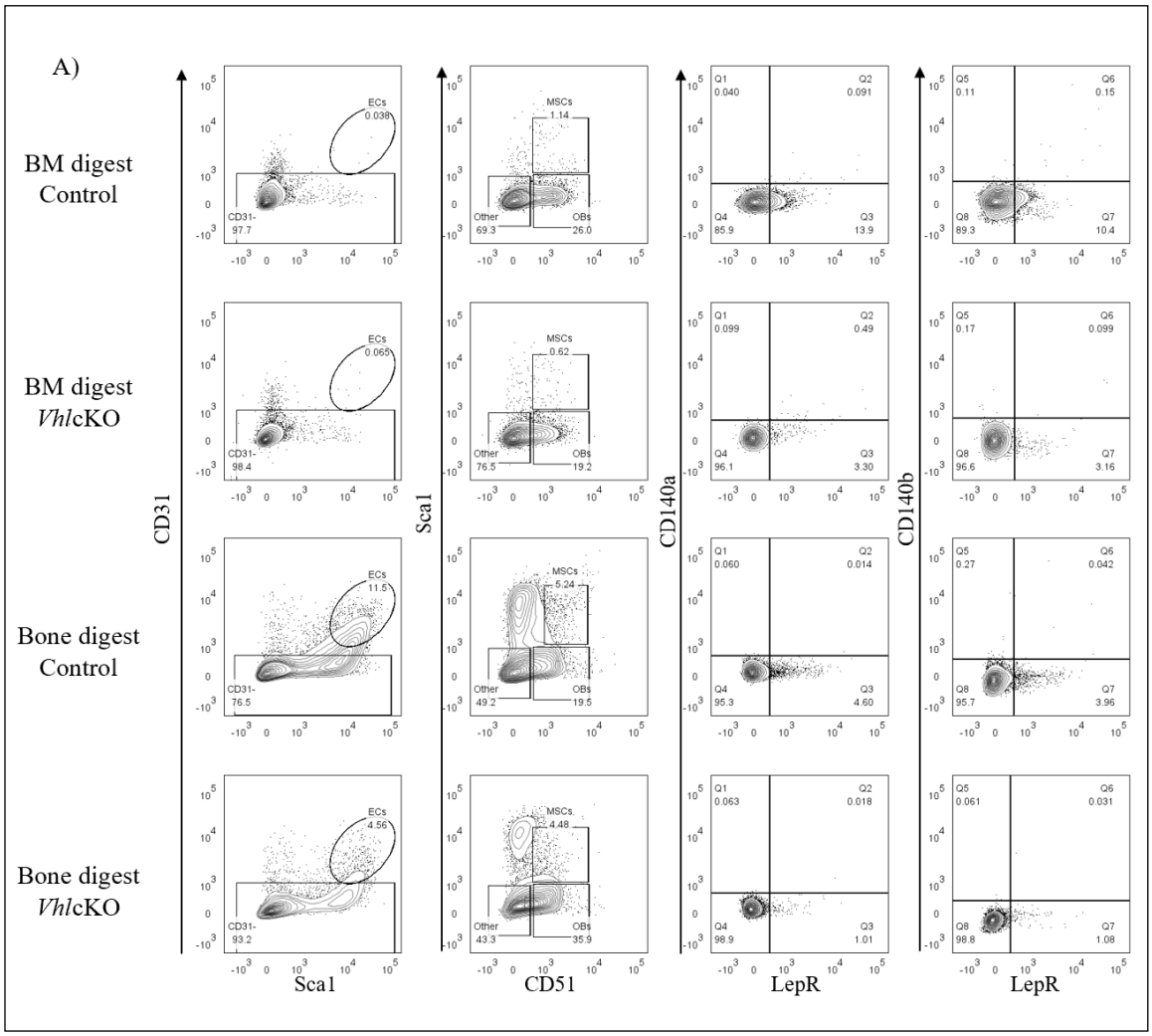
A)
BM digest Control
BM digest *Vhl*cKO
Bone digest Control
Bone digest *Vhl*cKO
CD31
Sca1
Sca1
CD51
CD140a
LepR
CD140b
LepR
ECs 0.038
CD31- 97.7
MSCs 1.14
Other 69.3
OBs 26.0
Q1 0.040
Q2 0.091
Q4 85.9
Q3 13.9
Q5 0.11
Q6 0.15
Q8 89.3
Q7 10.4
ECs 0.065
CD31- 98.4
MSCs 0.62
Other 76.5
OBs 19.2
Q1 0.099
Q2 0.49
Q4 96.1
Q3 3.30
Q5 0.17
Q6 0.099
Q8 96.6
Q7 3.16
ECs 11.5
CD31- 76.5
MSCs 5.24
Other 49.2
OBs 19.5
Q1 0.060
Q2 0.014
Q4 95.3
Q3 4.60
Q5 0.27
Q6 0.042
Q8 95.7
Q7 3.96
ECs 4.56
CD31- 93.2
MSCs 4.48
Other 43.3
OBs 35.9
Q1 0.063
Q2 0.018
Q4 98.9
Q3 1.01
Q5 0.061
Q6 0.031
Q8 98.8
Q7 1.08

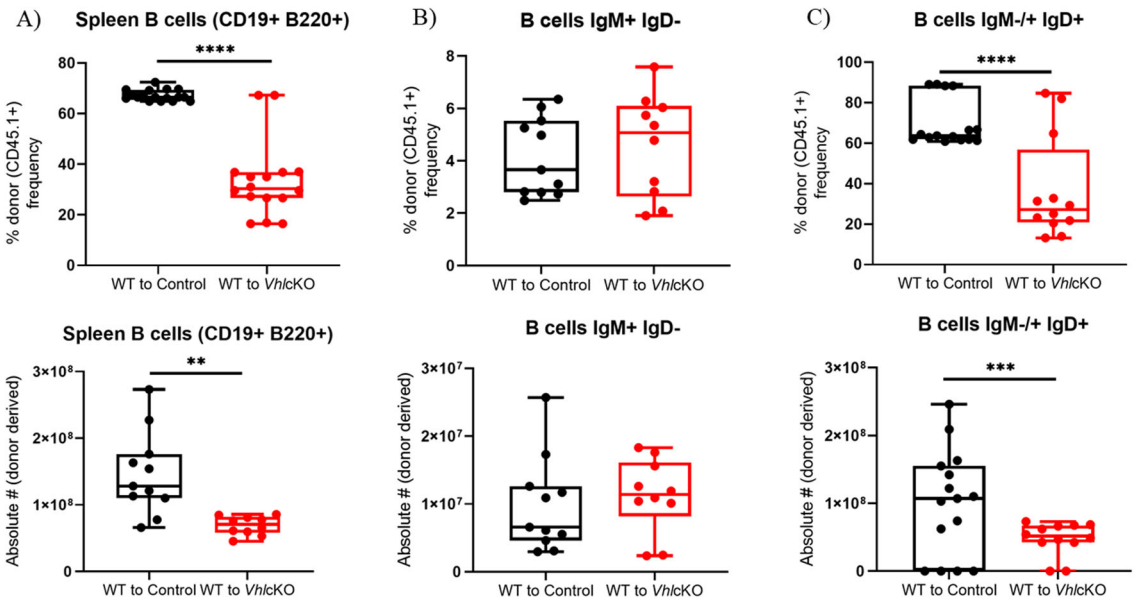


**Figure 15. *Vhl*cKO mice have reduced B cells after transplant of WT→*Vhl*cKO.** Whole bone marrow was transplanted into lethally irradiated mice and analyzed 16 weeks post-transplant. A) Frequency (top) and absolute numbers (bottom) of splenic B cells ($B220^{+}$ $CD19^{+}$); and B) $IgM^{-/+}IgD^{-}$ B cells corresponding to marginal zone B cells and B1 cells; and C) $IgM^{+/-}$ $IgD^{+}$ cells corresponding to follicular B cells. $p<0.05$*, $p<0.01$**, $p<0.001$***, $p<0.0001$**** two-tailed Student's t-test.

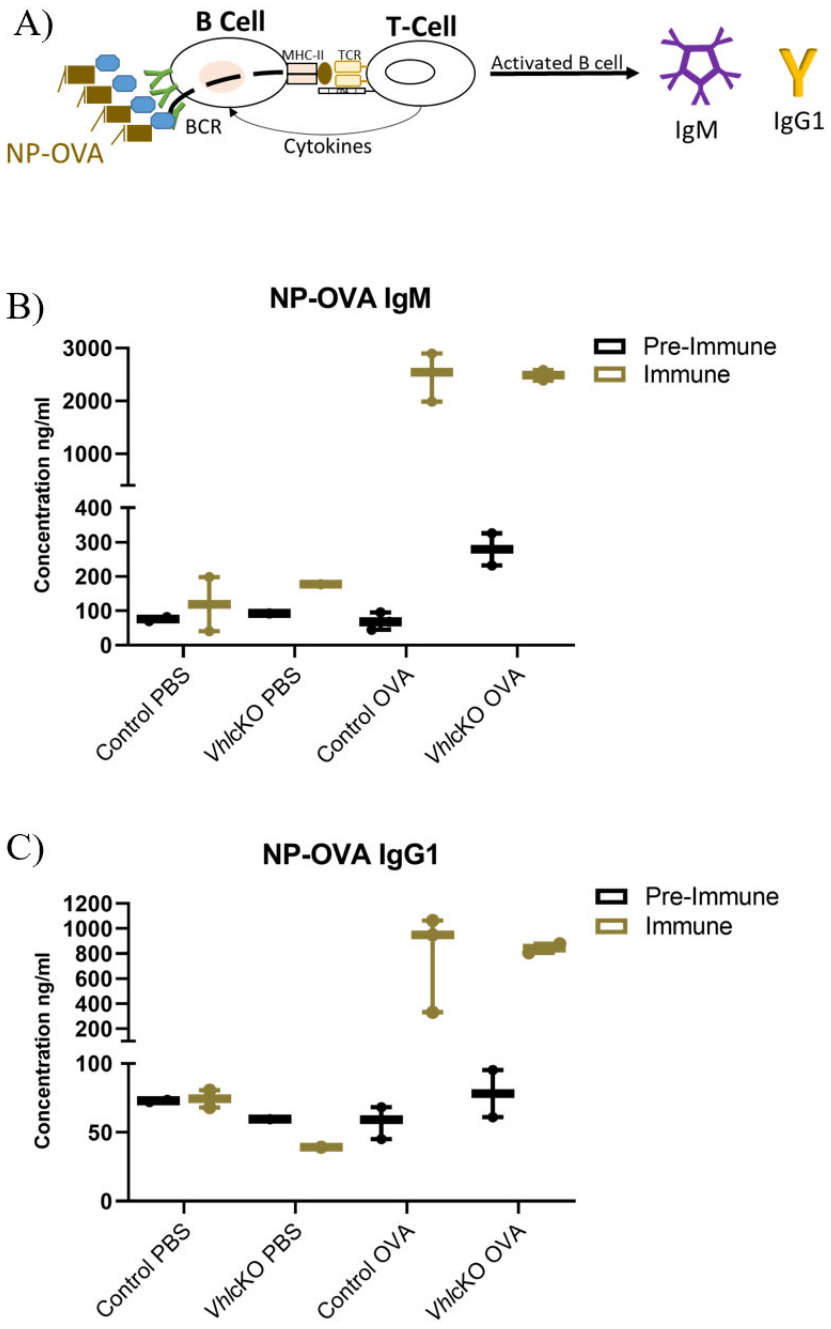


**Figure 16. NP-OVA T-dependent antibody response in *Vhl*cKO mice.** Mice were 10 weeks old at initial time of injection (pre-immune) and peripheral blood serum was collected 28 days after initial injection when mice were 14 weeks old (immune). IgM and IgG1 levels were measured by ELISA with NP20-BSA as a coating antigen.

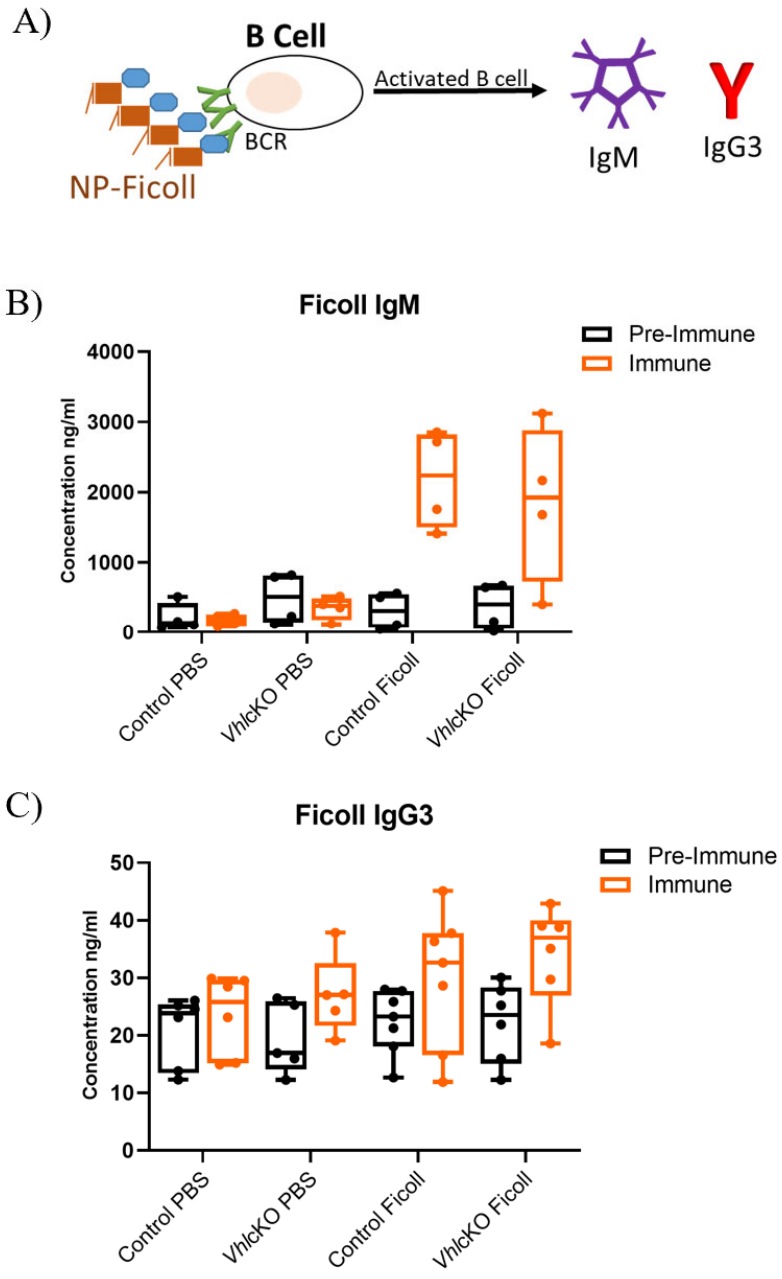


**Figure 17. NP-Ficoll T-independent antibody response in *Vhl*cKO mice.** Mice were 10 weeks old at initial time of injection (pre-immune) and peripheral blood serum was collected 28 days after initial injection when mice were 14 weeks old (immune). IgM and IgG3 levels were measured by ELISA with NP20-BSA as a coating antigen.

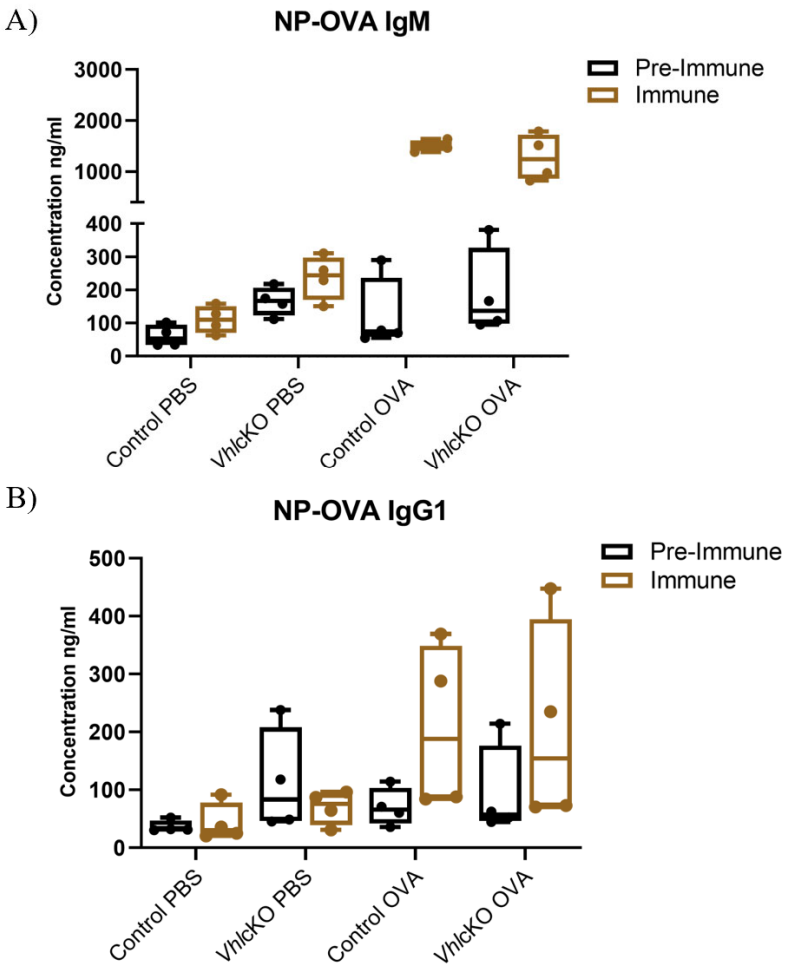


**Figure 18. NP-OVA T-dependent high affinity antibody response in *Vhl*cKO mice.** Mice were 10 weeks old at initial time of injection (pre-immune) and peripheral blood serum was collected 28 days after initial injection when mice were 14 weeks old (immune). IgM and IgG1 levels were measured by ELISA with NP2-BSA as a coating antigen.

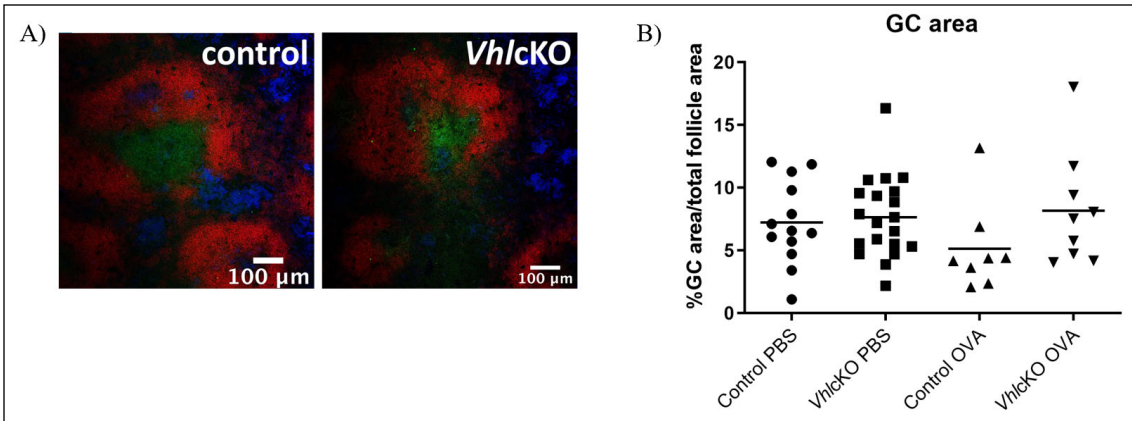


**Figure 19. *Vhl* deletion in *Dmp1*-expressing cells does not impair germinal center B-cell formation.** Mice were injected with NP-OVA **(**50 ug/100ul) at D1 and D21 and spleens were collected and frozen at D28, mice were 10 weeks old at time of initial injection and 14 weeks old at time of spleen collection. A) Immunofluorescence staining of splenic germinal centers in control (left) and VhlcKO (right) mice. B cells (red, IgD), GCs (blue, GL-7), and T cells (green, CD4 and CD8a); B) summary of % germinal center area by total follicle area. Scale bar ~100 µm. Data collected by Dr. David Gravano.

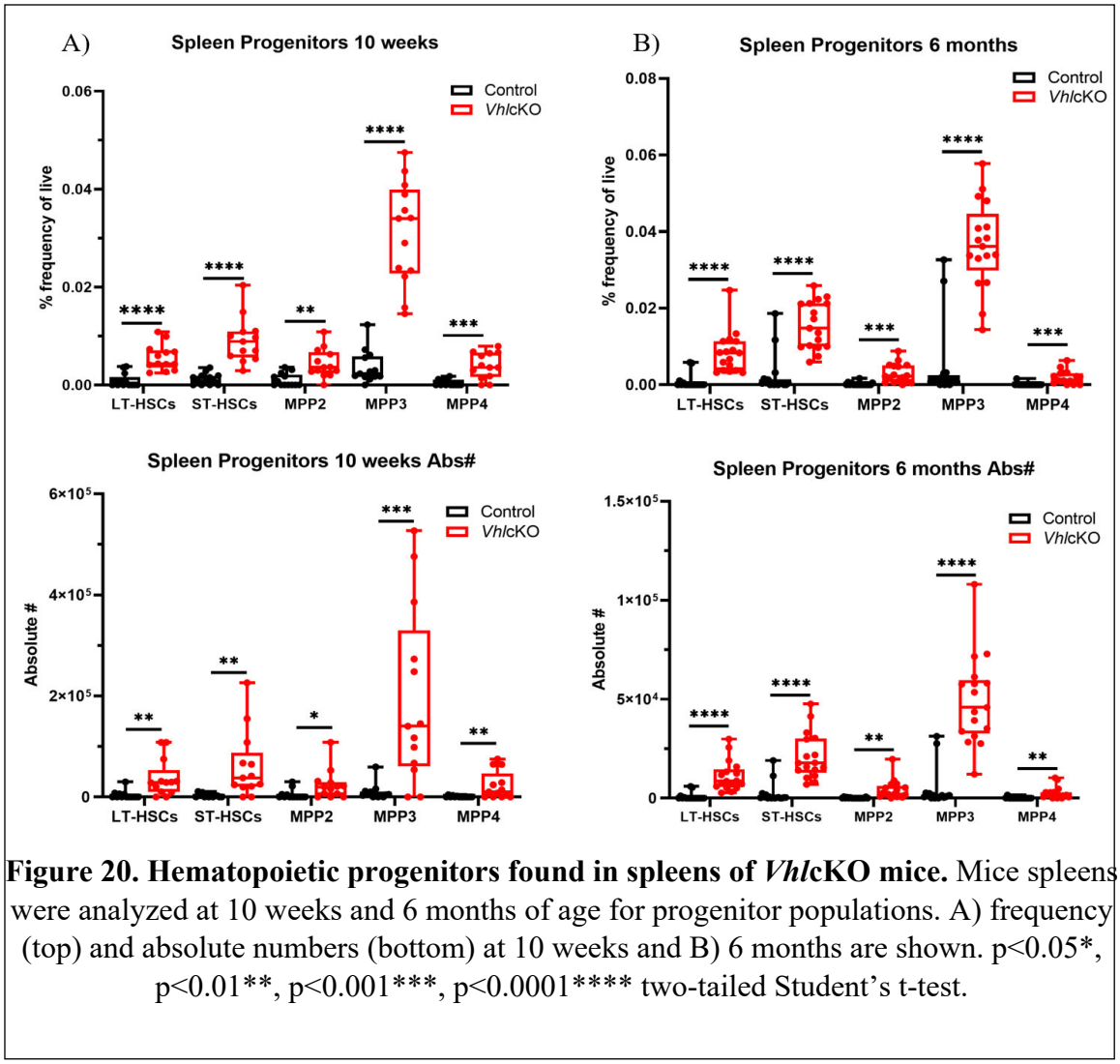


**Figure 20. Hematopoietic progenitors found in spleens of *Vhl*cKO mice.** Mice spleens were analyzed at 10 weeks and 6 months of age for progenitor populations. A) frequency (top) and absolute numbers (bottom) at 10 weeks and B) 6 months are shown. $p<0.05$*, $p<0.01$**, $p<0.001$***, $p<0.0001$**** two-tailed Student's t-test.

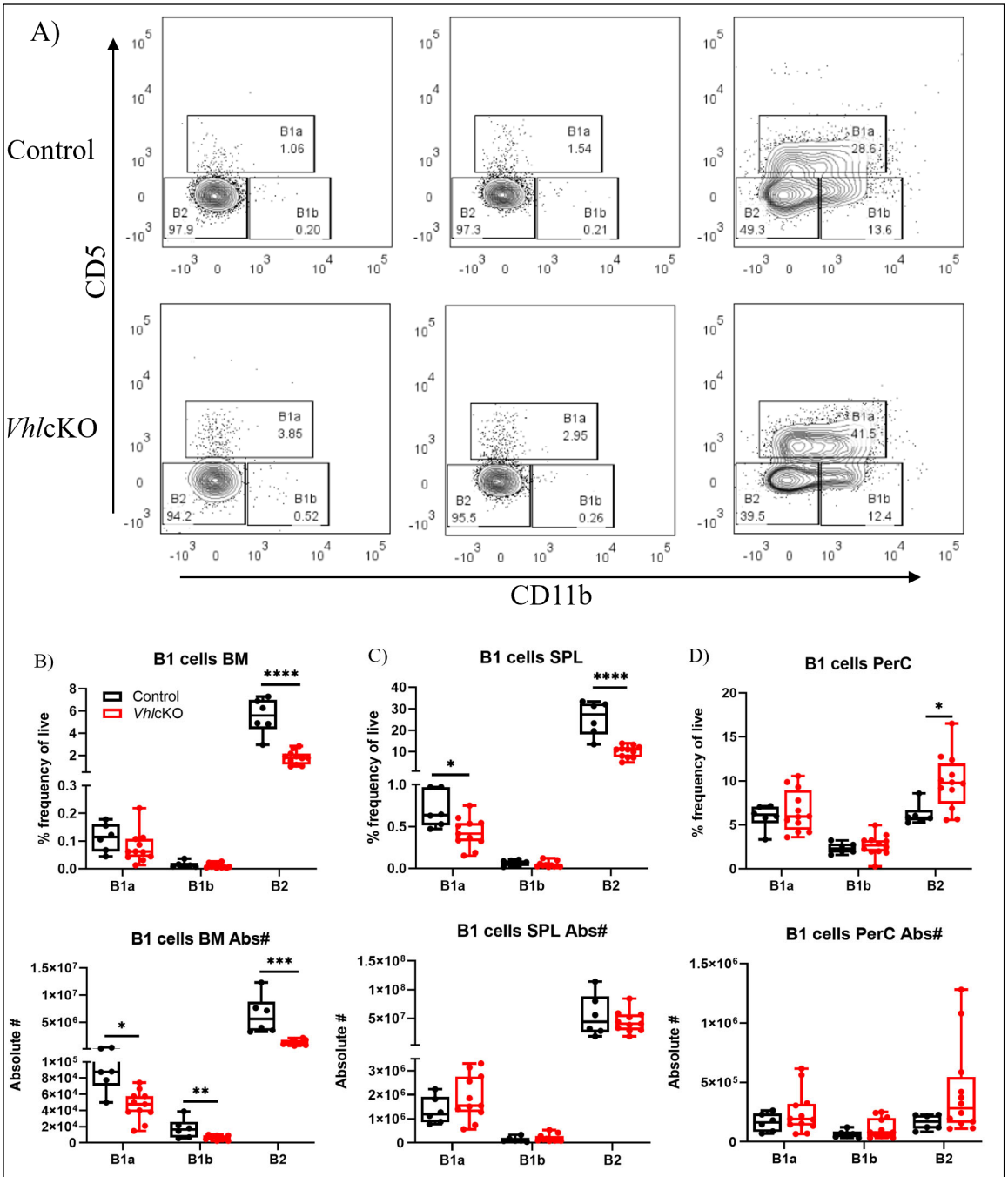


**Figure 21. Normal B1a % frequency in BM of *Vhl*cKO mice.** Mice between 10-19 weeks of age were analyzed for B1 cells A) flow cytometry gating strategy Gated: Live, Lin-, IgM+; B) bone marrow; C) spleens; D) peritoneal cavity % frequency of live (top) and absolute numbers (bottom). $p<0.05$*, $p<0.01$**, $p<0.001$***, $p<0.0001$**** two-tailed Student's t-test.

**Table 3**. **Isolated tdTomato+ cells from serial bone digest of Dmp1-Cre+;Ai9 mice.** Mice bone fragments were pooled (n=3) at 12-weeks-old and serial digested to isolate bone cells, D1-D3, D4-D6 and D7-D9 were pooled prior to staining to sort for tdTomato+ cells.

| Bone Digest | Total Cell count | Sorting | Sorted tdTomato+ |
|---|---|---|---|
| Digest 1 | 3262500 | D1-D3 pooled | 5004 |
| Digest 2 | 2000000 | | |
| Digest 3 | 1025000 | | |
| Digest 4 | 700000 | D4-D6 pooled | 7830 |
| Digest 5 | 400000 | | |
| Digest 6 | 687500 | | |
| Digest 7 | 150000 | D7-D9 pooled | 3896 |
| Digest 8 | 300000 | | |
| Digest 9 | 237500 | | |

## References


104. Chicana B, Abbasizadeh N, Burns C, Taglinao H, Spencer JA, Manilay JO. Deletion of Vhl in Dmp1-expressing cells causes microenvironmental impairment of B cell lymphopoiesis. bioRxiv (2022). doi: 10.1101/2021.09.10.459794

105. Bellido T, Delgado-Calle J. Ex Vivo Organ Cultures as Models to Study Bone Biology. JBMR Plus (2020) 4(3). doi: 10.1002/jbm4.10345

106. Millan AJ, Elizaldi SR, Lee EM, Aceves JO, Murugesh D, Loots GG, et al. Sostdc1 Regulates NK Cell Maturation and Cytotoxicity. J Immunol (2019) 202(8):2296-306. doi: 10.4049/jimmunol.1801157

107. Carlyle JR, Mesci A, Ljutic B, Belanger S, Tai LH, Rousselle E, et al. Molecular and genetic basis for strain-dependent NK1.1 alloreactivity of mouse NK cells. J Immunol (2006) 176(12):7511-24. doi: 10.4049/jimmunol.176.12.7511

108. Arase H, Saito T, Phillips JH, Lanier LL. Cutting edge: the mouse NK cell-associated antigen recognized by DX5 monoclonal antibody is CD49b (alpha 2 integrin, very late antigen-2). J Immunol (2001) 167(3):1141-4. doi: 10.4049/jimmunol.167.3.1141

109. Walzer T, Blery M, Chaix J, Fuseri N, Chasson L, Robbins SH, et al. Identification, activation, and selective in vivo ablation of mouse NK cells via NKp46. Proc Natl Acad Sci U S A (2007) 104(9):3384-9. doi: 10.1073/pnas.0609692104

110. Li S, Chen LX, Peng XH, Wang C, Qin BY, Tan D, et al. Overview of the reporter genes and reporter mouse models. Animal Model Exp Med (2018) 1(1):29-35. doi: 10.1002/ame2.12008

111. Hefley TJ. Utilization of FPLC-purified bacterial collagenase for the isolation of cells from bone. J Bone Miner Res (1987) 2(6):505-16. doi: 10.1002/jbmr.5650020607

112. Gu G, Hentunen TA, Nars M, Harkonen PL, Vaananen HK. Estrogen protects primary osteocytes against glucocorticoid-induced apoptosis. Apoptosis (2005) 10(3):583-95. doi: 10.1007/s10495-005-1893-0

113. Wong G, Cohn DV. Separation of parathyroid hormone and calcitonin-sensitive cells from non-responsive bone cells. Nature (1974) 252(5485):713-5. doi: 10.1038/252713a0

114. Schepers K, Hsiao EC, Garg T, Scott MJ, Passegue E. Activated Gs signaling in osteoblastic cells alters the hematopoietic stem cell niche in mice. Blood (2012) 120(17):3425-35. doi: 10.1182/blood-2011-11-395418

115. Winkler IG, Barbier V, Wadley R, Zannettino AC, Williams S, Levesque JP. Positioning of bone marrow hematopoietic and stromal cells relative to blood flow in vivo: serially reconstituting hematopoietic stem cells reside in distinct nonperfused niches. Blood (2010) 116(3):375-85. doi: 10.1182/blood-2009-07-233437

116. Stern AR, Stern MM, Van Dyke ME, Jahn K, Prideaux M, Bonewald LF. Isolation and culture of primary osteocytes from the long bones of skeletally mature and aged mice. Biotechniques (2012) 52(6):361-73. doi: 10.2144/0000113876

117. Shah KM, Stern MM, Stern AR, Pathak JL, Bravenboer N, Bakker AD. Osteocyte isolation and culture methods. Bonekey Rep (2016) 5:838. doi: 10.1038/bonekey.2016.65

118. Suire C, Brouard N, Hirschi K, Simmons PJ. Isolation of the stromal-vascular fraction of mouse bone marrow markedly enhances the yield of clonogenic stromal progenitors. Blood (2012) 119(11):e86-95. doi: 10.1182/blood-2011-08-372334

119. Decker M, Martinez-Morentin L, Wang G, Lee Y, Liu Q, Leslie J, et al. Leptin-receptor-expressing bone marrow stromal cells are myofibroblasts in primary myelofibrosis. Nat Cell Biol (2017) 19(6):677-88. doi: 10.1038/ncb3530
120. Morikawa S, Mabuchi Y, Kubota Y, Nagai Y, Niibe K, Hiratsu E, et al. Prospective identification, isolation, and systemic transplantation of multipotent mesenchymal stem cells in murine bone marrow. J Exp Med (2009) 206(11):2483-96. doi: 10.1084/jem.20091046
69. Green AC, Tjin G, Lee SC, Chalk AM, Straszkowski L, Kwang D, et al. The characterization of distinct populations of murine skeletal cells that have different roles in B lymphopoiesis. Blood (2021) 138(4):304-17. doi: 10.1182/blood.2020005865
121. Moroz E, Carlin S, Dyomina K, Burke S, Thaler HT, Blasberg R, et al. Real-time imaging of HIF-1alpha stabilization and degradation. PLoS One (2009) 4(4):e5077. doi: 10.1371/journal.pone.0005077
122. Jiang BH, Liu LZ, Schafer R, Flynn DC, Barnett JB. A novel role for 3, 4-dichloropropionanilide (DCPA) in the inhibition of prostate cancer cell migration, proliferation, and hypoxia-inducible factor 1alpha expression. BMC Cancer (2006) 6:204. doi: 10.1186/1471-2407-6-204
123. Fujita N, Chiba K, Shapiro IM, Risbud MV. HIF-1alpha and HIF-2alpha degradation is differentially regulated in nucleus pulposus cells of the intervertebral disc. J Bone Miner Res (2012) 27(2):401-12. doi: 10.1002/jbmr.538
124. Corfe SA, Paige CJ. The many roles of IL-7 in B cell development; mediator of survival, proliferation and differentiation. Semin Immunol (2012) 24(3):198-208. doi: 10.1016/j.smim.2012.02.001
125. Dias S, Silva H, Jr., Cumano A, Vieira P. Interleukin-7 is necessary to maintain the B cell potential in common lymphoid progenitors. J Exp Med (2005) 201(6):971-9. doi: 10.1084/jem.20042393
48. Cain CJ, Rueda R, McLelland B, Collette NM, Loots GG, Manilay JO. Absence of sclerostin adversely affects B-cell survival. J Bone Miner Res (2012) 27(7):1451-61. doi: 10.1002/jbmr.1608
126. de Vinuesa CG, O'Leary P, Sze DMY, Toellner KM, MacLennan ICM. T-independent type 2 antigens induce B cell proliferation in multiple splenic sites, but exponential growth is confined to extrafollicular foci. European Journal of Immunology (1999) 29(4):1314-23. doi: 10.1002/(SICI)1521-4141(199904)29:04<1314::AID-IMMU1314>3.0.CO;2-4
127. Devera TS, Shah HB, Lang GA, Lang ML. Glycolipid-activated NKT cells support the induction of persistent plasma cell responses and antibody titers. Eur J Immunol (2008) 38(4):1001-11. doi: 10.1002/eji.200738000
38. Choi YS, Dieter JA, Rothaeusler K, Luo Z, Baumgarth N. B-1 cells in the bone marrow are a significant source of natural IgM. Eur J Immunol (2012) 42(1):120-9. doi: 10.1002/eji.201141890
32. Owen JJ, Cooper MD, Raff MC. In vitro generation of B lymphocytes in mouse foetal liver, a mammalian 'bursa equivalent'. Nature (1974) 249(455):361-3. doi: 10.1038/249361a0
33. Baumgarth N. B-1 Cell Heterogeneity and the Regulation of Natural and Antigen-Induced IgM Production. Front Immunol (2016) 7:324. doi: 10.3389/fimmu.2016.00324

34. Montecino-Rodriguez E, Dorshkind K. B-1 B cell development in the fetus and adult. Immunity (2012) 36(1):13-21. doi: 10.1016/j.immuni.2011.11.017
35. Montecino-Rodriguez E, Leathers H, Dorshkind K. Identification of a B-1 B cell-specified progenitor. Nat Immunol (2006) 7(3):293-301. doi: 10.1038/ni1301
36. Esplin BL, Welner RS, Zhang Q, Borghesi LA, Kincade PW. A differentiation pathway for B1 cells in adult bone marrow. Proc Natl Acad Sci U S A (2009) 106(14):5773-8. doi: 10.1073/pnas.0811632106
128. Baumgarth N. The double life of a B-1 cell: self-reactivity selects for protective effector functions. Nat Rev Immunol (2011) 11(1):34-46. doi: 10.1038/nri2901
129. Kantor AB, Herzenberg LA. Origin of murine B cell lineages. Annu Rev Immunol (1993) 11:501-38. doi: 10.1146/annurev.iy.11.040193.002441
92. Cho SH, Raybuck AL, Stengel K, Wei M, Beck TC, Volanakis E, et al. Germinal centre hypoxia and regulation of antibody qualities by a hypoxia response system. Nature (2016) 537(7619):234-8. doi: 10.1038/nature19334
93. Xu S, Huo J, Huang Y, Aw M, Chen S, Mak S, et al. von Hippel-Lindau Protein Maintains Metabolic Balance to Regulate the Survival of Naive B Lymphocytes. iScience (2019) 17:379-92. doi: 10.1016/j.isci.2019.07.002
130. Spijker S. Dissection of Rodent Brain Regions. In: Li KW, editor. Neuroproteomics. Totowa, NJ: Humana Press; 2011. p. 13-26.

# CHAPTER 3

## *Vhl* deficiency in Dmp1-expressing cells affects myeloid development and erythropoiesis

Publication in preparation

Citation: ***Chicana B**, *Emery J, Taglinao H, Donham C, Manilay JO. *Vhl* deficiency in Dmp1-expressing cells affects myeloid development and erythropoiesis: possible effects on myeloerythroid metabolism. *Shared first authorship

## Abstract

The specific types of bone marrow (BM) stromal cells and local BM microenvironments that contribute to the regulation of myelopoiesis are not fully understood. The von-Hippel Lindau protein (VHL) controls responses to hypoxia and could regulate immune metabolism. We investigated this in *Dmp1*-Cre$^{+}$; *Vhl* conditional knockout mice (*Vhl*cKO), where *Vhl* is deleted in mesenchymal stem cells, osteoblasts (OBs) and osteocytes. We found elevate EPO levels in *Vhl*cKO peripheral blood serum and BM fluid by 3 weeks of age, and evidence for dysregulated erythropoiesis. Moreover, the *Vhl*cKO displayed an increased frequency of common myeloid progenitors by 10 weeks of age. We hypothesize EPO and Epo-receptor (EpoR) signaling to be directly affecting myeloiderythroid development in the BM. EpoR is expressed on osteoprogenitors, macrophages, dendritic cells, and B cells, but whether it is expressed on myeloid progenitors is unclear. These studies are relevant for the understanding of BM microenvironmental changes that can trigger adaptations in myelopoiesis.

## Introduction

Blood cells are continuously replenished by differentiation and maturation of hematopoietic stem cells (HSCs) into either lymphoid or myeloid lineage cells; this process is known as hematopoiesis. The lymphoid and myeloid cell lineages are the two major branches of hematopoietic cells. Lymphoid lineage cells include B cells, T cells and natural killer (NK) cells, while myeloid lineage cells include monocytes, granulocytes, macrophages, megakaryocytes, and erythrocytes (11, 12). These two lineages are separable at the progenitor level. Multipotent progenitors (MPPs) give rise to oligopotent progenitors, either common lymphoid progenitors (CLPs) (13, 14) or common myeloid progenitors (CMPs) (15). CLPs can develop into B cells, T cells or NK cells, all which leave the bone marrow into the periphery to finish development in other organs such as the spleen or thymus. CMPs have myeloid, erythroid, and megakaryocytic potential and can form granulocyte-macrophage progenitors (GMPs) and megakaryocyte-erythrocyte progenitors (MEPs). MEPs can develop into erythrocytes or megakaryocytes. Megakaryocytes break into platelets. GMPs differentiate into granulocytes such as neutrophils, basophils and eosinophils, or into monocytes which in turn become macrophages, osteoclasts, or myeloid dendritic cells (DCs) (15-19). The BM microenvironment that supports lymphoid and myeloid development has been described (12, 56, 57, 65, 131-133), but the detailed contributions of the microenvironment that maintain and regulate myeloid-erythroid development in the healthy bone marrow remains. A detailed understanding of how bone marrow microenvironments affect myeloid-erythroid development could provide strategies towards novel therapeutic approaches to immune deficiencies.

Erythropoietin (EPO) is a glycoprotein hormone produced by the kidneys that stimulates erythropoiesis in the bone marrow. Clinically it is used to stimulate erythropoiesis in anemic patients with kidney disease (134-136). EPO binds to the erythropoietin receptor (EpoR) (137), which has been traditionally thought of as an erythroid-specific signal. Deletion of EPO or EpoR in mice leads to embryonic lethality due to severe anemia at embryonic day 13 (138, 139). In recent years, EPO has been revealed to exert other roles in other myeloid lineages, angiogenesis, bone formation, and muscle repair, suggesting a broader biological role for EPO signaling (140-142). Whether EPO promotes bone formation (142-145) or bone loss (146-149) has been a topic of debate, with studies finding opposite roles. In humans, high levels of EPO in serum has been shown to predict incident fractures in elderly men with normal kidney function (150), while local EPO administration promoted bone healing in a study of 60 patients with tibiofibular fractures (151). Studies indicate that EPO can modulate osteoblast activity via mTOR and Ephrin B2/EphB4 signaling (142-146). Mice lacking EpoR in mature osteoblasts (using osteocalcin-Cre) were protected from Epo-induced bone loss (152). Mice lacking EpoR in osteoprogenitors using the osterix-Cre line, exhibit a low bone formation rate and high bone mass due to inhibition of osteoclastogenesis via the RANKL/OPG pathway (153). These studies reveal that the Epo/EpoR signaling is essential for bone remodeling.

Additionally, studies have found that EpoR is also expressed in non-erythroid cell types, such macrophages, dendritic cells, endothelial cells, bone marrow stromal cells and

B cells (154-157). EPO has been linked to impair skeletal homeostasis and B cell development (158). Ito et al. found that administration of EPO reduced immature and mature B cells in the bone marrow, while also decreasing surface VCAM1 and CXCL12 from endothelial cells, both signals that are essential for B cell development (155). B cells produce receptor activator of nuclear factor kappa-B ligand (RANKL) and osteoprotegerin (OPG), two key regulators of bone metabolism. EPO treatment *in vivo* increased RANKL expression in bone marrow B cells activating osteoclastogenesis (159). Deletion of EpoR from B cells (using Mb1-Cre) attenuated EPO- induced trabecular bone loss (160). These studies highlight B cells as an important target of Epo-EpoR signaling that regulates bone homeostasis.

The role of EPO in erythroid and non-erythroid lineages has been extensively characterized revealing a mediating signal on myeloid lineage cells. Megakaryocytes (MKs) are responsible for the production of blood thrombocytes (platelets), which are necessary for normal blood clotting. Thrombopoietin (TPO) has been known as the major regulator for platelet production through the Mpl receptor. However, EPO has also been identified as a stimulator for MKs (161-163) and EpoR has been found in 59% of total MKs (164), revealing a role in MK development. EPO administration has been shown to activate platelets and induce platelet production (165-167). Furthermore, TPO is able to restore erythroid differentiation in EpoR-deficient erythroid progenitors (168). These studies reveal the ability of EPO and TPO to stimulate each other targets lineages, and more recently found to conjointly regulate platelet size (169). Neutrophils, are phagocytes and a highly abundant granulocyte population, are the first line of defense (innate immunity) against pathogens. In rat studies, high levels of EPO was found to induce down regulation of neutrophils, but no reductions were observed *in vivo* (170). In more recent mice studies, EPO administration elevated neutrophil counts in peripheral blood, but no changes in count or function of different neutrophil populations (171). These studies suggest that EPO most likely does have a mediating effect on neutrophils. Macrophages, are phagocytes and another essential component of innate immunity, involved in detection and phagocytosis of pathogens as well as apoptotic cell clearance. Macrophages have been shown to express EpoR (172) and EPO administration enhances macrophage pro-inflammatory activity and function (173). EPO increased phagocytosis of apoptotic cells and deficiency of EpoR in macrophages impaired the clearance of apoptotic cells (172). In bone marrow-derived macrophages (BMDM), EpoR expression and activation by EPO results in the activation of signaling pathway MAPK, PI3K and NFκB, which are known for macrophage activation (173). These results indicate a direct target of Epo/EpoR signaling in macrophages that enhances its inflammatory activity and function. Dendritic cells (DCs) are phagocytes known to initiate the immune response by presenting antigens (also knowns as antigen-presenting cells (APC)), play an important role in adaptive immune system. Bone marrow DCs (BMDCs) have been shown to express EpoR, and EPO administration can activate the NFkB and MAPK signaling pathways, and induce a higher expression of CD80, CD86 and MHC class II (157, 174). All together these studies provide information of the cell-specific targets of EPO/EpoR signaling, providing insight to the immune regulatory functions of EPO.

The von-Hippel Lindau protein (VHL) regulates hypoxia-inducible factor (HIF) degradation, which is involved in cellular adaptation to low oxygen environments (hypoxia). HIF1α stabilization promotes the transcriptional activation of genes, including EPO to regulate erythropoiesis (175). HIF increases EPO production in kidney and liver in response to systemic hypoxia to increase red blood cell (RBC) production in the bone marrow (176, 177). Loss of *Vhl* in myeloid cells using the LysM-Cre (which targets monocytes, mature macrophages and granulocytes), leads to an increase in myeloid cell infiltration and activation of acute inflammatory responses, demonstrating that HIF-1α activation directs regulation of myeloid cells (178). We have previously found that conditional deletion of *Vhl* using *Dmp1*-Cre$^{+}$;*Vhl*$^{fl/fl}$ conditional knockout mice (*Vhl*cKO), display high bone mass and severe defect in B cell development, but appeared to have enhanced monocyte and granulocyte production in the bone marrow (89, 104). In this study, we investigate how changes in bone homeostasis in *Vhl*cKO mice affects myeloid and erythroid development.

## Method

### Experimental Animals

Mice on the C57Bl/6 background were used. B6N.FVB-Tg1Jqfe/BwdJ (*Dmp1*-Cre) (179) and B6.129S4(C)-Vhl tm1Jae/ J (*Vhl*$^{fl/fl}$) (180) were purchased from The Jackson Laboratory. These two lines of mice were crossed to generate *Vhl* conditional knockouts in *Dmp1*-expressing cells (*Vhl*cKO). Genotyping was confirmed following protocols from Jackson Laboratory for JAX Stock #021047 and #012933. Mice were housed under specific pathogen-free conditions in the University of California, Merced's vivarium with autoclaved feed and water, and sterile microisolator cages. The University of California Merced Institutional Animal Care and Use Committee approved all animal work.

### Bone Marrow Collection

Bone marrow collection was processed in the same manner as previously published (104). In brief, mice were euthanized by carbon dioxide asphyxiation followed by cervical dislocation as a second form of euthanasia. Femurs and tibias were dissected and cleaned of muscle tissues. Bones were crushes with a mortar and pestle in M199+ with 2% FBS to release BM cells, which were then filtered through 70-micron nylon mesh. Isolated cells were treated with ACK lysis buffer to remove erythrocytes for myeloid lineage and progenitor analysis. Cell counts were obtained using a hemocytometer and Trypan Blue staining to exclude dead cells.

To harvest the red blood cells residing in the bone marrow, bones were crushed using a mortar and pestle in M199 with 2% FCS (M199+). The cells were filtered through 70-micron nylon mesh and centrifuged for 5 minutes at 1500 rpm. Cell pellet was resuspended in M199+ media and stored at 4°C until staining for flow cytometry.

To collect BM fluid, femurs were cleaned of any muscle tissue and the epiphyses were cut off and discarded. The bone shaft was then placed into a 0.2 mL tube in which a hole was introduced using a needle. Thirty µL of 1x phosphate buffered saline (PBS) was placed on the top end of the bone shaft, using a 25g needle, and then the tube containing the bone was placed into a 1.5 ml microcentrifuge tube and centrifuged for 30 seconds at 15,000rpm. The BM supernatant was collected and stored at -80C until analysis.

**Peripheral blood collection**

Mice were heated under a heat lamp to increase blood circulation and then restrained. Blood collection was performed via tail bleeds by making an incision with a scalpel blade over the ventral tail vein. No more than ten drops were collected (< 0.5 mL) into centrifuge tubes without heparin and allowed to clot for 30 minutes at room temperature. The samples were then centrifuged for 10 minutes at 4000 rpm at 4°C. Blood serum was collected and stored at -80°C until the day of analysis.

**Quantification of Cytokines**

Cytokine measurements were performed using a customized bead-based multiplex (13-LEGENDplex assay) from Biolegend, Inc. with the analytes IL-3, IL-5, IL-6, IL-7, IL-15, IL-34, M-CSF, TPO, GM-CSF, LIF, EPO, CXCL12, SCF for the analysis of BM serum and peripheral blood serum of VhlcKO and control mice. Concentrations of cytokines were determined from samples following manufacturer's instructions and software.

**Real-Time qPCR measurement**

Whole bone marrow cells were isolated from long bones as described above. Cells were pelleted and resuspended in RNeasy RLT Lysis Buffer (Qiagen) with 1% of 2-mercaptoethanol. Total RNA was purified using the Qiagen RNeasy Micro Kit (Qiagen) according to manufacturer's protocol. RNA concentration and purity was analyzed using the NanoDrop One Spectrophotometer (Thermo Fisher Scientific). The same amount of RNA from each sample was mixed with qScript XLT One-Step, RT-qPCR ToughMix (Quantabio) together with specific TaqMan expression primers. Real-time qPCR was ran on the Applied Biosystems thermocycler using QuantStudio3 software (ThermoFisher) at the following specifications: 1 cycles at 50°C for 10 minutes for cDNA synthesis, 1 cycle at 95°C for 1 minute for initial denaturation and then 40 cycles of amplification at 95°C for 5 seconds then 60°C for 45 seconds. The following TaqMan gene expression assays (Thermo Fisher Scientific) were used: housekeeping *Actb*-VIC (Mm02619580_g1), target genes *Epo*-FAM (Mm01202755_m1) and *EpoR*-FAM (Mm00833882_m1).

**Flow Cytometry Analysis and Antibodies**

Bone marrow cells were stained for flow cytometry and included a pre-incubation step with unconjugated anti-CD16/32 (clone 93) to block Fc receptors as previously described, except for myeloid progenitor pannel (48, 104, 181). The antibody cocktails used for different sets of stains are listed in **Table 4**. For viability staining, DAPI (Sigma-

Aldrich, 1 μg/ml final concentration) or propidium iodide (Sigma-Aldrich, 1 μg/ml final concentration) was used. Single color stains were used for setting compensations and gates were determined with fluorescent-minus one controls, isotype-matched antibody controls, or historical controls. Flow cytometry data was acquired on the BD LSR II and on the ZE5. The data was analyzed using FlowJo Software version 10.7.1.

**Statistical analysis**

A G*Power statistical (182) power analysis (a=0.05 and power of 0.95) based on myeloid progenitor data and total BM cellularity determined that a minimum of n=8 mice per group was needed for our studies. The total sample size for each experiment was >8 performed in three independent experiments. Age-matched mice of both sexes *Vhl*cKO and control mice (*Vhl*$^{fl/fl}$, *Dmp1-Cre*-negative mice) were used. Comparisons between groups were performed using a two-tailed Student's t-test was used to test differences between mean and median values with Graph-Pad Prism and were considered significant if $p<0.05$.

## Results

To address the defects on myelopoiesis in the *Vhl*cKO mice, we first measured myeloid lineage frequency and numbers in the bone marrow (BM) at different ages using flow cytometry. We classify neutrophils as CD45$^+$Ly6G$^+$CD11b$^+$, classical monocytes divided into CD45$^+$Ly6G$^-$ CD11b$^+$F4/80$^-$CD115$^+$Ly6C$^{hi}$CD43$^-$ and CD45$^+$Ly6G$^-$ CD11b$^+$F4/80$^-$CD115$^+$Ly6C$^{hi}$CD43$^+$, non-classical monocytes CD45$^+$Ly6G$^-$ CD11b$^+$F4/80$^-$CD115$^+$Ly6C$^-$CD43$^+$, and dendritic cells CD45$^+$Ly6G$^-$CD11b$^+$F4/80$^-$ CD115$^+$Ly6C$^-$CD43$^+$MHC-II$^+$CD11c$^+$ (183). We found no changes in frequency of neutrophils, monocytes, or dendritic cells, in the *Vhl*cKO bone marrow (**Figure 22A-B**). However, we observed a decrease of neutrophils, dendritic cells, and Ly6C$^+$CD43$^+$ monocytes in the *Vhl*cKO bone marrow compared to control mice, suggesting a defect in myelopoiesis (**Figure 22C**).

To further investigate if the defect in myelopoiesis occurred upstream of lineage-committed cells, we analyzed myeloid progenitor compartments in the BM of *Vhl*c*KO* mice. Common myeloid progenitor (CMP: CD45$^+$Lin$^-$cKIT$^+$Sca1$^-$CD16/32$^+$CD34$^+$), granulocyte/monocyte progenitor (GMP: CD45$^+$Lin$^-$cKIT$^+$Sca1$^-$CD16/32$^-$CD34$^+$) and megakaryocyte/erythroid progenitor (MEP: Lin$^-$CD45$^+$cKIT$^+$Sca1$^-$CD16/32$^-$CD34$^-$) were quantified using flow cytometry (**Figure 23A**). The results showed an increase in frequency of CMPs and MEPs at 10-weeks-old, and an increase in CMP and GMPs at 24-weeks-old (**Figure 23B-C**). Absolute numbers of CMPs, MEPs and GMPs were comparable at 10-weeks-old, but significantly decreased at 24-weeks-old. The *Vhl*cKO GMP population displayed a reduction of CD34 expression, which was quantified and found more severely reduced in 24-week-old mice (**Figure 23B-C**).

The CMP and MEP increase observed in Figure 2 suggests a possible effect on erythropoiesis. To address any defects in erythropoiesis, we analyzed erythroid development in BM of *Vhl*cKO mice using flow cytometry (**Figure 24A**). We utilized Ter119 and CD71 cellular markers, which allows for identification of developmentally distinct RBC progenitor populations (Region 1: CD71$^+$Ter119$^-$, Region 2: CD71$^+$Ter119$^+$,

Region 3: $CD71^{int}Ter119^{+}$, and Region 4: $CD71^{-}$ $Ter119^{+}$) (181, 184). Regions 1-4 correlate with progressive stages of RBC differentiation with region 1 comprising the least and region 4 most mature RBCs. Region 1 predominantly proerythroblast, basophilic erythroblast in region 2, late basophilic and chromatophilic erythroblast in region 3 and orthochromatophilic erythroblast in region 4 (184). Results of RBC development reveal that at 10-weeks-old and 24-weeks-old, *Vhl*cKO mice displayed a significant decrease in regions 1-3 corresponding to erythroid progenitors and an increase at stage 4, corresponding to orthochromatophilic erythroblasts (**Figure 24**). These results indicate a significant increase in erythropoiesis, suggesting a possible role of EPO known to stimulates the production of mature RBCs from the bone marrow.

The increased late erythroid production suggested that EPO may be dysregulated in *Vhl*cKO mice. To confirm this, we investigated levels of EPO in the *Vhl*cKO mice. EPO concentrations in the peripheral blood serum and bone marrow fluid were comparable in both control and *Vhl*cKO mice at 3-to-6-weeks-old. However, at 10-to-24-weeks-old, *Vhl*cKO mice had significantly higher EPO levels than control mice (**Figure 25A**). TPO has also been linked as a stimulator of erythropoiesis in addition to its main role in platelet production, we observed increase levels of TPO in the peripheral blood serum, but not in bone marrow fluid of *Vhl*cKO mice (**Figure 25B**). To investigate if the high levels of EPO found in the *Vhl*cKO bone marrow fluid was being secreted by bone marrow cells, we measured *Epo* mRNA levels by real-time qPCR and 1 out of 4 control mice bone marrow had detectable levels of *Epo*, while the other 3 mice had no detectable levels as of 40 cycles of qPCR. Due to this we couldn't calculate relative expression of *Epo* because control mice had little to none *Epo* mRNA present. However, the *Vhl*cKO bone marrow cells did express a measurable level of *Epo* mRNA, we report the delta cycle-threshold (CT) values (difference between target gene and housekeeping CT value), we found lower delta CT values of *Epo* mRNA present in bone marrow cells indicating a high expression of *Epo* mRNA (**Figure 25C**). We also measured *EpoR* mRNA expression from bone marrow cells and found a decrease in *EpoR* relative expression in the *Vhl*cKO mice (**Figure 25D**).

## Discussion

In Chapter 3, we explore the *Vhl*cKO BM microenvironment effects on myelopoiesis and erythropoiesis. In our initial studies presented in Chapter 2, we observed a decrease of cellularity in the VhlcKO mice accompanied with reduced CD45+ cells as the mice ages. Preliminary results show no change in frequencies, but a decreased in cellular number of neutrophils, dendritic cells, and classical monocytes $Ly6C^{+}CD43^{+}$ in 24-week-old *Vhl*cKO mice. At the myeloid progenitor stage, we observe a decrease in CMPs in 10-week-old mice that's more severe at 24-weeks old. We initially predicted in Chapter 2 that the myeloid lineage would be increased, we were in part correct that progenitors were increased, but myeloid lineages remain unchanged or decreased. These results suggest that the VhlcKO bone marrow is able to retain comparable levels of myeloid lineage populations as controls, at the expense of the lymphoid lineage population. We analyzed erythroid development and observed an increased in late erythropoiesis (region 4: orthochromatophilic erythroblasts). Altogether, these results suggest a shift from lymphoid to the myeloid compartment and more specifically towards erythropoiesis. We

found elevate EPO levels in *Vhl*cKO peripheral blood serum and BM fluid by 3-6 weeks of age, and evidence for dysregulated erythropoiesis. We hypothesize that alterations to the EPO/EpoR signaling is directly affecting the myeloerythroid development in the BM. We continue to address these questions as we prepare our manuscript.

# Figures

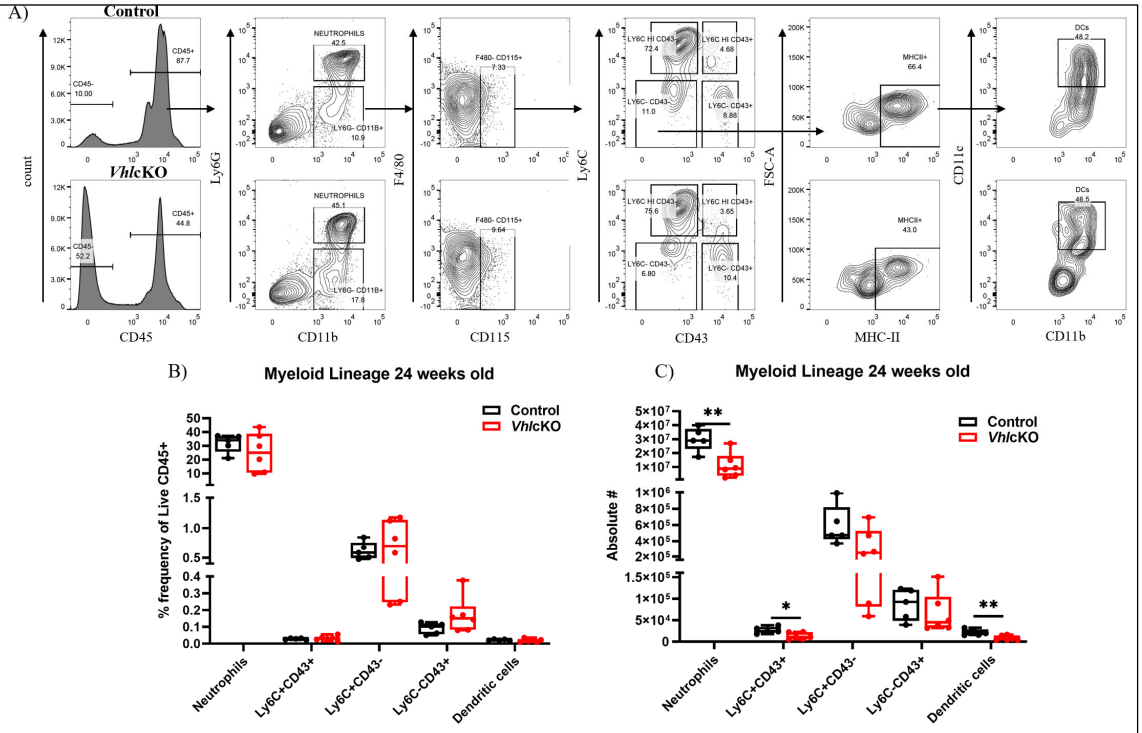


**Figure 22. Bone marrow defects in myelopoiesis of *Vhl*cKO mice.** Longitudinal study of bone marrow myeloid monocytes/macrophages A) flow cytometry gating strategy; B) frequency out of Live CD45+ and C) cellularity of myeloid populations in bone marrow at different ages; p<0.01**, two-tailed Student's t-test.

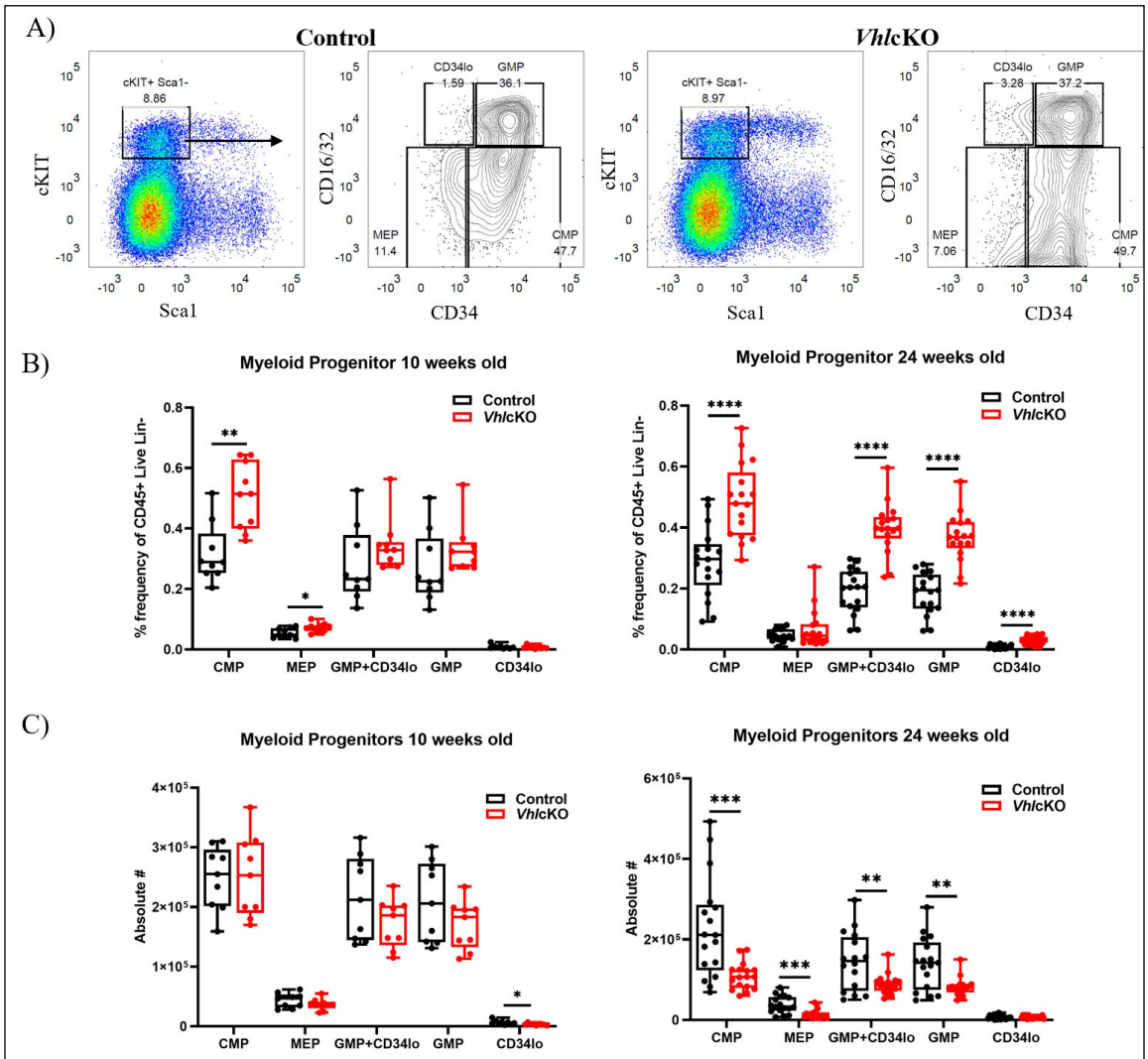


**Figure 23. Myeloid progenitor defects in bone marrow of *Vhl*cKO mice.** Longitudinal study of bone marrow cells A) example gating flow cytometry; B) % frequency of CMPs, MEPs, and GMPs with and without the $CD34^{lo}$ population present in *Vhl*cKO mice; and C) cellularity of these myeloid progenitors at different ages in control and *Vhl*cKO mice. p<0.05*, p<0.01**, p<0.001***, p<0.0001**** two-tailed Student's t-test.

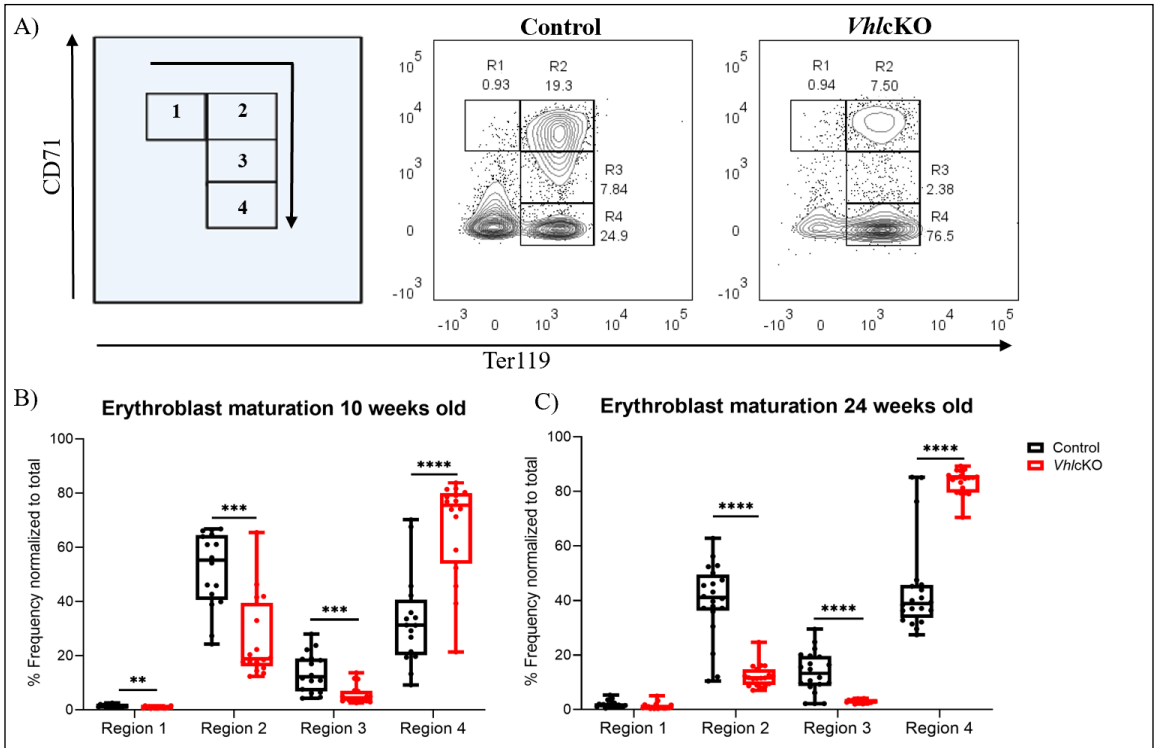


**Figure 24. *Vhl*cKO mice have altered erythropoiesis an increased frequency of orthochromatophilic erythroblasts.** (A) Flow cytometry gating of red blood cells (RBCs) in control and *Vhl*cKO. Stage 1-4 indicates the 1 being the least mature to 4 the most mature. Quantification of flow cytometry data for RBC in bone marrow of B) 10-weeks-old, and C) 24-weeks old. Data was normalized out of the 4 stages: (1 region/ sum of 4 regions) x 100. $p<0.05$*, $p<0.01$**, $p<0.001$***, $p<0.0001$**** two-tailed Student's t-test. Data initially collected by Cristine Donham, and subsequently collected and analyzed by Hanna Taglinao.

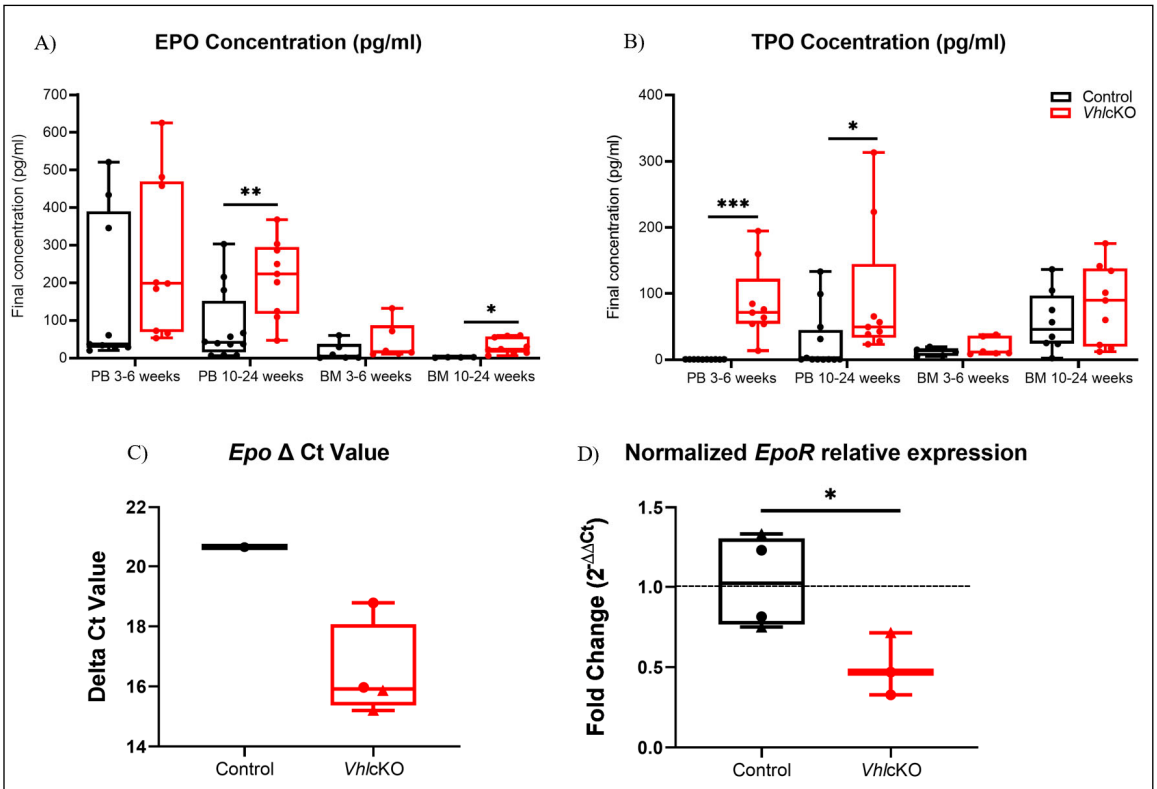


**Figure 25. *Vhl*cKO bone marrow has elevated levels of EPO and TPO, but reduced levels of *EpoR*.** A) EPO and B) TPO cytokine level measurements in bone marrow fluid of combined 3-6-weeks-old and 10-24-weeks old control or *Vhl*cKO mice; C) mRNA expression of *Epo* and D) *EpoR* levels from whole bone marrow of 10-week-old (circles) and 24-week-old (triangles) of control or *Vhl*cKO mice. $p<0.05$*, $p<0.01$**, $p<0.001$***, two-tailed Student's t-test.

**Table 4. List of the fluorochrome-labeled monoclonal antibodies used for flow cytometry in Chapter 3 organized by experimental cocktail**

| Cocktail | Antigen | Clone | Fluorochrome | Source |
|---|---|---|---|---|
| Myeloid Lineage | CD11b | M1/70 | FITC | Biolegend |
| | CD11c | N418 | PE | Biolegend |
| | CD19 | 6D5 | BV421 | Biolegend |
| | CD43 | S7 | BV605 | BD Biosciences |
| | CD45 | 30-F11 | BV711 | Biolegend |
| | Ly6G | 1A8 | APC | Biolegend |
| | F4/80 | BM8 | APC-eFluor 780 | Invitrogen |
| | Ly6C | HK1.4 | PerCP Cy5.5 | Biolegend |
| | CD115 | AFS98 | PE-Cy7 | Biolegend |
| | MHC-II | M5/114.15.2 | biotin | Biolegend |
| | Streptavidin | - | BUV395 | BD Biosciences |
| | DAPI (4′,6-diamidino-2-phenylindole) | | Viability Dye | Sigma-Aldrich |
| Myeloid Progenitor | CD3 | 145-2C11 | biotin | Biolegend |
| | CD4 | Gk1.5 | biotin | Biolegend |
| | CD8 | 53.6.7 | biotin | Biolegend |
| | CD5 | 52-7.3 | biotin | Biolegend |
| | CD19 | 6D5 | biotin | Biolegend |
| | Nk1.1 | PK136 | biotin | Biolegend |
| | TER119 | TER119 | biotin | Biolegend |
| | Gr1 | RB6-8C5 | biotin | Biolegend |
| | F4/80 | BM8 | biotin | Biolegend |
| | CD34 | RAM34 | FITC | Invitrogen |
| | CD45 | 30-F11 | BV421 | Biolegend |
| | Sca1 (Ly-6A/E) | D7 | BV510 | Biolegend |
| | CD16/32 | 93 | APC | Biolegend |
| | CD117 (cKit) | 2B8 | APC-Cy7 | Biolegend |
| | Streptavidin | - | PE-Cy5 | Life Technologies |
| | Propidium iodide (PI) | | Viability Dye | Sigma-Aldrich |
| Red Blood Cell Maturation | CD71 | RI7217 | PE | Biolegend |
| | TER119 | TER119 | APC | Biolegend |

## References


11. Kondo M, Wagers AJ, Manz MG, Prohaska SS, Scherer DC, Beilhack GF, et al. Biology of hematopoietic stem cells and progenitors: implications for clinical application. Annu Rev Immunol (2003) 21:759-806. doi: 10.1146/annurev.immunol.21.120601.141007

12. Kondo M. Lymphoid and myeloid lineage commitment in multipotent hematopoietic progenitors. Immunol Rev (2010) 238(1):37-46. doi: 10.1111/j.1600-065X.2010.00963.x

13. Karsunky H, Inlay MA, Serwold T, Bhattacharya D, Weissman IL. Flk2+ common lymphoid progenitors possess equivalent differentiation potential for the B and T lineages. Blood (2008) 111(12):5562-70. doi: 10.1182/blood-2007-11-126219

14. Kondo M, Weissman IL, Akashi K. Identification of clonogenic common lymphoid progenitors in mouse bone marrow. Cell (1997) 91(5):661-72. doi: 10.1016/s0092-8674(00)80453-5

15. Akashi K, Traver D, Miyamoto T, Weissman IL. A clonogenic common myeloid progenitor that gives rise to all myeloid lineages. Nature (2000) 404(6774):193-7. doi: 10.1038/35004599

16. Manz MG, Traver D, Miyamoto T, Weissman IL, Akashi K. Dendritic cell potentials of early lymphoid and myeloid progenitors. Blood (2001) 97(11):3333-41. doi: 10.1182/blood.v97.11.3333

17. Roodman GD. Advances in bone biology: the osteoclast. Endocr Rev (1996) 17(4):308-32. doi: 10.1210/edrv-17-4-308

18. Wei W, Zeve D, Wang X, Du Y, Tang W, Dechow PC, et al. Osteoclast progenitors reside in the peroxisome proliferator-activated receptor gamma-expressing bone marrow cell population. Mol Cell Biol (2011) 31(23):4692-705. doi: 10.1128/MCB.05979-11

19. Friedman AD. Transcriptional control of granulocyte and monocyte development. Oncogene (2007) 26(47):6816-28. doi: 10.1038/sj.onc.1210764

56. Ding L, Morrison SJ. Haematopoietic stem cells and early lymphoid progenitors occupy distinct bone marrow niches. Nature (2013) 495(7440):231-5. doi: 10.1038/nature11885

57. Ding L, Saunders TL, Enikolopov G, Morrison SJ. Endothelial and perivascular cells maintain haematopoietic stem cells. Nature (2012) 481(7382):457-62. doi: 10.1038/nature10783

65. Greenbaum A, Hsu YM, Day RB, Schuettpelz LG, Christopher MJ, Borgerding JN, et al. CXCL12 in early mesenchymal progenitors is required for haematopoietic stem-cell maintenance. Nature (2013) 495(7440):227-30. doi: 10.1038/nature11926

131. Tokoyoda K, Egawa T, Sugiyama T, Choi BI, Nagasawa T. Cellular niches controlling B lymphocyte behavior within bone marrow during development. Immunity (2004) 20(6):707-18. doi: 10.1016/j.immuni.2004.05.001

132. Cariappa A, Mazo IB, Chase C, Shi HN, Liu H, Li Q, et al. Perisinusoidal B cells in the bone marrow participate in T-independent responses to blood-borne microbes. Immunity (2005) 23(4):397-407. doi: 10.1016/j.immuni.2005.09.004

133. Pillai S, Cariappa A. The bone marrow perisinusoidal niche for recirculating B cells and the positive selection of bone marrow-derived B lymphocytes. Immunol Cell Biol (2009) 87(1):16-9. doi: 10.1038/icb.2008.89
134. Verhoef GE, Zachee P, Ferrant A, Demuynck H, Selleslag D, Van Hove L, et al. Recombinant human erythropoietin for the treatment of anemia in the myelodysplastic syndromes: a clinical and erythrokinetic assessment. Ann Hematol (1992) 64(1):16-21. doi: 10.1007/BF01811466
135. Skali H, Parving HH, Parfrey PS, Burdmann EA, Lewis EF, Ivanovich P, et al. Stroke in patients with type 2 diabetes mellitus, chronic kidney disease, and anemia treated with Darbepoetin Alfa: the trial to reduce cardiovascular events with Aranesp therapy (TREAT) experience. Circulation (2011) 124(25):2903-8. doi: 10.1161/CIRCULATIONAHA.111.030411
136. Eschbach JW, Egrie JC, Downing MR, Browne JK, Adamson JW. Correction of the anemia of end-stage renal disease with recombinant human erythropoietin. Results of a combined phase I and II clinical trial. N Engl J Med (1987) 316(2):73-8. doi: 10.1056/NEJM198701083160203
137. D'Andrea AD, Lodish HF, Wong GG. Expression cloning of the murine erythropoietin receptor. Cell (1989) 57(2):277-85. doi: 10.1016/0092-8674(89)90965-3
138. Zeigler BM, Vajdos J, Qin W, Loverro L, Niss K. A mouse model for an erythropoietin-deficiency anemia. Dis Model Mech (2010) 3(11-12):763-72. doi: 10.1242/dmm.004788
139. Wu H, Liu X, Jaenisch R, Lodish HF. Generation of committed erythroid BFU-E and CFU-E progenitors does not require erythropoietin or the erythropoietin receptor. Cell (1995) 83(1):59-67. doi: 10.1016/0092-8674(95)90234-1
140. Nakano M, Satoh K, Fukumoto Y, Ito Y, Kagaya Y, Ishii N, et al. Important role of erythropoietin receptor to promote VEGF expression and angiogenesis in peripheral ischemia in mice. Circ Res (2007) 100(5):662-9. doi: 10.1161/01.RES.0000260179.43672.fe
141. Jia Y, Suzuki N, Yamamoto M, Gassmann M, Noguchi CT. Endogenous erythropoietin signaling facilitates skeletal muscle repair and recovery following pharmacologically induced damage. FASEB J (2012) 26(7):2847-58. doi: 10.1096/fj.11-196618
142. Shiozawa Y, Jung Y, Ziegler AM, Pedersen EA, Wang J, Wang Z, et al. Erythropoietin couples hematopoiesis with bone formation. PLoS One (2010) 5(5):e10853. doi: 10.1371/journal.pone.0010853
142. Li C, Shi C, Kim J, Chen Y, Ni S, Jiang L, et al. Erythropoietin promotes bone formation through EphrinB2/EphB4 signaling. J Dent Res (2015) 94(3):455-63. doi: 10.1177/0022034514566431
144. Wan L, Zhang F, He Q, Tsang WP, Lu L, Li Q, et al. EPO promotes bone repair through enhanced cartilaginous callus formation and angiogenesis. PLoS One (2014) 9(7):e102010. doi: 10.1371/journal.pone.0102010
145. Kim J, Jung Y, Sun H, Joseph J, Mishra A, Shiozawa Y, et al. Erythropoietin mediated bone formation is regulated by mTOR signaling. J Cell Biochem (2012) 113(1):220-8. doi: 10.1002/jcb.23347

146. Hiram-Bab S, Liron T, Deshet-Unger N, Mittelman M, Gassmann M, Rauner M, et al. Erythropoietin directly stimulates osteoclast precursors and induces bone loss. FASEB J (2015) 29(5):1890-900. doi: 10.1096/fj.14-259085
147. Rauner M, Franke K, Murray M, Singh RP, Hiram-Bab S, Platzbecker U, et al. Increased EPO Levels Are Associated With Bone Loss in Mice Lacking PHD2 in EPO-Producing Cells. J Bone Miner Res (2016) 31(10):1877-87. doi: 10.1002/jbmr.2857
148. Suresh S, Alvarez JC, Dey S, Noguchi CT. Erythropoietin-Induced Changes in Bone and Bone Marrow in Mouse Models of Diet-Induced Obesity. Int J Mol Sci (2020) 21(5). doi: 10.3390/ijms21051657
149. Kolomansky A, Hiram-Bab S, Ben-Califa N, Liron T, Deshet-Unger N, Mittelman M, et al. Erythropoietin Mediated Bone Loss in Mice Is Dose-Dependent and Mostly Irreversible. Int J Mol Sci (2020) 21(11). doi: 10.3390/ijms21113817
150. Kristjansdottir HL, Lewerin C, Lerner UH, Herlitz H, Johansson P, Johansson H, et al. High Plasma Erythropoietin Predicts Incident Fractures in Elderly Men with Normal Renal Function: The MrOS Sweden Cohort. J Bone Miner Res (2020) 35(2):298-305. doi: 10.1002/jbmr.3900
151. Bakhshi H, Kazemian G, Emami M, Nemati A, Karimi Yarandi H, Safdari F. Local erythropoietin injection in tibiofibular fracture healing. Trauma Mon (2013) 17(4):386-8. doi: 10.5812/traumamon.7099
152. Suresh S, Lee J, Noguchi CT. Erythropoietin signaling in osteoblasts is required for normal bone formation and for bone loss during erythropoietin-stimulated erythropoiesis. FASEB J (2020) 34(9):11685-97. doi: 10.1096/fj.202000888R
153. Rauner M, Murray M, Thiele S, Watts D, Neumann D, Gabet Y, et al. Epo/EpoR signaling in osteoprogenitor cells is essential for bone homeostasis and Epo-induced bone loss. Bone Res (2021) 9(1):42. doi: 10.1038/s41413-021-00157-x
154. Zhang H, Wang S, Liu D, Gao C, Han Y, Guo X, et al. EpoR-tdTomato-Cre mice enable identification of EpoR expression in subsets of tissue macrophages and hematopoietic cells. Blood (2021) 138(20):1986-97. doi: 10.1182/blood.2021011410
155. Ito T, Hamazaki Y, Takaori-Kondo A, Minato N. Bone Marrow Endothelial Cells Induce Immature and Mature B Cell Egress in Response to Erythropoietin. Cell Struct Funct (2017) 42(2):149-57. doi: 10.1247/csf.17018
156. Suresh S, de Castro LF, Dey S, Robey PG, Noguchi CT. Erythropoietin modulates bone marrow stromal cell differentiation. Bone Res (2019) 7:21. doi: 10.1038/s41413-019-0060-0
157. Lifshitz L, Prutchi-Sagiv S, Avneon M, Gassmann M, Mittelman M, Neumann D. Non-erythroid activities of erythropoietin: Functional effects on murine dendritic cells. Mol Immunol (2009) 46(4):713-21. doi: 10.1016/j.molimm.2008.10.004
158. Singbrant S, Russell MR, Jovic T, Liddicoat B, Izon DJ, Purton LE, et al. Erythropoietin couples erythropoiesis, B-lymphopoiesis, and bone homeostasis within the bone marrow microenvironment. Blood (2011) 117(21):5631-42. doi: 10.1182/blood-2010-11-320564
159. Deshet-Unger N, Kolomansky A, Ben-Califa N, Hiram-Bab S, Gilboa D, Liron T, et al. Erythropoietin receptor in B cells plays a role in bone remodeling in mice. Theranostics (2020) 10(19):8744-56. doi: 10.7150/thno.45845

160. Neumann D, Gabet Y, Wielockx B, Rauner M, Mittelman M, Oster HS, et al. B Cell Specific Knockdown of the Erythropoietin (EPO) Receptor Attenuates EPO-Induced Bone Loss in Mice. Blood (2019) 134(Supplement_1):939-. doi: 10.1182/blood-2019-127092
161. Ishibashi T, Koziol JA, Burstein SA. Human recombinant erythropoietin promotes differentiation of murine megakaryocytes in vitro. J Clin Invest (1987) 79(1):286-9. doi: 10.1172/JCI112796
162. Tsukada J, Misago M, Kikuchi M, Sato T, Ogawa R, Ota T, et al. Interactions between recombinant human erythropoietin and serum factor(s) on murine megakaryocyte colony formation. Blood (1992) 80(1):37-45. doi: 10.1182/blood.V80.1.37.37
163. Metcalf D, Di Rago L, Mifsud S. Synergistic and inhibitory interactions in the in vitro control of murine megakaryocyte colony formation. Stem Cells (2002) 20(6):552-60. doi: 10.1002/stem.200552
164. Pronk CJ, Rossi DJ, Mansson R, Attema JL, Norddahl GL, Chan CK, et al. Elucidation of the phenotypic, functional, and molecular topography of a myeloerythroid progenitor cell hierarchy. Cell Stem Cell (2007) 1(4):428-42. doi: 10.1016/j.stem.2007.07.005
165. McDonald TP, Cottrell MB, Clift RE, Cullen WC, Lin FK. High doses of recombinant erythropoietin stimulate platelet production in mice. Exp Hematol (1987) 15(6):719-21.
166. McDonald TP, Cottrell MB, Steward SA, Clift RE, Swearingen CJ, Jackson CW. Comparison of platelet production in two strains of mice with different modal megakaryocyte DNA ploidies after exposure to hypoxia. Exp Hematol (1992) 20(1):51-6.
167. McDonald TP, Clift RE, Cottrell MB. Large, chronic doses of erythropoietin cause thrombocytopenia in mice [see comments]. Blood (1992) 80(2):352-8. doi: 10.1182/blood.V80.2.352.352
168. Kieran MW, Perkins AC, Orkin SH, Zon LI. Thrombopoietin rescues in vitro erythroid colony formation from mouse embryos lacking the erythropoietin receptor. Proc Natl Acad Sci U S A (1996) 93(17):9126-31. doi: 10.1073/pnas.93.17.9126
169. Hacein-Bey-Abina S, Estienne M, Bessoles S, Echchakir H, Pederzoli-Ribeil M, Chiron A, et al. Erythropoietin is a major regulator of thrombopoiesis in thrombopoietin-dependent and -independent contexts. Exp Hematol (2020) 88:15-27. doi: 10.1016/j.exphem.2020.07.006
170. Koenig JM, Christensen RD. Effect of erythropoietin on granulocytopoiesis: in vitro and in vivo studies in weanling rats. Pediatr Res (1990) 27(6):583-7. doi: 10.1203/00006450-199006000-00009
171. Avneon M, Lifshitz L, Katz O, Prutchi-Sagiv S, Gassmann M, Mittelman M, et al. Non-erythroid effects of erythropoietin: are neutrophils a target? Leuk Res (2009) 33(10):1430-2. doi: 10.1016/j.leukres.2009.03.020
172. Luo B, Gan W, Liu Z, Shen Z, Wang J, Shi R, et al. Erythropoeitin Signaling in Macrophages Promotes Dying Cell Clearance and Immune Tolerance. Immunity (2016) 44(2):287-302. doi: 10.1016/j.immuni.2016.01.002
173. Lifshitz L, Tabak G, Gassmann M, Mittelman M, Neumann D. Macrophages as novel target cells for erythropoietin. Haematologica (2010) 95(11):1823-31. doi: 10.3324/haematol.2010.025015

174. Newmann D, Mittelman M, Markovitz M, Sagiv SP, Lifchitz L. Dendritic Cells as a Novel Target for Erythropoietin: Studies in Murine Models. Blood (2007) 110(11):2417-. doi: 10.1182/blood.V110.11.2417.2417
175. Lee FS, Percy MJ. The HIF pathway and erythrocytosis. Annu Rev Pathol (2011) 6:165-92. doi: 10.1146/annurev-pathol-011110-130321
176. Haase VH. Regulation of erythropoiesis by hypoxia-inducible factors. Blood Rev (2013) 27(1):41-53. doi: 10.1016/j.blre.2012.12.003
177. Franke K, Gassmann M, Wielockx B. Erythrocytosis: the HIF pathway in control. Blood (2013) 122(7):1122-8. doi: 10.1182/blood-2013-01-478065
178. Cramer T, Yamanishi Y, Clausen BE, Förster I, Pawlinski R, Mackman N, et al. HIF-1α Is Essential for Myeloid Cell-Mediated Inflammation. Cell (2003) 112(5):645-57. doi: 10.1016/s0092-8674(03)00154-5
89. Loots GG, Robling AG, Chang JC, Murugesh DK, Bajwa J, Carlisle C, et al. Vhl deficiency in osteocytes produces high bone mass and hematopoietic defects. Bone (2018) 116:307-14. doi: 10.1016/j.bone.2018.08.022
104. Chicana B, Abbasizadeh N, Burns C, Taglinao H, Spencer JA, Manilay JO. Deletion of Vhl in Dmp1-expressing cells causes microenvironmental impairment of B cell lymphopoiesis. bioRxiv (2022). doi: 10.1101/2021.09.10.459794
179. Lu Y, Xie Y, Zhang S, Dusevich V, Bonewald LF, Feng JQ. DMP1-targeted Cre expression in odontoblasts and osteocytes. J Dent Res (2007) 86(4):320-5. doi: 10.1177/154405910708600404
180. Haase VH, Glickman JN, Socolovsky M, Jaenisch R. Vascular tumors in livers with targeted inactivation of the von Hippel-Lindau tumor suppressor. Proc Natl Acad Sci U S A (2001) 98(4):1583-8. doi: 10.1073/pnas.98.4.1583
48. Cain CJ, Rueda R, McLelland B, Collette NM, Loots GG, Manilay JO. Absence of sclerostin adversely affects B-cell survival. J Bone Miner Res (2012) 27(7):1451-61. doi: 10.1002/jbmr.1608
181. Gravano DM, Manilay JO. Inhibition of proteolysis of Delta-like-1 does not promote or reduce T-cell developmental potential. Immunol Cell Biol (2010) 88(7):746-53. doi: 10.1038/icb.2010.30
182. Faul F, Erdfelder E, Lang AG, Buchner A. G*Power 3: a flexible statistical power analysis program for the social, behavioral, and biomedical sciences. Behav Res Methods (2007) 39(2):175-91.
183. Yanez A, Coetzee SG, Olsson A, Muench DE, Berman BP, Hazelett DJ, et al. Granulocyte-Monocyte Progenitors and Monocyte-Dendritic Cell Progenitors Independently Produce Functionally Distinct Monocytes. Immunity (2017) 47(5):890-902 e4. doi: 10.1016/j.immuni.2017.10.021
184. Socolovsky M, Nam H, Fleming MD, Haase VH, Brugnara C, Lodish HF. Ineffective erythropoiesis in Stat5a(-/-)5b(-/-) mice due to decreased survival of early erythroblasts. Blood (2001) 98(12):3261-73. doi: 10.1182/blood.v98.12.3261

# CHAPTER 4

## Conclusions and Future Directions

## Contributions to the field

*Cell extrinsic role of Vhl and altered bone homeostasis on immune cell development*

The network of interactions regulating the bone and bone microenvironment is complex and there are still gaps in the knowledge of how these interactions affect long-term immunity and development (49, 185, 186). The information generated in this dissertation focused on significant changes to the microenvironment niche of the *Vhl*cKO mice and its effects on hematopoiesis (lymphoid and myeloid), helping define the role of *Vhl* and altered bone homeostasis has on immune cell development. These results help further explain the complex relationship between bone, niche, and hematopoiesis in the bone marrow in the interdisciplinary field of osteoimmunology (187). We found that the bone marrow of the *Vhl*cKO has an age-related difference in hypoxic stress and in B cell development. While also having reduced supporting cytokines such as CXCL12 and IL7, and increased EPO. The results of this work could contribute to the development of new therapies for exogenous CXCL12 and EPO antagonists, to preserve and improve bone marrow function during bone niche changes or stress. The studies in this dissertation have clinical relevance in revealing potential side effects on the immunity of patients treated with anabolic bone building drugs for treatment of bone-weakening diseases, like osteoporosis.

*Possible implications of hypoxia controlling drugs on the immune system*

Deletion of *Vhl* to stabilize HIF1α in skeletal cells like OB and OCY, have been shown to increase bone mass, revealing the critical role of HIF1α (hypoxic conditions) in bone formation (**Table 2**). Different modes of hypoxic conditioning have been proposed as possible routes against bone diseases (188, 189). One often forgotten effect of HIF1α stabilization, is its effects on B cell proliferation, antibody class-switching, generation of high affinity antibodies, antibody responses, impaired metabolic balance, all which is essential for B cell survival (92, 93). Furthermore, this dissertation revealed the cell extrinsic effects that HIF1α stabilization in skeletal cells has on B cells (104). A detailed understanding of these interactions is crucial for developing hypoxic controlling bone-building therapies that will spare immune complications and deficiencies. Based on the NIH clinical trials website, there are still not many studies currently undergoing clinical trials for the use of hypoxia controlling drugs for treatment of osteoporosis. However, one study that was completed July 2021, studied the effects of "Strength training in hypoxia to improve bone and cardiovascular health on elderly", have yet to publish the results of the study, but based on the reports there was no quantification or measurement of the effects that such conditions would have on the immune system. On the other hand, a study using Salidroside (SAL), a known anti-hypoxic drug commonly used in Chinese medicine, has been shown to ameliorate hypoxia induce bone loss, by enhancing osteogenesis (190). Although this study shows promising results, they also did not measure any effects on immunity, but I predict it would have less severe effects than hypoxia inducible drugs. We recommend hypoxia controlling drugs to address its possible implications on the immune system, in particular on B cells.

## Future Directions

*Determine if B cell functionality is truly affected in the VhlcKO mice*

Although antibody levels remain similar as shown in Chapter 2 Figure 9-11, we did not further test for antibody affinity, which is an essential component of B cell antibody functionality. We also have not measured plasma cells or memory B cells after activation to see if the *Vhl*cKO mice are able to maintain memory B cells comparable to controls, neither have we tested 6-month older mice, which have more severe B cell reduction in the BM. Therefore, to fully conclude that there are no functional defects in the *Vhl*cKO mice, requires further experimentation.

*Perform rescue experiments to normalize aberrant hematopoiesis in VhlcKO bone marrow*

We have presented cytokines involved in the aberrant hematopoiesis observed in this model, such as CXCL12, EPO, and IL7 (Chapter 2), but whether restoring these cytokine signals would rescue aberrant hematopoiesis remains to be explored. To normalize aberrant hematopoiesis in the bone marrow of *Vhl*cKO mice, we could perform "adding-back" experiments. For example, *in vitro* assays in which B cells from control mice can be co-cultured with *VhlcKO* stromal niche cell(s) and supplemented with exogenous cytokines (CXCL12 and IL7). I hypothesize that in such *invitro* setting B cells could develop similar to controls. Or possible *in vivo* assays to supplement mice with EPO antagonists and exogenous CXCL12 or IL7, to rescue hematopoiesis. Whether these assays could restore hematopoiesis in such high bone mass remains to be explored.

*Determine the bone marrow cells contributing to EPO production in the VhlcKO mice*

As we presented in Figure 25 in Chapter 3, we found that whole bone marrow *Vhl*cKO cells produce a high level of *Epo* mRNA. This suggest that there is a population(s) in the bone marrow capable of secreting EPO. The main source of EPO are the kidneys, but hepatocytes from the liver have also been found to produce significant levels of EPO (191). Studies have also found mRNA expression of *Epo* in the brain, spleen, hair follicles, reproductive organs, and renal fibroblasts (192-199). Whether bone marrow can contribute EPO remains unclear. The *Vhl*cKO mice provides a great model to tease out specific BM populations that can contribute significant EPO to the bone marrow.

*Need for conditional knockout models that target osteocytes*

One limitation in our studies has been the off-target gene deletion in the *Dmp1-Cre* mice we utilized. The *Dmp1-Cre* mice strain is currently the main model available to study osteocytes (200). However, despite its widespread use, the *Dmp1-Cre* displays off-target expression in skeletal muscle fibers, gastrointestinal mesenchyme, arteries, kidneys, and brain (200-203). Deletion of *Vhl* at the MSC, OB and OCY stages display similar physical bone characteristics and altered bone marrow microenvironment (Table 2). These studies imply that the phenotypes could have been generated at an earlier osteoprogenitor stage (MSCs) and not exclusively to more mature osteolineages (OBs and OCYs). There is a need for new osteolineage mouse models that are non-overlapping between MSCs, OBs, and OCYs to allow the specific contributions of each stage to hematopoiesis. In initial studies, St. John et al. 2014 performed invitro RNA-seq revealing the specific

transcriptional changes in osteoblasts during differentiation towards an osteocyte-like phenotype (204). In a more recent study, Youlten et al. 2021 defined an osteocyte transcriptome signature of 1239 unique genes that distinguishes osteocytes from other cells, and of which 77% are of unknown role. There's still a need for single cell RNA-sequencing of skeletal cells (205), and as these studies are coming out, they reveal key markers that could be used to differentiate osteoblasts from osteocytes. For now, usage of the tamoxifen induced mouse strains *Dmp1-Cre-ER$^{T2}$* or *Sost-Cre-ER$^{T2}$* can help avoid some of the off target expression and a more targeted expression to mature osteocytes (200, 206).

*Using Dmp1-Cre;Ai9 mice for analysis of niche cells in the VhlcKO mice*

During flow cytometry after bone digest, we found that the distribution of the stromal cell populations was not affected in the *Vhl*cKO, except for CD31+ ECs, which were reduced (Supplemental Figure 6 in Chicana et al. 2022). This was surprising due to the increase in vessel volume that was observed from the ex vivo imaging analysis of *Vhl*cKO bones. The differences in the results suggested that there was a limitation in the bone digestion protocol that was used for analyzing BMSCs by flow cytometry, which was of an enzymatic digestion for 2 hours. In addition, the increased density of *Vhl*cKO bone made it challenging to digest completely and all bone cells may not have been released. To address this limitation, we started testing a serial bone digest that is more promising at releasing bone cells (Chapter 2, Figure 10). This addresses the isolation limitation of bone cells from highly dense bones, but the limitation of markers needed for the isolation of Dmp1$^{+}$ expressing cells remains. One solution is having the *Vhl*cKO mice in a reporter background, which would help sort isolate DMP1 expressing cells from serial digested bones for further testing (gene expression, co-cultures, imaging). Here are some recommendations:

| | Mouse Strain | Common Name | Allele Type | Chromosome | Brief description | Jax Stock No. |
|---|---|---|---|---|---|---|
| Used in our studies | B6N.FVB-Tg(Dmp1-cre)1Jqfe/BwdJ | Dmp1-Cre$^{+}$ | Transgenic | UN | Cre target | 023047 |
| | B6.129S4(C)-*Vhl$^{tm1Jae}$*/J | Vhl$^{fl/fl}$ | Targeted | 6 | Flox target | 012933 |
| | B6.Cg-*Gt(ROSA)26Sor$^{tm9(CAG-tdTomato)Hze}$*/J | Ai9 | Targeted | 6 | Cre reporter | 007909 |
| Other Reporters | Tg(CAG-Bgeo,-DsRed*MST)1Nagy/J | Z/RED | Transgenic | UN | Double reporter | 005438 |
| | B6.129(Cg)-Tg(CAG-Bgeo/GFP)21Lbe/ | Z/EG | Transgenic | 5 | Double reporter | 004178 |
| | B6;129S6-*Igs7$^{tm213(CAG-EGFP,CAG-mOrange2,CAG-mKate2)Hze}$*/J | Ai213 | Targeted | 9 | Triple reporter | 034113 |
| | B6;129S-*Gt(ROSA)26Sor$^{tm1(CAG-cre*,-mKate2)Yzwa}$*/J | Rosa26$^{PA-Cre\ A20}$ | Targeted | 6 | Photoactivatable | 033544 |

## Summary

These studies reveal the implications that HIF stabilization in skeletal cells have in immune development in the bone marrow. We further characterized the microenvironment that influences hematopoiesis in the context of altered bone homeostasis. We have provided evidence that *Vhl*-deficiency in osteocytes results in structural and molecular changes in the BM microenvironments that insufficiently produces niche cells and cytokines required to appropriately support hematopoiesis in the BM, in particular of B cell development. We continue to explore if the alterations in skeletal glucose metabolism directly affect myeloerythroid development in the BM through increased Epo-receptor (EpoR) signaling. This dissertation expands on the potential mechanisms by which VHL/HIF signaling in Dmp1 expressing cells may serve as a niche for distinct hematopoietic lymphoid and myeloid lineages in the BM, further elucidating and expanding our definition of "niche" to include bone embedded cells and anatomical changes. The culmination of this dissertation provides a unique view of how alterations in the bone can change the bone marrow hematopoiesis.

## References


49. Manilay JO, Zouali M. Tight relationships between B lymphocytes and the skeletal system. Trends Mol Med (2014) 20(7):405-12. doi: 10.1016/j.molmed.2014.03.003

185. Mori G, D'Amelio P, Faccio R, Brunetti G. The Interplay between the bone and the immune system. Clin Dev Immunol (2013) 2013:720504. doi: 10.1155/2013/720504

186. Ponzetti M, Rucci N. Updates on Osteoimmunology: What's New on the Cross-Talk Between Bone and Immune System. Front Endocrinol (Lausanne) (2019) 10:236. doi: 10.3389/fendo.2019.00236

187. Ginaldi L, De Martinis M. Osteoimmunology and Beyond. Curr Med Chem (2016) 23(33):3754-74.

188. Hannah SS, McFadden S, McNeilly A, McClean C. "Take My Bone Away?" Hypoxia and bone: A narrative review. J Cell Physiol (2021) 236(2):721-40. doi: 10.1002/jcp.29921

189. Camacho-Cardenosa M, Camacho-Cardenosa A, Timon R, Olcina G, Tomas-Carus P, Brazo-Sayavera J. Can Hypoxic Conditioning Improve Bone Metabolism? A Systematic Review. Int J Environ Res Public Health (2019) 16(10). doi: 10.3390/ijerph16101799

92. Cho SH, Raybuck AL, Stengel K, Wei M, Beck TC, Volanakis E, et al. Germinal centre hypoxia and regulation of antibody qualities by a hypoxia response system. Nature (2016) 537(7619):234-8. doi: 10.1038/nature19334

93. Xu S, Huo J, Huang Y, Aw M, Chen S, Mak S, et al. von Hippel-Lindau Protein Maintains Metabolic Balance to Regulate the Survival of Naive B Lymphocytes. iScience (2019) 17:379-92. doi: 10.1016/j.isci.2019.07.002

104. Chicana B, Abbasizadeh N, Burns C, Taglinao H, Spencer JA, Manilay JO. Deletion of Vhl in Dmp1-expressing cells causes microenvironmental impairment of B cell lymphopoiesis. bioRxiv (2022). doi: 10.1101/2021.09.10.459794

190. Li L, Qu Y, Jin X, Guo XQ, Wang Y, Qi L, et al. Protective effect of salidroside against bone loss via hypoxia-inducible factor-1alpha pathway-induced angiogenesis. Sci Rep (2016) 6:32131. doi: 10.1038/srep32131

191. Koury ST, Bondurant MC, Koury MJ, Semenza GL. Localization of cells producing erythropoietin in murine liver by in situ hybridization [see comments]. Blood (1991) 77(11):2497-503. doi: 10.1182/blood.V77.11.2497.2497

192. Bachmann S, Le Hir M, Eckardt KU. Co-localization of erythropoietin mRNA and ecto-5'-nucleotidase immunoreactivity in peritubular cells of rat renal cortex indicates that fibroblasts produce erythropoietin. J Histochem Cytochem (1993) 41(3):335-41. doi: 10.1177/41.3.8429197

193. Bernaudin M, Bellail A, Marti HH, Yvon A, Vivien D, Duchatelle I, et al. Neurons and astrocytes express EPO mRNA: Oxygen-sensing mechanisms that involve the redox-state of the brain. Glia (2000) 30(3):271-8. doi: Doi 10.1002/(Sici)1098-1136(200005)30:3<271::Aid-Glia6>3.3.Co;2-8

194. Lacombe C, Da Silva JL, Bruneval P, Fournier JG, Wendling F, Casadevall N, et al. Peritubular cells are the site of erythropoietin synthesis in the murine hypoxic kidney. J Clin Invest (1988) 81(2):620-3. doi: 10.1172/JCI113363

195. Maxwell PH, Osmond MK, Pugh CW, Heryet A, Nicholls LG, Tan CC, et al. Identification of the renal erythropoietin-producing cells using transgenic mice. Kidney Int (1993) 44(5):1149-62. doi: 10.1038/ki.1993.362
196. Marti HH, Gassmann M, Wenger RH, Kvietikova I, Morganti-Kossmann MC, Kossmann T, et al. Detection of erythropoietin in human liquor: intrinsic erythropoietin production in the brain. Kidney Int (1997) 51(2):416-8. doi: 10.1038/ki.1997.55
197. Yasuda Y, Masuda S, Chikuma M, Inoue K, Nagao M, Sasaki R. Estrogen-dependent production of erythropoietin in uterus and its implication in uterine angiogenesis. J Biol Chem (1998) 273(39):25381-7. doi: 10.1074/jbc.273.39.25381
198. Bodo E, Kromminga A, Funk W, Laugsch M, Duske U, Jelkmann W, et al. Human hair follicles are an extrarenal source and a nonhematopoietic target of erythropoietin. FASEB J (2007) 21(12):3346-54. doi: 10.1096/fj.07-8628com
199. Kobayashi T, Yanase H, Iwanaga T, Sasaki R, Nagao M. Epididymis is a novel site of erythropoietin production in mouse reproductive organs. Biochem Bioph Res Co (2002) 296(1):145-51. doi: Pii S0006-291x(02)00832-X
Doi 10.1016/S0006-291x(02)00832-X
200. Kalajzic I, Matthews BG, Torreggiani E, Harris MA, Divieti Pajevic P, Harris SE. In vitro and in vivo approaches to study osteocyte biology. Bone (2013) 54(2):296-306. doi: 10.1016/j.bone.2012.09.040
201. Dallas SL, Xie Y, Shiflett LA, Ueki Y. Mouse Cre Models for the Study of Bone Diseases. Curr Osteoporos Rep (2018) 16(4):466-77. doi: 10.1007/s11914-018-0455-7
202. Dasgupta K, Lessard S, Hann S, Fowler ME, Robling AG, Warman ML. Sensitive detection of Cre-mediated recombination using droplet digital PCR reveals Tg(BGLAP-Cre) and Tg(DMP1-Cre) are active in multiple non-skeletal tissues. Bone (2020) 142:115674. doi: 10.1016/j.bone.2020.115674
203. Lim J, Burclaff J, He G, Mills JC, Long F. Unintended targeting of Dmp1-Cre reveals a critical role for Bmpr1a signaling in the gastrointestinal mesenchyme of adult mice. Bone Res (2017) 5:16049. doi: 10.1038/boneres.2016.49
204. St John HC, Bishop KA, Meyer MB, Benkusky NA, Leng N, Kendziorski C, et al. The osteoblast to osteocyte transition: epigenetic changes and response to the vitamin D3 hormone. Mol Endocrinol (2014) 28(7):1150-65. doi: 10.1210/me.2014-1091
205. Ayturk U. RNA-seq in Skeletal Biology. Curr Osteoporos Rep (2019) 17(4):178-85. doi: 10.1007/s11914-019-00517-x
202. Maurel DB, Matsumoto T, Vallejo JA, Johnson ML, Dallas SL, Kitase Y, et al. Characterization of a novel murine Sost ER(T2) Cre model targeting osteocytes. Bone Res (2019) 7:6. doi: 10.1038/s41413-018-0037-4